DC Corona Electroporation

Submitted by

Nevendra Krishniah Chetty

In fulfilment of the degree of

Doctor of Philosophy in Electrical Engineering from the University of KwaZulu-Natal

Date of submission

December 2015

Supervised by

Dr. I E Davidson

and

Co-supervised by

Dr. L Chetty, Prof. T Govender and Prof. N M Ijumba

SUPERVISOR'S APPROVAL

As the candidate's supervisor, I have approved this thesis for submission.

Signed: ……

Date: ……...

DECLARATION

I, Nevendra Krishniah Chetty, declare that

1. The research reported in this thesis, except where otherwise indicated, is my original research.

2. This thesis has not been submitted for any degree or examination at any other university.

3. This thesis does not contain other persons' data, pictures, graphs or other information, unless specifically acknowledged as being sourced from other persons.

4. This thesis does not contain other persons' writing, unless specifically acknowledged as being sourced from other researchers. Where other written sources have been quoted, then:
    a. Their words have been re-written but the general information attributed to them has been referenced
    b. Where their exact words have been used, then their writing has been placed in italics and inside quotation marks, and referenced.

5. This thesis does not contain text, graphics or tables copied and pasted from the Internet, unless specifically acknowledged, and the source being detailed in the thesis and in the References sections.

Signed

……

ABSTRACT

Cells are surrounded by a semi-permeable bilayer lipid membrane that acts as a barrier against the entry of foreign molecules. In the fields of molecular biology, biotechnology, and medicine, the ability to breach the cell membrane and introduce molecules into cells for therapeutic purposes is often necessary. Molecules, which are considered foreign to the cell like drugs and extraneous genetic materials, are administered to cells for numerous applications including the treatment and prevention of diseases. There are many accepted methods of facilitating the delivery of molecules to cells. Of all these methods, one important and well-established physical method is electroporation which has been utilised for decades.

Electroporation is a widely adopted procedure for the temporary permeabilization of cell membranes due to the application of short electrical pulses. It is a phenomenon resulting from the effects of pulsed electric fields, which induces biochemical and physiological changes to a cell membrane. As a result, some of the molecules that are ordinarily unable to pass through the membrane are thereafter able to gain access to the cell interior via pores that are formed in the membrane.

Even though electroporation is fairly safe, there are some drawbacks associated with this method. The traditional method of electroporation requires direct contact of high voltage electrodes and fairly high currents are involved. As a result, the procedure can cause pain, muscle spasms, discomfort, burning and cell and tissue damage.

Alternative methods of molecular delivery are therefore being researched, especially non-contact methods such as the use of high voltage plasma and high voltage corona discharge. Successful cell permeabilization with corona discharge ions and plasma has been previously demonstrated. These methods offer the advantage of contact-free treatment with low associated current.

In this thesis, the research investigates the delivery of tracer molecules, SYTOX Green, into HeLa cells and the consequential cell destruction by the phenomenon of corona discharge. A high voltage DC, multipoint-to-plane atmospheric-air corona discharge apparatus was designed and constructed to investigate the conditions as well as the characteristics of the corona discharge current pulses that resulted in an acceptable balance between high cell

permeabilization and low cell destruction. Firstly, the salient variables that affect molecular delivery and cell destruction were established. Secondly, the variables were optimized to allow for reliable molecular delivery to cells with acceptable levels of cell destruction. Thirdly, the nature and variation of the corona discharge current pulses and its effect on molecular delivery and cell destruction were investigated. Finally, a new method of assessing cell destruction, which combined the measurements of cell viability and cell lysis were used.

The variables that were identified, over the course of many experiments, were exposure time to corona discharge, incubation time with SYTOX Green, volume of liquid during exposure, and inter-electrode distance. Further experiments show that when the variables of the experiment are set at optimal values, cell permeabilization is reliable with minimal damage to cells. Once these conditions were obtained and optimised, the effect of different applied voltages on the level of cell permeabilization and the short-term destructive effects on cells were investigated. The general trend is an increase in fluorescence and therefore, molecular delivery, with an increase in applied voltage. Cell destruction also tends to increase with increasing applied voltage.

The characteristics of the corona current pulses that were analyzed include amplitudes, repetition rates, widths, and rise-times. The characteristic frequencies of single pulses, obtained from the application of a discrete fast Fourier transform, were also analyzed.

For the corona-generating device constructed and the voltages tested, it was found that the only characteristic that varies appreciably with voltage is the pulse repetition rate. A higher pulse repetition rate relates to a greater number of pulses per unit time and therefore, a greater exposure of the cells to the applied electric field. This would, therefore, translate to a higher extent of molecular delivery and a higher accompanying level of cell destruction.

This study shows that permeabilization of HeLa cells due to corona discharge can be reliably achieved and the results provide a greater understanding of cell permeabilization due to the influence of corona discharge. It therefore forms an important basis for future research on practical applications that would promote the establishment and acceptance of corona discharge as a procedure for molecular delivery to cells.

ACKNOWLEDGEMENTS

I would like to express my gratitude and appreciation to my supervisor, Dr. I E Davidson and to my co-supervisors Dr. L Chetty, Prof. T Govender and Prof. N M Ijumba for their guidance, advice, encouragement and financial support during the course of this study.

I would also like to express my gratitude and appreciation to Dr. R Parboosing from the Virology Department for accommodating me in the laboratory, providing me with the necessary facilities to conduct my experiments and for his expert guidance during the course of the experiments. Thank you also to Gugu and Louis for their assistance in the laboratory and for teaching me the biological protocols and procedures.

I am grateful to the technical staff of electrical engineering and mechanical engineering for their assistance in the design and fabrication of the experimental apparatus.

To my family, thank you for your support, encouragement and immense sacrifice, without which this undertaking would not have been possible.

To God, thank you for always watching over me.

CONTENTS

LIST OF TABLES

LIST OF FIGURES

LIST OF ACRONYMS

DNA:	Deoxyribonucleic Acid
RNA:	Ribonucleic Acid
DFFT:	Discrete Fast Fourier Transform
DC:	Direct Current
FBS:	Fetal Bovine Serum
EMEM:	Eagle's Minimum Essential Medium
DMSO:	Dimethyl Sulfoxide
PBS:	Phosphate Buffered Saline
DAPI:	4',6-Diamidino-2-Phenylindole
PFA:	Paraformaldehyde
RFU:	Relative Fluorescent Units
RPMI:	Roswell Park Memorial Institute
UV:	Ultraviolet
NIH:	National Institutes of Health
AIDS:	Acquired Immunodeficiency Syndrome
NIAID:	National Institute of Allergy and Infectious Diseases
BNC:	Bayonet Neill-Concelman
ATCC:	American Type Culture Collection
CCL:	Continuous Cell Line

CHAPTER 1

Introduction

1.1 Background and Motivation

Molecular delivery to the interior of cells, across the semi-permeable cell membrane, is a well-established and indispensable procedure in the fields of molecular biology, biotechnology and medicine. Foreign molecules like drugs and genetic materials are administered to cells for various therapeutic applications, including the treatment and prevention of diseases.

The cell membrane acts as a barrier to the entry of these foreign molecules and these molecules can only enter the cell when the cell membrane is compromised by an external stimulus [1]. There are various methods of introducing molecules into cells and all methods have their distinct advantages. Each application is different and, therefore, each method can be deemed a preferred choice for a particular application [2].

Often, the success of a drug or gene depends not only on the substance itself but also on the delivery method. Their effectiveness can, therefore, sometimes be enhanced just by improving the delivery method [2]. For the delivery of some of the latest formulations of drugs, new and innovative delivery methods are often required to enhance their potency [2]. New methods of delivery could also enable the use of previously engineered formulations that were ineffective before, simply because of the lack of a suitable delivery method [2]. New delivery methods even allow for the reformulation of existing drugs that could not have been considered previously because of delivery limitations [2]. Continual research into producing variations of existing methods or newer methods of molecular delivery is therefore necessary.

An important facet of drug delivery systems is the advancement in the systems for delivery, which includes research involving multidisciplinary approaches. Considerable research into advanced drug delivery systems is continuing worldwide. The revenue associated with this classification of delivery systems in 2013, for example, was approximately $151.3 billion, and this figure is projected to rise to $173.8 billion in 2018 [3].

Other challenges exist in the effective administration of drugs and genetic material to cells. Firstly, many drugs are unable to pass through the cell membrane and are, therefore, ineffective when introduced into the body [4]. Secondly, pharmaceutical substances are not selective when it comes to affecting cells. For example, drugs intended to kill cancer cells are just as likely to kill healthy cells as well [4]. Therefore, it is often the case that the efficacy of a drug can be enhanced by the method of administration [4].

Cancer is among the leading causes of death in the world and research into finding effective treatments and cures receives high priority [5]. According to the World Health Organisation, in 2012, 14 million new cases of cancer were detected worldwide with approximately 8.2 million people dying from cancer related causes [6].

Two methods of treating cancer that require molecular delivery into cells across the cell membrane, and which have been receiving increasing attention recently, are electro-chemotherapy [7, 8] and gene therapy [9, 10]. Both methods are well established tools in the effort to treat cancer and will continue to be so in the foreseeable future [11].

Electro-chemotherapy has become a reliable and inexpensive method of cancer treatment whilst posing minimal risk to the patient [7]. This procedure is mainly used in Europe where, in 2012, there were more than 100 clinical facilities in 16 countries that offered this form of treatment [12]. In this method of treatment, anti-cancer drugs like bleomycin and cisplatin are administered to cells with the aid of electric pulses [12]. Because these drugs are unable to pass through the cell membrane, the use of electric pulses to permeabilize cells increases its uptake and therefore, its effectiveness [7, 8, 13]. The quantity of drug required is reduced thereby minimising systemic toxicity [8, 13]. This method also has the advantage of being localised and allows for the targeting of a specific treatment area with the correct placement of electrodes [13, 14].

Gene therapy involves the insertion of genetic material into cells with the aim of treating or preventing diseases. It is an accepted option in the treatment of cancer, AIDS, and hepatitis [15]. Many of the currently approved gene therapy protocols worldwide are related to the treatment of cancer [9]. There are different methods of gene transfer. Each method has its advantages which can render it more suitable to a particular application [5]. The methods of gene transfer can be classified into two broad categories, namely viral methods and non-viral methods [16]. Viral vectors are genetically modified viruses which are unable to replicate,

and are commonly used tools to introduce molecules like drugs and nucleic acids into cells [17, 18]. This method has a high efficiency and is effective on a wide range of cell types [17]. This method, however, has some disadvantages. The use of viral methods poses numerous risks to the patient as well as personnel in the general environment [19, 20]. These methods can also trigger an immune response when detected by the body and can also produce carcinogenic effects [17]. Besides viral methods, non-viral methods are also used which include chemical and physical methods. Chemical methods involve the transfer of genetic material by carriers that are formulated chemical compounds [21]. Physical methods include application of electric fields, pressurised vascular delivery, ultrasound, and other less efficient methods like laser, magnetic fields and ballistic delivery [22]. Even though they have a lower transfection rate than viral vectors, these methods have a lower associated risk and have the advantage of being able to transfer larger molecules into cells [18] . Another advantage of non-viral methods is that they do not run the risk of triggering an immune response from the body like viral methods do. Therefore, in cases of long-term gene expression as an example, physical methods might often be the preferred ones [5].

Amongst the various delivery methods is one important physical method called electroporation, which has been used for decades for the transfer of various types of molecules like drugs, DNA, RNA, proteins, and ions into cells [7, 20, 23]. Electroporation is a phenomenon resulting from the application of short electrical pulses, which induces biochemical and physiological changes to a cell membrane and has proven useful in various biological and medical applications [1, 24-27]. It is an accepted and established technique and is still an indispensable procedure today [28, 29]. It is a necessary step in electro-chemotherapy and, for gene therapy, the use of electroporation is increasing. Gene transfection on human subjects using electroporation has been conducted over the last few years and has the possibility of becoming a routine procedure in the future [28]. Because of its safety and efficiency, it is highly probable that this method will develop into one of the main methods of gene transfer [28].

As a result of the wide acceptance of electroporation, research into applications using this method, including electrochemotherapy and gene transfer, are currently receiving wide attention [4, 11]. There are, however, certain disadvantages associated with electroporation. Further investigation into alternative methods of applying electric fields across cell membranes to permeabilize them is therefore warranted.

1.2 Problem Formulation

Even though electroporation is fairly safe there are some drawbacks associated with this method. The traditional method of electroporation requires direct contact of high voltage electrodes and, therefore, fairly high currents are involved. Peak currents of between 0.1A to 3.0A for skin electroporation have been reported [30]. This results in pain, muscle spasm, burning and general discomfort [31-33]. It has also been established that electroporation does cause damage to cells and tissues [34-37].

Alternative methods of molecular delivery using electric fields are, therefore, being investigated, especially non-contact methods such as the use of high voltage plasma. Research into the medical use of plasmas has recently attracted great interest and a new facet of medicine called "*plasma medicine*" has recently emerged [38]. Research into a wide-ranging array of gas plasmas has and is being conducted [39, 40]. Successful cell permeabilization with both plasma [41] and corona ions [42] has been previously demonstrated.

Corona discharge is especially appealing because it is simple to generate and occurs in air at atmospheric condition. Corona discharge is also a non-contact method with the added advantage of having low associated current. Further, conventional electroporation relies on the application of electrodes to the treatment area, in many cases, the surface area to be treated is restricted. The use of corona discharge can allow for greater surface areas to be treated, depending on the design of the corona-producing device. It is anticipated that with on-going research investigations in this field, new devices could be developed for treating large surfaces including limbs or the whole body. For these reasons, the method chosen for further research in our investigation is corona discharge.

For the method of electroporation, the literature shows that the pulse magnitude, pulse width and number of pulses are all significant characteristics that have a bearing on the efficacy of the procedure. Ramachandran et al. [42] theorized that the ions produced by the corona discharge are responsible for the application of electric fields across the cell membrane. In an attempt to draw a parallel between conventional electroporation and corona permeabilization, it is important to note that the corona discharge current is composed of a series of current pulses. In positive corona, positive ions, formed due to electron avalanches, accumulate in the gap and are responsible for the corona pulses [43]. The current pulses,

therefore, are as a result of the creation and movement of the ions that are assumed to be responsible for the application of the electric fields across the cell membrane. Just as the characteristics of the applied pulses play an important role in pore formation in the conventional method of electroporation, it is envisaged that so too would the current pulses in the corona discharge method of cell permeabilization.

This research investigation sets out to analyze the corona current pulses of DC applied voltages and relate these characteristics to the levels of cell permeabilization and cell destruction, as an important contribution to knowledge. The characteristics of the corona pulses analyzed in this investigation include pulse amplitudes, pulse repetition rates, pulse widths, and pulse rise-times. The characteristic frequencies of single pulses, obtained from the application of a discrete fast Fourier transform (DFFT), was also analyzed. An analysis of the corona current pulses and their effect on cell permeabilization and cell destruction is an important step in understanding how corona discharges can be tuned and adapted to specific applications.

Prior to this investigation, it was necessary to firstly establish the experimental variables that affect molecular delivery and cell destruction and, secondly, to establish the optimal values of these parameters that resulted in a high level of permeabilization with minimal cell destruction.

1.3 Research Hypotheses, Research Question and Aims

The hypotheses for this research are:

- Reliable cell permeabilization with minimal cell destruction can be achieved due to the exposure of the cells to corona discharge,
- The levels of cell permeabilization and cell destruction depend on the rate of ionisation and, therefore, the nature of the corona discharge current pulses.

The research questions central to this thesis are:

- What are the characteristics of the corona discharge current pulses that affect both molecular delivery to cells and the associated cell destruction?
- What is the mechanism behind the interaction of the corona discharge with the cell membrane?

Therefore, the aims of this research investigation are:

- To determine the salient variables that would affect cell permeabilization and the associated cell destruction due to the influence of corona discharge,
- To establish the manner in which these variables would affect the levels of cell permeabilization and cell destruction,
- To determine the characteristics of the corona discharge current pulses that affect molecular delivery and cell destruction,
- To establish a theory behind the mechanism of the interaction of the corona discharge with the cell membrane.

1.4 Outline of Thesis

Briefly, the outline of the thesis is as follows.

Chapter 1 provides a background to the research study, presents a motivation for the need for this study, provides a brief outline of the problem area, elucidates the research question, aims and objectives of the study, and outlines the structure of the thesis.

Chapter 2 provides a review of the literature of two of the most important subjects, a thorough understanding of which is necessary for the success of the study, namely electroporation and high voltage DC corona. The detailed analyses of these two subjects were necessary for investigating the merits of corona discharge as an alternative to the conventional method of electroporation.

Chapter 3 provides a detailed description of the design and construction of the experimental apparatus, the different cell lines chosen and the evolution of the techniques, procedures and protocols utilized in this research study. The details of the final experiments, which were conducted using one of the devices and one cell line, are also included.

Chapter 4 provides the results obtained and also presents an analysis and discussion of these results.

Chapter 5 details the conclusions of the research investigation and proposes areas of potential future research.

1.5 Main Contributions of Thesis

The main contributions of this thesis are as follows:

- A multipoint-to-plane atmospheric air corona-generating device was designed and constructed to successfully deliver molecules to cells.
- Successful permeabilization of a mammalian cancer cell line, the HeLa cell, using high voltage DC corona discharge was achieved.
- A new and more accurate method of assessing cell destruction was established using a combination of cell viability (trypan blue assay) and cell lysis (fluorescence of supernatant) measurements.
- Identification and optimization of variables that would result in an acceptable balance between cell permeabilization and cell destruction where permeabilization is maximized and cell destruction is minimized. The identified variables were:
    - Volume of liquid
    - Exposure time to corona discharge
    - Incubation time with SYTOX Green
    - Inter-electrode distance
    - Magnitude of applied voltage
- It was demonstrated that higher applied voltages resulted in an increase in permeabilization with an increase in cell destruction.
- For the constructed corona-generating instrument, it was established that of all the pulse characteristics investigated, only the average corona discharge pulse repetition rate was found to have an appreciable effect on cell permeabilization and cell destruction.
- A theory for the mechanism of DC corona electroporation is proposed.

1.6 Publications Emanating from or Related to this Study

1.5.1 **N. K. Chetty** and L. Chetty, "A Review of Factors that Affect Corona Electroporation of In-vitro Samples in a High-voltage Point-plane Gap Test Apparatus", South African Universities Power Engineering Conference, Potchefstroom, South Africa, Pp. 44-50, 31 January and 1 February 2013.

1.5.2 L. Chetty, N. M. Ijumba, **N. K. Chetty**, Y. Singh and K. G. Ilunga, "Evaluating the Effect of Paint Coatings on the Corona Performance of Conductor Surfaces", 18th

International Symposium on High Voltage Engineering, Hanyang University, Seoul, Korea, 25 August – 30 August 2013.

1.5.3 **N. K. Chetty**, L. Chonco, N. M. Ijumba, L. Chetty, I. E. Davidson, T. Govender, and R. Parboosing, "Factors Affecting the Permeabilization and Destruction of HeLa Cells by Corona Discharge", (Submitted for review, IEEE Transactions on Plasma Science, 2015)

1.5.3 **N. K. Chetty**, L. Chonco, N. M. Ijumba, L. Chetty, I. E. Davidson, T. Govender, and R. Parboosing, "Analysis of Current Pulses in HeLa-Cell Permeabilization Due to High Voltage DC Corona Discharge" (Submitted for review, IEEE Transactions on Nanobioscience, 2015)

CHAPTER 2

Literature Review

2.1 Introduction

In Chapter 1, the high prevalence of cancer and its major contribution to the mortality rate worldwide was highlighted. The critical and urgent need for newer and more effective methods of treatment cannot be overstated.

It was established that corona discharge could prove to be a viable alternative to the conventional form of electroporation for the applications of electro-chemotherapy and gene therapy, two effective and approved protocols for the treatment of cancer. In order to facilitate the establishment of corona discharge as an accepted method, a deeper understanding of how corona discharge could facilitate the transfer of molecules into cells is mandatory. In order to do this, a detailed investigation of the two concepts of electroporation and high voltage corona discharge was conducted. Electroporation is an established procedure and the lessons learned from decades of research could be utilized to understand and optimize DC corona electroporation as a tool for permeabilizing cells. Electroporation is an electric field dependent phenomenon and so too is corona discharge induced molecular delivery. Understanding the phenomena of electroporation and corona discharge would assist in understanding the concept of DC corona electroporation.

The choice of corona discharge, which is a form of plasma, as a viable alternative is further enhanced by the fact that research on plasma discharges in the fields of biology and medicine is fast gaining momentum. In fact, this field has been receiving so much attention recently that a new facet of medicine, termed "*plasma medicine*", has emerged [38].

2.2 Plasma Medicine

Non-equilibrium atmospheric pressure discharges have many important applications especially in the fields of the environment, biology and medicine [38, 44]. Plasmas are used in many applications due to their effectiveness in killing bacteria and their ability to penetrate areas that are difficult to access [40]. The advantage of using plasmas is that they are effective on rough surfaces and can also access small gaps and openings [45].

Low temperature plasmas at atmospheric pressure are used directly in medicine for various medical treatments [38-40, 44, 45]. Direct medical applications of plasmas includes wound healing, blood coagulation, homeostasis, cancer treatment, dentistry, fungal eradication, treatment of skin infections, transfer of genetic material into cells, bacterial inactivation and cosmetic surgery [38-40, 45]. Indirect applications of plasma in the medical field primarily include sterilization and decontamination [40, 45].

The interaction of plasmas with living systems is varied due to the complex and diverse biological characteristics of these systems and, therefore, invoke complicated responses from cells [38]. However, it has been shown that the basic and initial interaction with the living systems is with the cell membrane and once this initial interaction occurs, other mechanisms, like biological responses occur [38]. For molecular delivery, the interaction of the plasma with the cell membrane is critical, since the cell membrane is the point of entry of the molecules. The active species generated by the plasma include ions, electrons, excited atoms, reactive gases, radicals, atoms, molecules and ultraviolet radiation [40, 44, 45]. Of all these species produced in the plasma, it has been shown that the ions play a major role in the interaction of plasmas with cell membranes [38]. The exact mechanism of the interaction of the ions with the cell membrane is unknown, however, some theories have been proposed. Dobrynin et al. [38] proposed that the effect of the interaction is chemical in nature. The ions, both positive and negative, are responsible for peroxidation of the phospholipid layer in eukaryote cells and the polysaccharide layer of prokaryote cells [38]. Ramachandran et al. [46] also showed that ions are responsible for the interaction with the cell membrane by permeabilizing cell membranes using corona ions. However, a different mechanism to that proposed by Dobrynin et al. [38] is afforded. He showed, by using a dye called Di-8-ANEPPS, that a change in the intrinsic transmembrane potential as well as the compactness of the lipids in membrane occurs due to the influence of corona ions [46]. From this observation, we are therefore inclined to agree with the theory proposed by Ramachandran, which is similar to the theory that is accepted for the conventional form of electroporation. In this case, the ions are responsible for charging the cell membrane and resulting in the formation of pores.

Even though the ions are considered the most important for interaction with the cell, the other elements produced by the plasma, whether they contribute to cell permeabilization, cell destruction or both, cannot be discounted. Therefore, in our investigation, we have used the complete discharge as compared to just the corona ions as used by Ramachandran et al. [42].

This is an important distinction since, as has been pointed out, the discharge has many other constituents which might also have an interaction with the cell and the cell membranes.

2.3 Biological and Medical Applications of Corona Discharge

The biggest attraction of using corona discharge over plasma jets is that the corona discharge is very simple to produce and operates in air at atmospheric conditions. Corona discharges also, can be produced to extend over a much larger surface area than plasmas, hence enabling larger treatment areas. For these reasons, further investigation into cell permeabilization using corona discharges is warranted.

Corona discharge has already been adopted in many direct and indirect applications in the medical and biological fields. It has been used successfully in applications like bacterial decontamination of water [47], sterilization of water [48], inactivation of surface bacteria [49], destruction of dust mites and cat allergens [50] and electroporation of cell membranes in the wine-making industry [51]. With ongoing research, this phenomenon has the potential of being utilised for further applications in the medical field.

For these corona discharge applications, various theories on the interaction of the corona discharge on living systems are proposed. For the decontamination of water, the anti-bacterial effect was attributed to the charged particles and chemically-active species in the discharge, like radicals. A greater concentration of peroxides was found with greater number of corona discharges [47]. For the sterilization of water, it was proposed that the ions produced by the corona discharge react with water to produce ozone, hydrogen peroxide and hydroxyls. Together with UV light, it was thought that these chemical substances are able to kill the organisms in the water [48]. For surface inactivation of bacteria, it was proposed that the ions produced by the corona discharge result in the peroxidation of bacterial membrane by increasing the transport rate of the peroxide species [49]. For the destruction of dust mites, the interaction of the corona discharge with the allergens has been likened to the process that occurs during surface treatment of polymers in industrial applications. Some of the bonds found in polymers are similar to those found in proteins. These bonds are broken by the species found in the corona discharge [50]. In the wine-making industry, it was assumed that the process is similar to that of conventional electroporation in which pores are formed in the membrane due to polarisation with the applied, external electric field [51]. However, just as was discussed in 2.2, the initial interaction involves charging of the cell

membrane, and this phenomenon is of interest to our investigation on molecular delivery to cells.

2.4 Corona Applications of Cell Permeabilization

For the cancer treatment options of electro-chemotherapy and gene therapy, the widespread use and importance of electroporation has already been highlighted. Because of the disadvantages presented by the conventional method of electroporation such as pain, burning, muscle spasms and cell and tissue damage, and because of the importance for research into innovative drug delivery methods to enhance the effectiveness of drug formulations, other methods of molecular delivery are, therefore, being researched such as the use of high voltage plasma and high voltage corona discharge. Successful cell permeabilization with plasma discharge [41] and corona ions [42] have been previously demonstrated and these methods are non-contact, with low associated current [42].

In our research, the alternative method of corona discharge is proposed. It is anticipated that devices generating corona discharge can be refined and optimized to reliably permeabilize cells. The benefit of using corona discharge would be twofold. Firstly, it would result in the minimization of the harmful effects that are experienced with conventional electroporation. Secondly, it could provide an opportunity for the treatment of larger surface areas.

2.5 Electroporation

2.5.1 Definition and Overview of Electroporation

Electroporation is a phenomenon resulting from the application of high-voltage pulses, which induces biochemical and physiological modifications to a cell membrane and has proven useful in various biological and medical applications [1, 24-26]. It is a universal cell membrane phenomenon in that it is found to occur in all cell membranes [1]. This phenomenon has been observed in various types of cells with the only common molecular structure being the lipid bilayer. It is, therefore, assumed that the electroporation mechanism occurs in the lipid bilayer [52]. The exact mechanism of electroporation is still not completely understood. However, it is widely accepted that the essence of electroporation is the formation of water-filled pores in the membrane [25, 52-55]. These pores allow molecules, which are normally impermeable to cells, to transgress the cell membrane [1, 25,

52, 56]. Once the electrical pulses cease, the cell membrane has a high probability of reconstituting, whereby the pores diminish in size and eventually disappear until the cell regains its normal physiological characteristics and function [1, 25, 56-59].

According to J. C. Weaver [24], the requirements for and processes that occur during electroporation are:

- The application of electrical pulses of a short duration,
- The charging of the cell membrane by the applied pulse,
- The rearrangement of the constituents of the cell membrane under the influence of the electric field,
- The formation of aqueous pores in the membrane,
- The resultant increase in the movement of ions and molecules into and out of the cell.

2.5.2 The Importance of Electroporation

Electroporation has numerous applications in the fields of molecular biology, biotechnology and medicine, which include the destruction of bacteria and yeasts [60, 61], electro-insertion of macromolecules like proteins into the cell membrane [62], transdermal molecular delivery [63], gene transfection in plants [64-66], gene transfection in animals [67-74] and electro-chemotherapy [7, 13, 75-80]. In almost all applications, the standard method of the application of high voltage DC electric pulses to alter the structure of the membrane was used. Only Zheng et al. [74] used a pulsed radio-frequency electric field, however, the principle is identical in all cases.

Despite the existence of several other technologies, electroporation is still widely accepted because of its numerous advantages, such as: it retains a favourable cell viability; is a relatively simple and easily reproducible procedure; and it results in high molecular transport [81]. The importance of electroporation can further be highlighted by the fact that in cellular gene transfer as an example, since the first demonstration by Neumann et al. [67], electroporation has become one of the most common methods of gene transfer [53, 81]. In some cases, it is the only method that is successful [53]. One of the most common applications of electroporation, and the focus of study in this research investigation, is molecular delivery to cells.

Figure 2.1 illustrates the movement of molecules into the cell during the process of electroporation. Figure 2.1 (a) shows the cell before electroporation surrounded by molecules that are unable to penetrate the lipid bilayer membrane. Figure 2.1 (b) shows the cell after electroporation with the fluorescent molecules already gaining entry into the cell through the hydrophilic pores. The membrane reconstitutes itself after the process has ended [24].

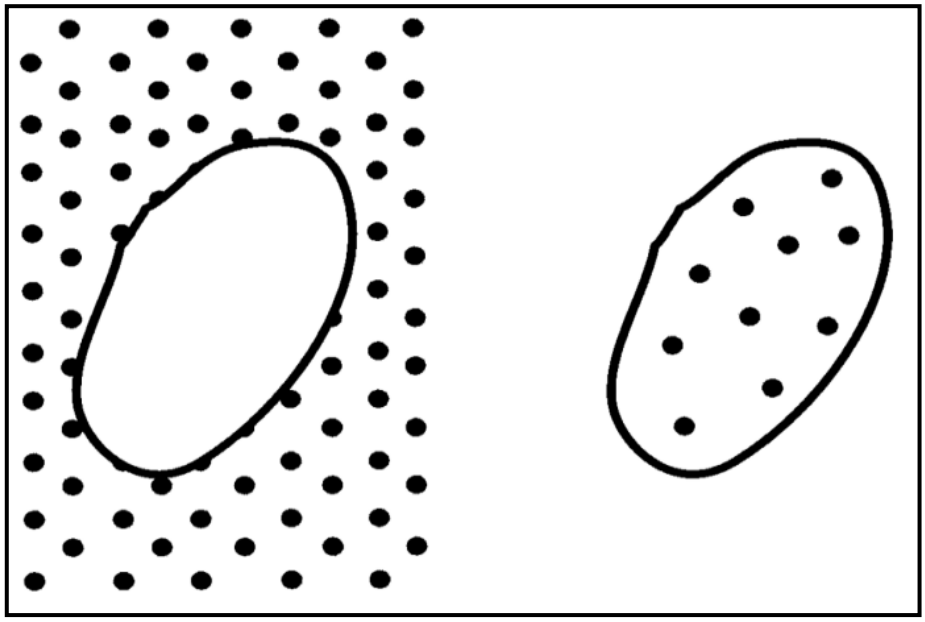

(a) (b)

Figure 2.1: Illustration showing inclusion of fluorescent molecules into the cell [24]

2.5.3 Structure of the Cell Membrane

In order to study alternate or refined methods of electropermeabilization, it is important to first understand the mechanism of the interaction of electric fields with the cell membrane. To achieve this, a fundamental understanding of the structure of the cell membrane is necessary.

All biological cells are surrounded by a cell membrane which is made up of two layers of phospholipid molecules and is therefore termed a lipid bilayer membrane [25, 82]. Protein molecules are also embedded in this membrane [52, 83, 84]. A cell membrane is extremely thin, in the region of 5 to 6 nm [52, 82-84]. The structure of a lipid molecule is shown in figure 2.2: [52]

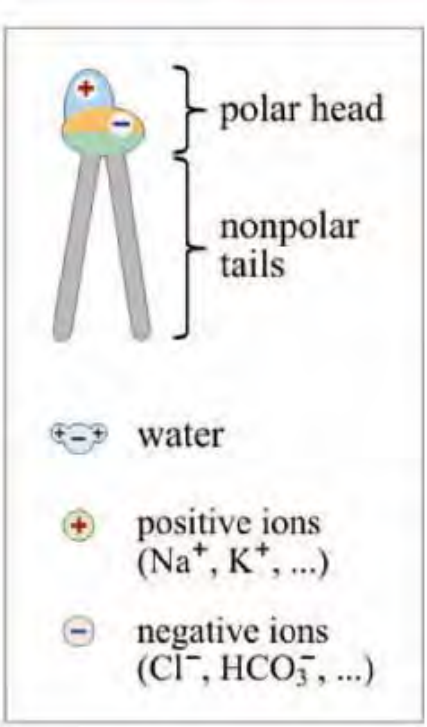

Figure 2.2: Illustration of a single lipid molecule [52]

Each lipid molecule has a polar and a non-polar part. The polar head is hydrophilic while the nonpolar tail is hydrophobic [85]. Because of the characteristics and features of the lipid molecules, they arrange themselves to form a structure consisting of two layers as illustrated in figure 2.3 [52]. The tails of the molecules come together while the polar heads face outwards. This results in the formation of a hydrophobic region within the membrane [52, 82]. The lipid bilayer is very stable and, because the interior of the bilayer is non-polar, polar molecules on either side of the membrane are unable to penetrate it [52].

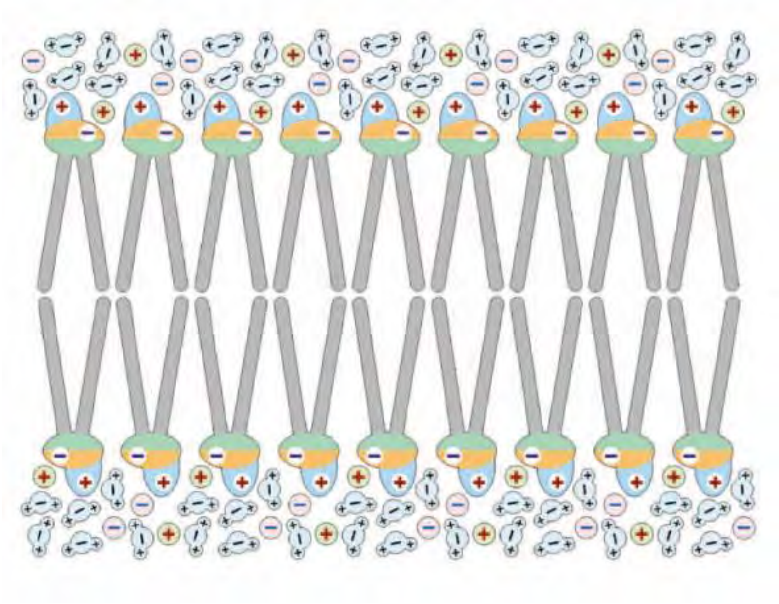

Figure 2.3: Orientation of lipid molecules to form the bilayer lipid membrane [52]

Aqueous electrolyte solutions are found on other side of the cell membrane [52] and the membrane acts as a barrier against the movement of many ions and hydrophilic molecules into and out of cells [25]. The membrane, however, is not totally impermeable since the survival and functioning of a cell depends on the movement of certain substances into and out of the cell. The membrane is therefore semi-permeable and this is made possible by the existence of proteins embedded in the membrane [52, 84]. These proteins can facilitate the movement of certain molecules into and out of the cell across the cell membrane [52]. They allow water and certain single atom ions to pass through [52, 82, 84].

2.5.4 Mechanism of Electroporation

2.5.4.1 Transmembrane Voltage

A unique characteristic of living cells is a naturally occurring transmembrane potential [86]. This potential exists because of the different type and concentration of ions on either side of the membrane resulting in a difference in potential between the inside and the outside of the cell [86, 87]. It has been established that, in most living cells, this intrinsic or natural transmembrane potential is approximately between 60 mV and 100 mV [1, 26, 55, 83, 88].

Electroporation can occur when an electric field is produced across the membranes due to the application of external voltages [25, 26, 52, 53, 55, 89]. When these electric fields are of

a sufficient magnitude and are applied for an adequate period of time, a redistribution of charge results [84]. Thus, a greater transmembrane voltage is induced over and above the intrinsic one [84]. When the transmembrane voltage exceeds a few hundred mV, the membrane structure begins to change and pathways begin to form [8]. In essence, permeability of the cell membrane is as a result of an increase in the transmembrane potential to a particular critical value [87]. When this critical value is reached, pores, which can be described as aqueous pathways, are formed in the membrane [1, 25]. These pathways result in an increase in the conductivity and permeability of the cell membrane [55]. Therefore, molecules are able to move within these pathways into and out of the cell. This rearrangement of the cell membrane due to the applied electric field is termed electroporation and the resultant movement of molecules into the cell is termed electropermeabilization [84].

2.5.4.2 Dielectric Breakdown of the Cell Membrane

Due to its properties, the cell membrane can be classified as an insulator [52]. Therefore, during the initial stages of research into electroporation, the phenomenon was found to be similar to dielectric breakdown, in the form of increased current flow, and has been observed in experiments with various cells [58, 59, 90]. It is often referred to as reversible, electrical breakdown of bilayer lipid membranes [25, 26, 52, 53]. In other words, breakdown of the cell membrane occurs when the electric field applied across the cell membrane is greater than the dielectric strength of the membrane [25, 55]. When this occurs, the electrical conductivity and permeability of the cell membrane has been observed to increase drastically [1, 25, 52, 55]. This breakdown was initially referred to as the "*punch-through*" effect [58].

Dielectric breakdown of the cell membranes occurs at a critical value of the transmembrane potential [59]. Once the critical value is reached, an increase over and above this value does not occur since an ionic current begins to flow through the pores and this prevents further increase in the membrane potential [88]. When pore formation occurs, the potential decreases slightly due to the ionic current that subsequently flows through the pores [88]. When the applied pulse ends, the membrane discharges within microseconds [1] and resealing of the membrane begins to occur [25].

Subsequent research showed that when pores are formed, charged molecules and ions are transported into and out of the cell. Because of the theory of pore formation, the sudden

increase in the conductivity of the cell membrane is actually due to the movement of charged molecules through the membrane and not due to dielectric breakdown. Therefore, the term dielectric breakdown commonly used in the earlier stages of research into electroporation might actually not be an appropriate term to describe cell membrane electroporation [24].

Cell membranes can withstand a trans-membrane potential of up to 1 V when short pulses of microseconds to milliseconds are applied [25]. For electric field strength measurements, it has been observed that, for various membranes, electric fields of between 133 V/cm to 2.5 kV/cm resulted in electroporation [1, 25, 88, 89, 91].

Corona discharge current pulses are in the nanosecond range and, therefore, would not result in prolonged application of the electric field. These short pulses would be tolerated by cell membranes and therefore, this fact alludes to corona discharge as being a potential alternative to conventional electroporation.

2.5.4.3 Pore Formation

The exact mechanism of electroporation is not known, however, the theory of aqueous pore formation is what is generally accepted to explain the phenomenon [52]. This theory is also consistent with the findings of many experimental observations made previously [82].

Pore formation in the membrane due to an electrical impulse is as a result of the influence of the impulse on the charges and dipoles of the membrane constituents [67]. The electric field increases dipole moments in the direction of the field and causes small changes in the position of the charges and dipoles [67]. This causes rearrangement of the lipid molecules which results in the formation of pores in the membrane [67]. A polarisation mechanism is therefore assumed to be responsible for the change in permeability of the membrane [92].
There are different stages to pore formation. Firstly, small hydrophobic pores are formed which have a short life-span. When the radius of these pores exceeds a certain value, the edges of the pores become inverted and the pores are transformed into hydrophilic pores [85]. Because of the formation of these hydrophilic pores, the membrane becomes conductive [85]. The formation of hydrophobic pores is merely a short-lived step towards the formation of hydrophilic ones [85].

Figure 2.4 illustrates the change in structure of the cell membrane during electroporation.

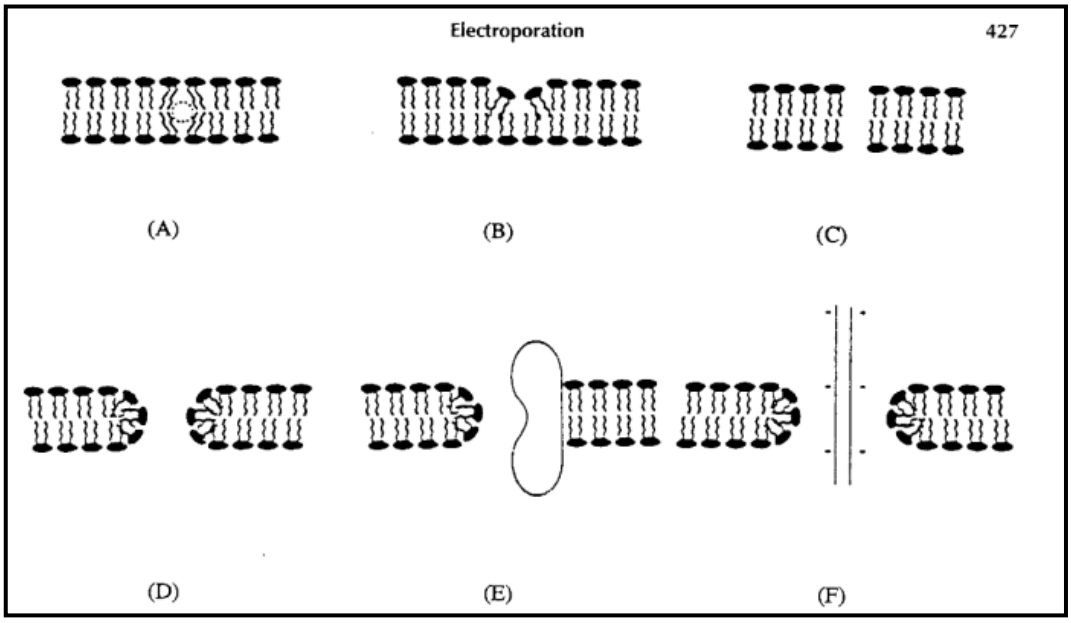

Figure 2.4: Illustration of the rearrangement of the lipid bilayer membrane [1]

The following is an explanation of the steps shown in figure 2.4:

A. Existing holes through which molecules can move into and out of a cell during normal cellular operation,
B. Compression of the membrane occurs and a depression is formed,
C. A hydrophobic pore is formed,
D. A hydrophilic pore is formed through which molecules can pass,
E. A protein channel that enables the insertion of a protein molecule into the cell membrane,
F. When transmembrane voltages are high enough, even long, charged molecules are able to enter through the hydrophilic pores.

The number of pores, the mean size and the level of conductivity of the pores all depend on the resultant membrane voltage [85]. The membrane voltage depends on various factors such as: the ionic strength of the medium, the magnitude of the applied potential and the pulse length of the applied potential [89]. This again reinforces the need for research into how corona discharge interacts with cell membranes since corona discharge current is in the form of pulses.

Since the size and number of pores depend on the nature of the pulses, it is therefore important to analyse the nature of the corona pulses.

The size of pores range from 1 nm to sizes a few times larger than this and it is impossible to physically observe them [1]. The pores are created in a very short space of time, in the region of 10^{-6} s [24]. The pores formed, however, can have a relatively long lifespan and can exist long after the membrane discharges [1, 24, 85, 93]. It takes between 1 to 10 milliseconds for the mean radius of the pores to decrease to 0.5 nm [85] and these pores have been found to exist for more than 1 s [24]. It has been shown that plasmid DNA uptake can continue for up to 10 minutes after the electric pulses have been applied [67].

A sharp reduction in conductivity does occur within a few milliseconds after application of the pulse [85]. However, this was not attributed to the disappearance of the pores since the number of pores was found to remain approximately the same [85]. It was, therefore, concluded that this reduction in conductivity was as a result of the decrease in the pore size [52, 85]. Therefore, it can be concluded that molecules of smaller diameter can still enter cells a while after the electric pulse has been removed.

This has important implications for molecular delivery due to corona discharge since it provides an indication of the window that is available after application of the corona discharge and before the membrane reseals. Firstly, molecules that need to be delivered to cells can be added after the application of corona discharge so that the discharge does not have an opportunity to denature the molecules. Further, the size of molecules differs and for DNA transfection, for example, genetic material is often relatively large and larger pores are required for successful delivery. Therefore, the correct time for the introduction of these molecules is important.

2.5.4.4 Membrane Recovery

The major advantage of electropermeabilization is that, because of the nature of the cell membrane, it can return to its original state in a fairly short space of time after removal of the electric field often with no observable adverse effects remaining [26, 52, 55, 94]. Once the applied voltage ceases, the cell enters the recovery phase where the pores diminish and eventually disappear [1, 52]. However, one must be cautious as its return to normal is not

guaranteed since, if the exposure is too high and/or too long, the cell constituents or the cell as a whole can be permanently damaged [25, 55, 94].

Therefore, since the nature of the applied electric fields affects cell destruction, during experimentation, it is important to monitor the effect of the pulse widths, rise-times, amplitudes and repetition rates on cell destruction.

2.5.4.5 Cell Stress and Death

Another important consideration of electroporation is cell survival and recovery [1]. Cell death can occur in various ways. One way is cell membrane rupture or irreversible breakdown which causes destruction of the cell [26]. This may occur when too high voltages are applied for relatively long periods of time after which the membrane reaches a point of no return [26]. The second is chemical imbalance of the cells due to movement of molecules into and out of the cells during the electroporation process [54]. This disrupts the normal physiological nature and functioning of the cell [1]. The third cause of cell death is cell lysis. It has been speculated that cell lysis is due to "*the colloidal osmotic pressure of the cytoplasmic macromolecules*" [25]. Cells can therefore die due to irreversible breakdown, chemical imbalance or because of colloidal osmotic pressure.

In assessing the effectiveness of corona electroporation, therefore, it is important to test any adverse effects by measuring both cell viability and cell lysis after the procedure. Testing merely the viability of cells is usually common practice as has also been done by Ramachandran et al. [42] and Connolly et al. [41].

2.5.4.6 Effect of Pulses

For the method of electroporation, the required electric fields are applied briefly, in the form of microseconds to milliseconds pulses [53]. The pulse magnitude, pulse width and number of pulses are all factors that impact on the effectiveness of the procedure. Previous investigations have indicated that pulse width [1, 26, 56, 57, 93, 95], pulse magnitude [27, 56, 62, 95] and the number of pulses [27, 95] all have an effect on permeabilization and cell destruction. For example: Shorter pulses ensure that membranes are not destroyed [26] and therefore ensure lower cell destruction. Longer pulses are required when larger molecules are introduced into cells [56]. Greater magnitude of the pulses increases permeabilization [95]

and allows for larger molecules to enter cells [95], however, cell viability may be compromised [27, 95]. A larger number of pulses ensures a greater rate of permeabilization [95]. In all cases, larger pulse widths, higher pulse magnitudes and a greater number of pulses increased the level of cell permeabilization and/or the level of cell destruction.

These findings regarding the nature of the applied voltage pulses provide a basis for research into the nature of the corona discharge and its influence on the rate of electroporation and cell destruction. Research involving molecular delivery to cells using corona discharge is very limited. According to our knowledge, no investigation has previously been conducted before on the characteristics of the corona discharge pulses and its effect on molecular delivery and cell destruction. Corona discharge occurs in the form of current pulses and, therefore, the findings of the characteristics of the applied pulses in conventional electroporation form a platform for initial investigations into corona electroporation.

2.6 High Voltage Plasma and Corona Discharge

2.6.1 Background to and Definition of Plasma

A plasma may be defined as "*a quasi-neutral gas of charged and neutral particles which exhibits collective behaviour*" [96]. Even though local concentrations of charges form within a plasma, they are shielded out within a short distance. Most of the plasma itself, therefore, does not have fields and potentials, and as a whole, the plasma is neutral. This behaviour is termed quasi-neutrality [96]. The quasi-neutrality of a plasma can be explained as follows [96]. A plasma has charged particles that are in motion. Particles of like charge can concentrate in a region and, therefore, there are regions of positive and negative charge within the plasma. These positive and negative regions result in the formation of electric fields within the plasma. Charged particles also move around and, as a result, generate currents which result in the formation of magnetic fields. Thus, we have electric and magnetic fields within the plasma. These electric and magnetic fields affect charged particles elsewhere in the plasma, even particles that are relatively far away. Therefore, the motion of particles depends, not only on the state of the conditions close by, but also depends on conditions further away. This is what is referred to as collective behaviour [96].

Another important characteristic of a plasma is its temperature. The temperature of a plasma is usually referred to in terms of energy, since there is a close relationship between the

temperature (T) and the average energy (E_{av}). It has, therefore, become common in plasma physics to refer to the temperature of the plasma in terms of energy [96]. The relationship between T and E_{av} is shown in the equations 2.1 and 2.2 for 1-D and 3-D plasmas.

The average kinetic energy of a 1-dimensional plasma is given by (2.1) [96].

$$E_{av} = \frac{1}{2}KT \qquad (2.1)$$

If extended to 3 dimensions, we have the relationship shown in equation (2.2) [96].

$$E_{av} = \frac{3}{2}KT \qquad (2.2)$$

Thus, there is a close relationship between T and E_{av}.

A brief discussion on the temperature of a plasma is as follows [39]. In a plasma, energy is transferred to electrons much faster than to the ions, which are larger and heavier. The temperature of the electrons will therefore increase much faster than the surrounding environment [39]. In a non-thermal plasma, the ions and neutral molecules lose heat much faster than the electrons. The gas therefore remains at low temperature. Non-thermal plasmas are also called non-equilibrium plasmas. In a thermal plasma, however, the temperature of the ions and neutral molecules and also the electrons are the same [39].

This is an important characteristic of a plasma since, for biological and medical applications, the temperature of the plasma cannot be too high so as to cause any adverse effects to cells and tissues. The suitable types of plasma are referred to as cold plasma. Corona discharge is classified as a cold plasma.

Plasmas do have a very low conductivity, and this small conductivity results in the existence of a very small electric current between two electrodes in a gas [97]. This current is conducted by charged particles or ions that move towards the electrodes under the influence of the electric field [97].

2.6.2 Corona Discharge

Corona discharge is a type of non-thermal plasma and is a partial gas discharge which occurs at or close to atmospheric conditions [98]. It is caused by the electric field concentrated at points of high electrical stress on high voltage electrodes [98-100]. When a sufficiently high voltage is applied to an electrode, a concentration of the electric field occurs at sharp edges, which ionizes the gas close to these regions [98]. If the gradient of the electric field is not high enough to cause arcing to the ground plane, the discharge is self-contained and is referred to as a corona discharge [98].

Ambient air is a good insulator and when it does reach the point of breakdown, it has the ability to return to its original state [100]. Due to the insulating properties of air, when a voltage is applied across it, only a very small current flows. As the applied voltage increases, so too does the current flowing between the electrode, until, at a sufficiently high voltage, electric breakdown occurs. At this point, a spark produced between the electrodes results in a short circuit between the electrodes [100, 101].

Breakdown of air occurs due to ionisation as a result of collisions [100]. Ionisation is when neutral atoms or molecules give rise to electrons and ions. Corona results in the formation of both positive and negative ions. The ions that are of opposite polarity to the stressed electrode are attracted to the electrode and neutralised by it [102]. Therefore, for positive applied voltage, the ions present are positive and for negative applied voltage, the ions are negative [102].

Corona discharges have been successfully used in many biological applications but one important application of corona discharge ions that has recently been attempted in the bio-medical field is molecular delivery to cells [42]. The phenomenon of corona discharge has the potential of gaining importance in applications like genetic engineering and drug delivery [103] and this further enhances the value of our research into corona discharge.

2.6.3 Theory of Corona Discharge

2.6.3.1 Triggering Electrons

For corona discharge to occur, one of the most basic conditions is the presence of free electrons which are accelerated by the electric field and can ionise gas molecules due to collisions [100].

2.6.3.2 Electron Avalanches

Avalanches, which are started by an electron, result in corona discharges. The process for the formation of an electron avalanche is as follows [100]. The free electrons that exist are accelerated by the electric field and collide with other molecules that exist in the region. If sufficient energy is imparted to the molecule, it results in ionisation of the molecule due to the expulsion of an electron. The original electron and the newly ejected electron are once again accelerated by the electric field resulting in further collisions with other molecules and further liberation of electrons. This process results in the formation of a large concentration of electrons and positive ions, resulting in an electron avalanche [100]. In both positive and negative corona, the current pulses are as a result of successive electron avalanches [100] An illustration of the electron avalanche is shown in figure 2.5.

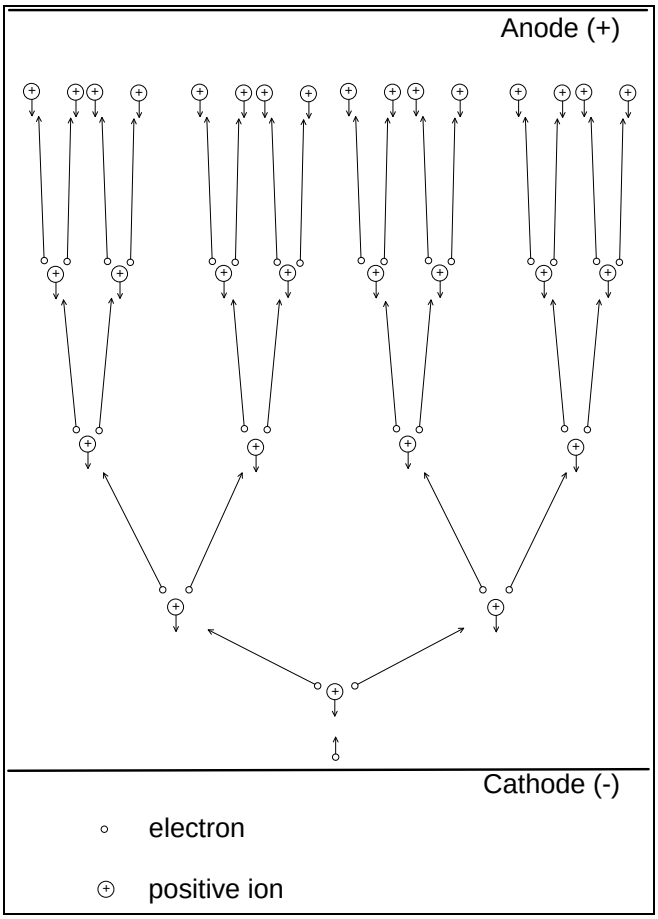

Figure 2.5: Illustration of the formation of an electron avalanche

The area close to the electrode is the area in which the charged particles are produced. The electric current that flows to the opposite electrode is determined by the drifting charged particles in the low electric field region that is outside this active corona region [104]. The drifting particles in positive corona are positive ions and either negative ions or electrons for the case of negative corona. The space charge formed by these drifting charged particles opposes the current formed by the same drifting charged particles [104]. It, therefore, follows that the movement of the dominant charged particles in the region outside the active corona is responsible for the corona discharge current [104].

The unique characteristic of a corona discharge is the drift region that connects the electrode at which the ionisation occurs to the passive electrode [105]. The species that are found in the drift region of unipolar coronas is the same polarity as the applied voltage [105]. The ions found in this drift region are what are presumed to be directly responsible for cell permeabilization and, therefore, the experimental apparatus was constructed in such a way that the cell sample could be placed within the drift region to take maximum advantage of

the effect of the ions. Figure 2.6 is an illustration of the regions within a corona discharge between two electrodes. In our apparatus, the cell sample is placed on the plane electrode so that the cells experience maximum exposure to the ions.

This is in contrast to the device constructed by Ramachandran et al. [42], in which the cell sample was placed beyond the ground electrode and the drifting ions are presumed to be the species that result in pore formation in the membrane.

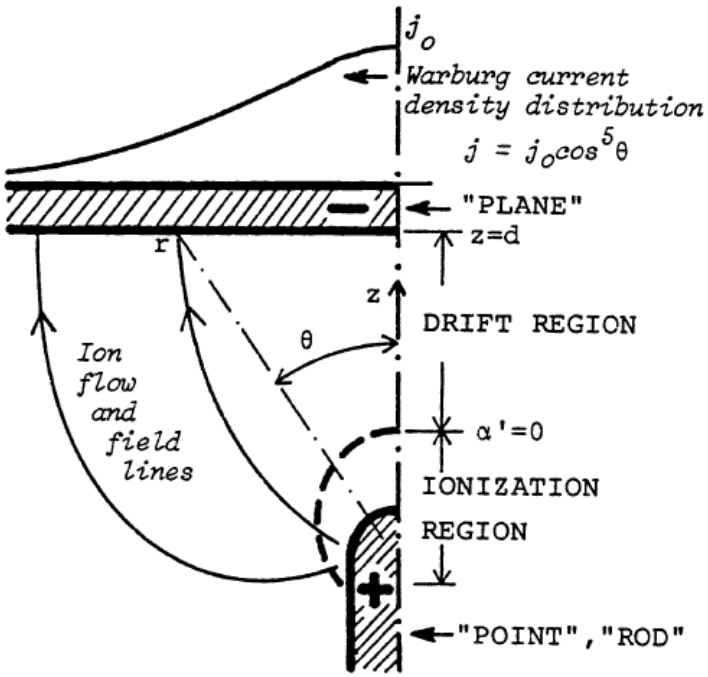

Figure 2.6: Illustration of the corona-discharge regions of a point-to-plane geometry [105]

2.6.3.3 Ionisation Processes

Ionisation is one of the fundamental processes involved in corona discharge. The ions produced are a requirement for the interaction of a plasma with the cell membrane [38]. There are various ways in which charged particles i.e. ions and electrons are produced in a gas either through ionization or electron emission [106]. When an atom or molecule absorbs sufficient energy, it allows for the liberation of an electron from this atom or molecule. As a result, an electron and a positive ion result. This process is called ionisation [106]. The release of an electron from a solid, however, is called electron emission. Electron emission is an important process in the production of charged particles in gas discharges and occurs mostly at the electrodes [106].

There are various ionisation processes and these can be classified as due to collisions, photo-ionisation and secondary ionisation [101].

2.6.4 Types of DC Corona

There are two types of DC corona that can occur in air.

- The first type of DC corona is unipolar conduction corona and is also referred to as positive glow coronas, negative Trichel pulse corona or negative glow coronas. In these types of corona discharge, the region of ionisation occurs in close proximity to the electrode to which the voltage is applied. This discharge is characterised by short pulses with a high repetition rate. The polarity of the active ions is of the same polarity as the applied voltage [105].

- The second type of corona discharge is bipolar or streamer corona discharge. This type of discharge occurs when currents between the point and plane electrodes are higher and is more prevalent when the point electrode is of positive polarity. In this case, a plasma is produced at a faster rate at which it can be taken up by the point electrode which results in the growth of a narrow plasma region of some 30 pm in diameter. This plasma region begins extending from the point electrode towards the ground electrode. The ionisation region that produces the plasma is positioned at the end of this plasma filament [105].

2.7 Conclusion

A review of the literature showed that limited research was conducted previously on molecular delivery to cells using corona discharge. To conduct our investigation, lessons therefore had to be drawn from the conventional form of electroporation which has been researched over decades. A detailed review of electroporation is therefore provided. To extract the relevant information from this review that would pertain to corona discharge, a review of corona discharge, with a focus on ionisation and the various forms of the discharge was conducted. The review of these two subjects therefore allowed us to obtain a clearer understanding of which characteristics of the corona discharge are relevant to cell permeabilization. This, therefore, provided clearer direction to our research investigation.

CHAPTER 3

Materials and Methods

3.1 Introduction

Three different configurations of corona-generating devices were designed and/or constructed and three different cell lines were chosen for this investigation on cell permeabilization. The equipment, electrical circuits, reagents, standard protocols, experimental method, and methods of analysis of the results are provided in detail in this chapter.

3.2 Cell Lines and Cell Culture

Three different cell lines were chosen from an existing stock of cell lines available at the virology department. Because the effects of corona discharge on different cell types was unknown at the beginning of this investigation, it was decided to try two cell lines of human origin and one of animal origin. Further, it was decided that one of the human cell lines will be a cancer cell since the investigation of permeabilization of cells is intended mainly for cancer research. For these reasons, the HeLa, MT4 and Vero cells were chosen for further experimentation. The HeLa and Vero cell lines are adherent cells while the MT4 cells are suspended cells.

These three cell lines provided sufficient variety for experiments.

3.2.1 HeLa Cells

The HeLa CD4-clone cell line is an immortalized human cell line obtained from cervical cancer tissue. Cells were grown in cell culture flasks for adherent cells (NUNC, 75 cm^2) with 90 % RPMI-1640 and 10 % Fetal Bovine Serum (FBS) and incubated at 37 °C with 5 % CO_2. Cells were fully confluent in flasks after 3 to 4 days at which point some of the cells were transferred to a new flask to continue propagation and some of the cells were seeded onto petri dishes in preparation for experiments.

HeLa cell maintenance required the following steps. The flask containing the HeLa cell culture was washed three times with 5 ml phosphate buffered saline (PBS). 2 ml of trypsin was added to the flask which was then incubated for ten minutes. After this time the flask was tapped gently to dislodge the cells. 5 ml growth medium (4.5 ml RPMI and 0.5 ml FBS) was added to the flask to counteract the action of trypsin. The cell suspension was pipetted up and down gently to break up any clumps. The concentration and viability of the cells was measured using the trypan blue assay. The required volume of cells was transferred to a new flask to which 16.2 ml RPMI and 1.8 ml FBS were already added. The quantity of cells transferred was 3.5 million cells for confluence after 3 days and 2.8 million cells for confluence after 4 days. The new flask was labelled and placed in the incubator.

Seeding of HeLa cells onto petri dishes for experiments required the following procedure. Cells were seeded in different concentrations to enable the availability of fully confluent petri dishes for experimentation every 2 to 3 days. For confluence after 2 days, 1.4 million cells were added, and for confluence after 3 days, 1.0 million cells were added. The volume of medium added to each petri dish brought the total volume to 4 ml.

Prior to seeding, the petri dishes were autoclaved then rinsed three times each with bleach, alcohol and de-ionised water. Thereafter, they were sterilised under UV light for 30 minutes.

The reagent was obtained through the NIH AIDS Reagent Program, Division of AIDS, NIAID, NIH: HeLa CD4 Clone 1022 from Dr. Bruce Chesebro [107-109].

3.2.2 MT4 Cells

Cells were grown in cell culture flasks for suspended cells (NUNC, 75 cm^2) with 90 % RPMI-1640 and 10 % FBS and incubated at 37 °C with 5 % CO_2. The cells were split into a new flask every 3 to 4 days. MT4 cell maintenance required the following protocol. The cell culture suspension in the flask was pipetted up and down gently to break up the clumps. 2 ml of cell suspension was added to a new flask into which 16.2 ml RPMI and 1.8 ml FBS were already added. The flask was labelled and placed in the incubator.

Prior to experiments, the petri dishes were autoclaved then rinsed three times each with bleach, alcohol and de-ionised water. Thereafter, they were sterilised under UV light for 30 minutes.

The reagent was obtained through the NIH AIDS Reagent Program, Division of AIDS, NIAID, NIH: MT-4 from Dr. Douglas Richman.

3.2.3 Vero Cells

This cell line, Vero (ATCC® CCL-81™), were grown in cell culture flasks for adherent cells (NUNC, 75 cm^2) with 98% Eagle's minimum essential medium (EMEM) and 2 % FBS and incubated at 37 °C with 5 % CO_2. Cells were fully confluent in flasks after 3 to 4 days at which point they were split into a new flask and seeded onto petri dishes in preparation for experiments.

Vero cell maintenance required the following procedure. The flask containing the cell culture was washed three times with 5 ml PBS. 1 ml trypsin was added to the flask which was then incubated for two minutes. Subsequently, the flask was tapped gently to dislodge the cells. 1 ml FBS was added to counteract the action of trypsin. The cell suspension was pipetted up and down to break up the clumps. 1 ml of the cell suspension was added to a new flask in which 19.6 ml EMEM and 0.4 ml FBS was already added. The flask was labelled and placed in the incubator.

Petri dishes for experimentation were seeded in the following manner. 4 ml of 2 % media was added to each petri dish. 400 µl of cell suspension was then added to each petri dish. The petri dishes were kept in an incubator at 37 °C and 5 % CO_2.

Prior to seeding, the petri dishes were autoclaved then rinsed three times each with bleach, alcohol and de-ionised water. Thereafter, they were sterilised under UV light for 30 minutes.

3.3 Construction of Corona-generating Instruments

Three corona-generating apparatus were constructed. Two of them were designed specifically for this investigation and the last one was replicated from a previous research study by Ramachandran et al. [42]. Three different designs were chosen for the investigation. The first allowed for direct exposure to the corona discharge in a multipoint-to-plane corona generating device. To the best of our knowledge, no investigation on direct exposure of the full corona discharge for the purpose of cell permeabilization has been undertaken before. The second was a replica of a previous design [42] in which the instrument was designed as

a corona generator which allowed for indirect exposure to the corona discharge thereby allowing the cells to be exposed to the corona ions of the discharge. The third configuration was one in which a cell suspension was exposed directly to corona discharge while the suspension was in direct contact with the ground electrode.

3.3.1 Device 1

A multi-point-to-plane atmospheric-air corona-generating device was designed and constructed for direct exposure of corona discharge on both suspended and adherent cells. Multiple high voltage electrodes were used. Mraihi et al. [110] showed that in a point-to-plane configuration, multiple tips produced a higher corona current and a greater concentration of active species. Further, Ramachandran et al. [42] showed that a corona-ion generator with multiple pins was more efficient at permeabilizing cells.

Ramachandran et al. [42] designed a corona-generating device that resulted in indirect exposure to the corona discharge, in which the sample was placed beyond the ground electrode and ions drifting out of the device resulted in permeabilization of the cells. Our device on the other hand is a different configuration and allows the sample to be placed between the two electrodes in the drift region thereby directly exposing them to the full corona discharge.

The detailed construction of the corona-generating device is illustrated in figures 3.1 and 3.4.

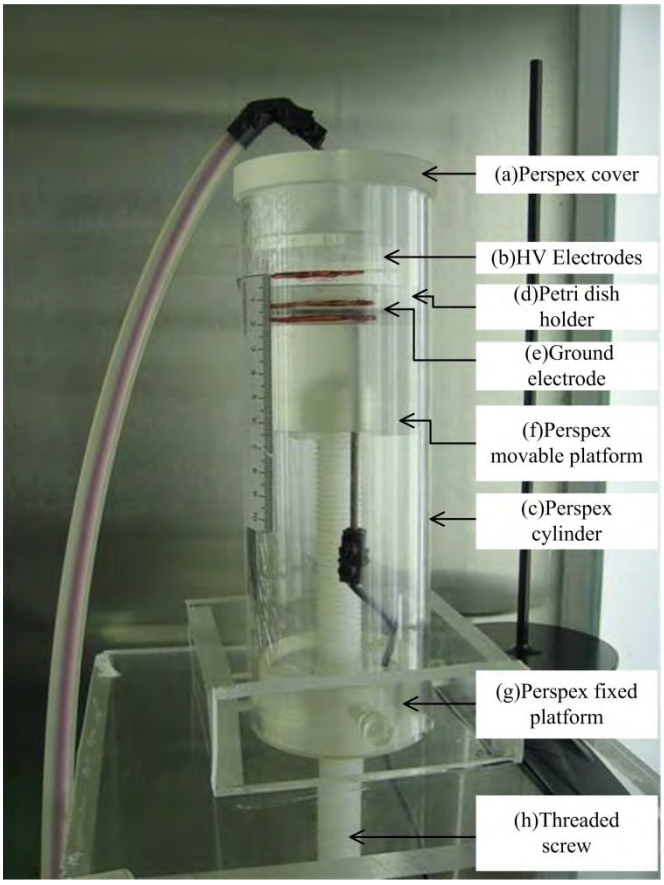

Figure 3.1: Atmospheric-air corona-generating instrument

The outer casing of the instrument was manufactured from a Perspex cylinder (c) with inner diameter of 70 mm, outer diameter of 80 mm and height of 225 mm. A threaded screw (h) was manufactured from a Teflon rod 22 mm in diameter and 290 mm in length. A platform (g) made of Perspex of thickness 35 mm was fixed to the inside wall of the cylinder. The platform was designed with a threaded hole so that the screw could be rotated either in a clockwise or anti-clockwise direction to enable the screw to move upwards or downwards respectively, thereby allowing the air gap between the electrodes to be adjusted. Another platform (f) of thickness 43 mm was attached to the top of the screw but not attached to the walls of the tube so that it could move in conjunction with the screw. A petri dish holder (d), which also houses the ground electrode, was placed on top of the platform. The glass petri dish containing the sample to be analyzed was placed on the ground electrode and was therefore positioned between the high voltage and ground electrodes.

The top of the device (a) was machined from a solid Perspex rod which had a hole drilled through the top. The high voltage electrodes (b) were stainless steel acupuncture needles (Suzhou Tianxie Acupuncture Instruments Co., Ltd.) and 13 of these were arranged in a

network and connected at the top. This was inserted through the hole at the top of the device and this point was connected to the high voltage amplifier.

The petri dish holder (d) was machined from a perspex disk and was 12 mm deep. The ground electrode (e) was a circular copper plate of 2 mm thickness. The sample dish could then be placed on the ground electrode. This arrangement was adopted so that the cell sample would be in the direct path of the corona discharge for optimal exposure to ions and other active elements.

3.3.2 Device 2

Device 2, as shown in figure 3.2, is a replica of the device constructed by Ramachandran et al. [42].

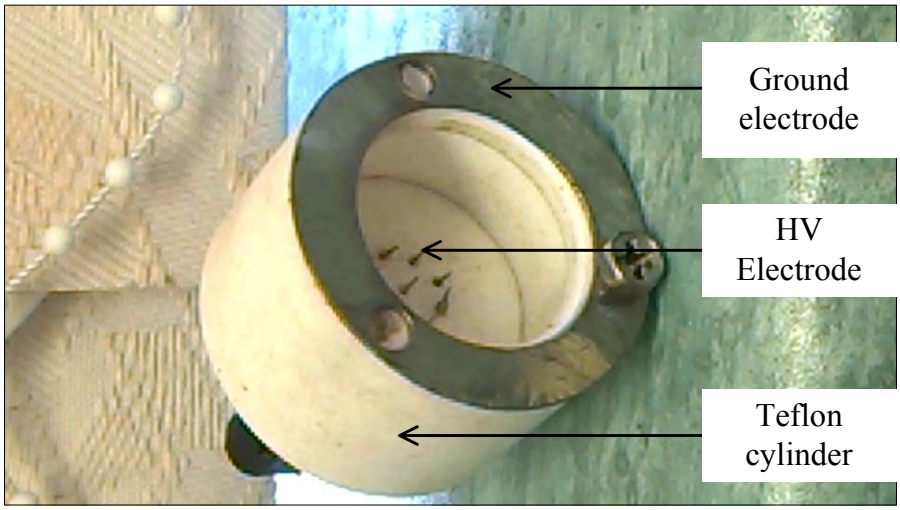

Figure 3.2: Replica of corona-ion generator [42]

This device is a corona ion generator in that the cell sample is placed below the ground electrode. There is no direct exposure to the corona discharge, however, some of the ions produced drift away from the device and settle on the sample surface below. It is presumed that these ions result in the charging of the cell membrane and, therefore, pore formation. The instrument was constructed from a Teflon rod with 38 mm outer diameter, 24 mm inner diameter and height of 25 mm. Nine stainless steel acupuncture needles (Suzhou Tianxie Acupuncture Instruments Co., Ltd.) were used as high voltage electrodes. The needles were arranged in a network and connected at the top. The needles were then connected to the high voltage supply.

3.3.3 Device 3

In this instrument, shown in figure 3.3, a perspex tube 100 mm in length and 20 mm in diameter with copper electrodes on either end was designed and constructed.

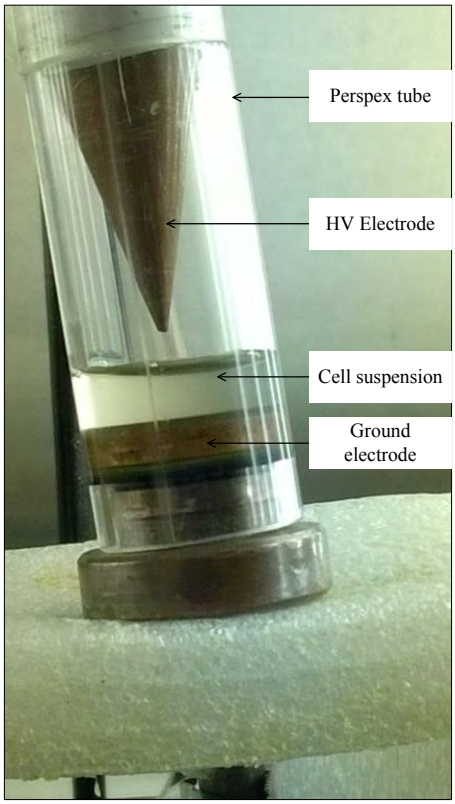

Figure 3.3: Corona generating device with submerged electrode

The high voltage electrode was designed with a sharp point and the ground electrode had a flat surface. The device was constructed such that an air gap was in existence between the two electrodes. The main idea of this device was that the cell suspension remains in contact with the ground electrode during exposure to the corona discharge so that the cell suspension itself becomes an integral part of the corona discharge. The ground electrode is fitted to the bottom of the cylinder and had a rubber seal around it that prevented liquid from leaking out. A pre-determined quantity of cell suspension was then added from the top of the cylinder. The high voltage electrode was placed on the top. The device was then connected to the circuit and the experiment conducted.

3.4 Circuit Diagrams

The electrical circuit employed for all three devices was identical and is shown in figures 3.4, 3.5 and 3.6.

3.4.1 Device 1

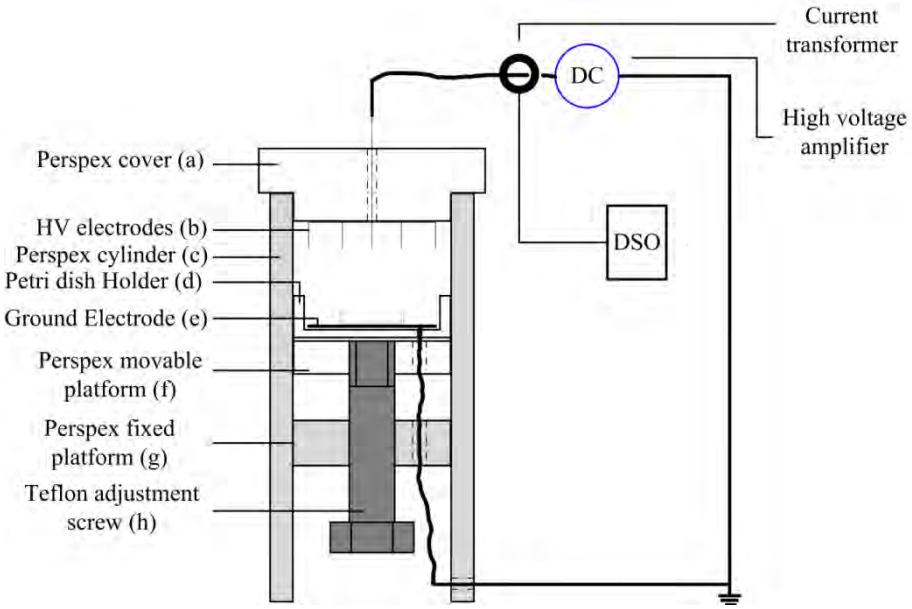

Figure 3.4: Diagram of the multipoint-to-plane atmospheric-air corona-generating device

3.4.2 Device 2

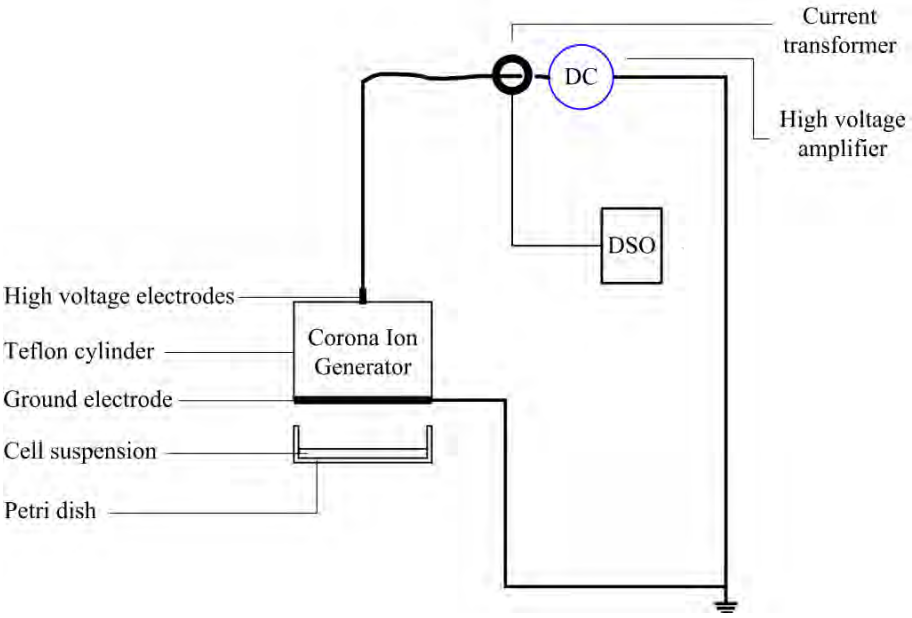

Figure 3.5: Diagram of the corona-ion generator

3.4.3. Device 3

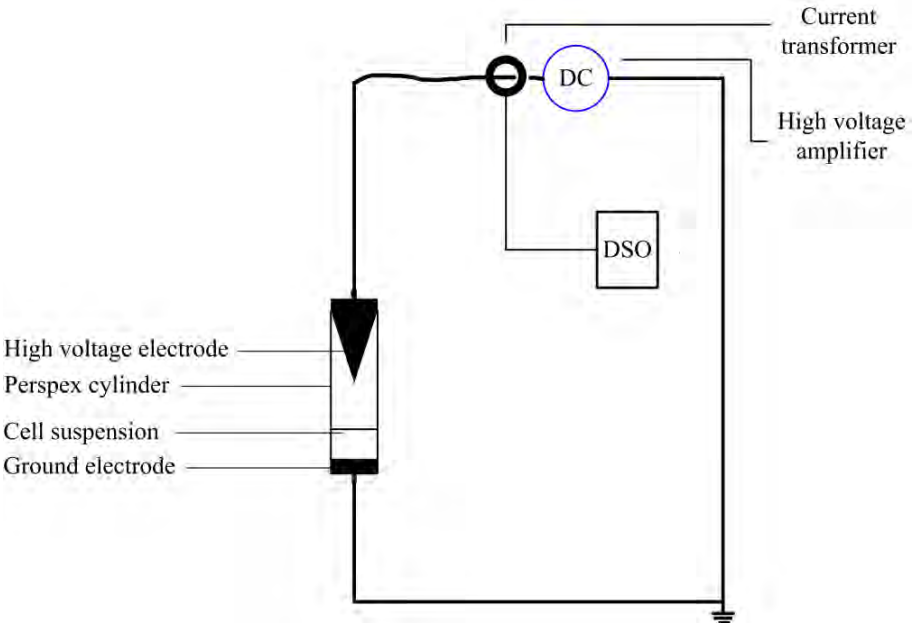

Figure 3.6: Diagram of submerged ground electrode corona-generating device

3.5 Equipment Used

A description of the equipment used in the experimental investigation is described below.

High voltage DC was supplied by a Trek 10/10B-HS high voltage amplifier with input provided by a Rigol DC3121A waveform generator. Current signals were captured on the high voltage side using a Bergoz CT-D5.0 BNC current transformer connected to an oscilloscope, a Picoscope 6404D. The data was transferred to a computer using the Picoscope version 6.9.18.1 software. Analysis of the data was carried out using Matlab 2014b software. Cells were enumerated and cell viability was established using the trypan blue assay with a Countess Automated Cell Counter (Invitrogen/Life technologies). A Promega Glomax multimode reader was used to perform the spectrofluorometric measurements and a Scientific Group Jouan BR4i centrifuge was used to centrifuge all samples.

3.6 Laboratory Conditions

All cell cultures and experiments were conducted in a laminar flow hood under sterile conditions. A laminar flow hood, as shown in figure 3.7, provides a sterile environment for

working with cells and is necessary for the prevention of contamination of the cell samples. By providing a constant flow of filtered air over the work area, dust and other contaminants are prevented from contaminating the work area and, therefore, the cell cultures.

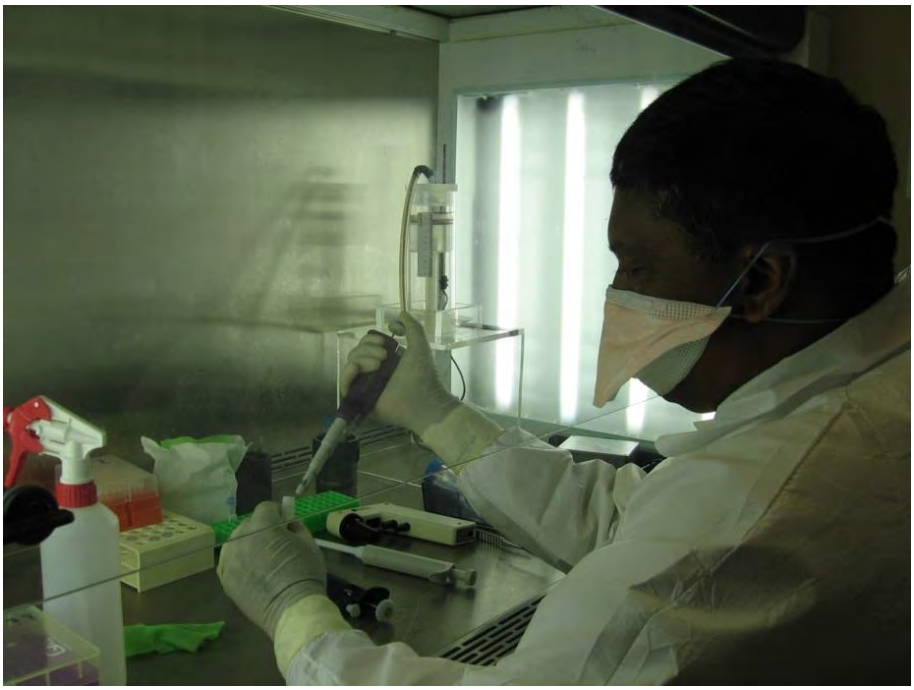

Figure 3.7: Working with cells in a laminar flow hood

An incubator, pictured in figure 3.8, is required for the cultivations of cells. The incubator provides an ideal environment for the cell cultures to thrive in by maintaining a temperature of 37 °C and environment with 5 % CO_2. These conditions are required for cell cultivation.

Figure 3.8: Incubator

3.7 Tracer Molecules and Concentration

SYTOX Green was used as tracer molecules to quantify the level of permeabilization of the cells (Life Technologies, 5 mM solution in Dimethyl Sulfoxide (DMSO)). This dye is impermeant to cells and only fluoresces brightly when it is bound to nucleic acids and excited by the 488 nm line of the argon ion laser [111]. SYTOX Green has an absorption maximum of 502 nm and an emission maximum of 523 nm [111].

Detection of an increase in the fluorescence of a cell is an indication that SYTOX Green molecules have passed through the cell membrane and have bound to the nucleic acids. SYTOX Green has been used successfully previously to investigate the permeabilization of cell membranes [41, 42, 112-115]. Various concentrations were tested during the course of the experimentation. For the final experiments, a 1 μM concentration of SYTOX green, made in PBS, was used.

3.8 Cell Destruction and Cell Concentration

An important consideration in assessing cell destruction is that cell destruction due to corona discharge includes both cells that become non-viable and cells that are lysed as shown in

figure 3.9. The non-viable cells remain largely intact but have a compromised membrane. The lysed cells result in cell fragments and free nucleic acids in solution.

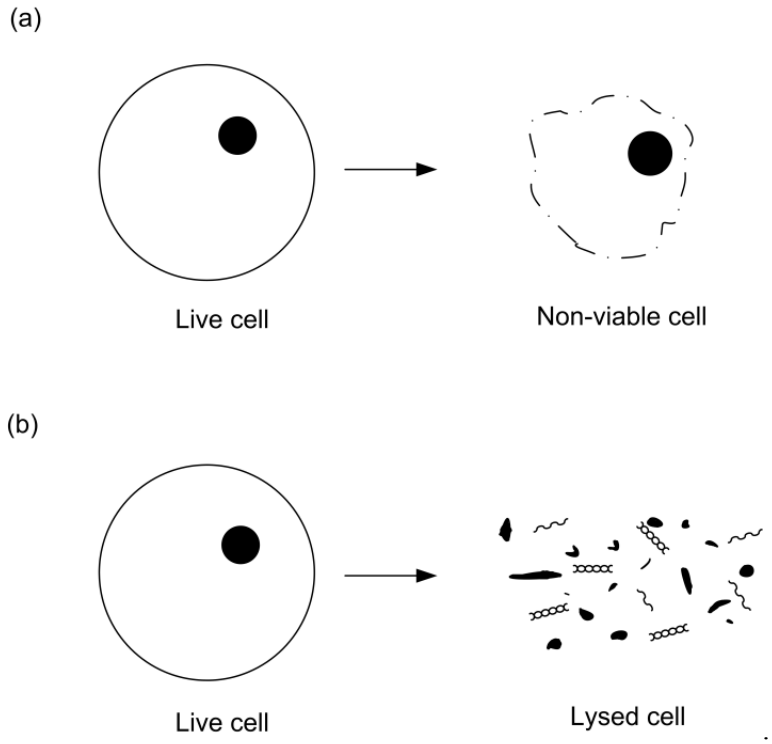

Figure 3.9: Cell destruction (a) Live cells that become non-viable (b) Live cells that are lysed

Previous studies [41, 42] have used the trypan blue exclusion test to establish cell viability to gauge the destructive effects of the permeabilization technique. The limitation of using the trypan blue exclusion test is that this assay is able to enumerate living and dead cells but not cells that have been lysed [116]. Therefore, the destructive effect of exposure to electrical pulses or plasma will be underestimated because cells that have been lysed are excluded from the count. In this research investigation, we sought to mitigate this inadequacy by measuring cell free DNA as a marker of cell lysis. DNA was quantified using the SYTOX Green method. SYTOX Green is a very sensitive dye and is ideal for quantifying DNA in solution and even binds to fragments of cells [117]. It has been used previously to detect DNA. For example, Gupta et al. [118] have used SYTOX Green to detect extracellular DNA. We therefore use this dye to detect DNA in solution in the supernatant after treatment with corona as a marker for cell lysis. This method, together with the trypan blue viability test, provides a more representative indication of the deleterious effects of the treatment.

Cells were enumerated using the trypan blue exclusion test [119] with a Countess Automated Cell Counter (Invitrogen/Life technologies). Cell destruction was measured using a combination of the trypan blue exclusion test and measurement of the free DNA in the supernatant after corona treatment using the fluorescence of SYTOX Green.

3.9 Experimental Method

The experimental methods for the different cell lines and their refinement over numerous experiments under varying conditions are presented in this chapter. It must be borne in mind that for the chosen cell lines, no documented evidence of success with permeabilization due to corona discharge was found. This implied that there was no standard procedure that could be adopted for the experiments but, instead, the experimental procedure had to be formulated using standard protocols and then refined by trial and error over numerous attempts using all three cell lines and devices. Successful permeabilization was only obtained with the HeLa cell line and devices 1 and 2. The main experiments were conducted using the HeLa cell line and device 1, the device that was specifically constructed for this research study and which allowed for the direct exposure of cells to the full corona discharge.

3.9.1 Vero Cells

Two fully confluent petri dishes were obtained from the incubator, one for the control and one for treatment with corona discharge. The growth medium was aspirated and both petri dishes were washed three times with 1 ml PBS. This allowed for the removal of all traces of growth media and unattached cells. The required volume of PBS was added to each petri for the experiment. The corona discharge was applied for the required time to the treatment sample while the control sample was left unexposed in the hood. Immediately after exposure, 0.5 µl of 5 mM SYTOX Green was added to both the control and treatment samples and the petri dishes were swirled to distribute the SYTOX green. The control and treatment samples were incubated for the required time to allow the SYTOX Green molecules to enter the cells. 250 µl of trypsin was added to each petri dish to detach the cells. After an incubation period of two minutes, the petri dishes were tapped gently to dislodge the cells. 1 ml of medium was added to counteract the effect of trypsin and to suspend the cells. The suspension was pipetted up and down gently to break up clumps. 200 µl each of the control and exposed sample were added to the wells of a plate reader and the spectrofluorometric analysis was

conducted. The viability and concentration of the cells were measured. The procedure was repeated to perform a set of three identical experiments.

The petri dishes were autoclaved after each experiment.

3.9.2 MT4 Cells

Two clean petri dishes were obtained, one for the control and one for treatment with corona discharge. The required volume and concentration of cells was added to each petri dish. One of the petri dishes was placed in the exposure area of the corona-generating device, while the control sample was left unexposed in the hood. The treatment sample was exposed to corona for the required time. The corona current was recorded with the current transformer and oscilloscope at predetermined intervals during exposure. Immediately after exposure, the required volume and concentration of SYTOX Green solution was added to both petri dishes. The samples were incubated for the required time to allow the SYTOX Green molecules to enter the cells. The suspension was pipetted up and down gently to break up any clumps. The fluorescence and viability of the treatment and control samples were measured. The procedure was repeated to perform a set of 3 identical experiments

The petri dishes were autoclaved after each experiment.

3.9.3 HeLa Cells

The procedure for HeLa cells was optimized over numerous experiments. After each set of experiments, an analysis was conducted to determine if there were any limitations to the method. If any limitations were identified, the procedure was amended to correct this limitation and a new batch of experiments was undertaken. This process continued until the final procedure was obtained.

3.9.3.1 Initial Procedure for HeLa Cells

After numerous experiments involving trial and error, the first general experimental procedure was established as follows. Two fully confluent petri dishes were obtained from the incubator, one for the control and one for treatment. The growth medium was aspirated and the petri dishes were washed three times with 1 ml PBS. The required volume of PBS

was added to samples. The treatment petri dish was placed in the exposure area of the corona-generating device and exposed to corona for the required time while the control petri dish was left unexposed in the hood. The corona current was recorded using the current transformer and the oscilloscope at predetermined intervals during exposure. Immediately after exposure, the required volume and concentration of SYTOX Green solution was added to both petri dishes. The petri dishes were incubated for the required time to allow the SYTOX Green molecules sufficient time to enter the cells. 750 µl of trypsin was added to both petri dishes and incubated for ten minutes. The petri dishes were tapped gently to dislodge cells. 1.5 ml of growth medium (colourless RPMI + 10 % FBS) was added to counteract the action of trypsin. The suspension was pipetted up and down to break up clumps. The fluorescence and viability were measured. The procedure was repeated to perform a set of three identical experiments. The petri dishes were autoclaved after each experiment.

3.9.3.2 Attempt to Solve Cell Clumping Problem with Post Lysis Fluorescence

During experiments using the procedure in 3.9.3.1, it was noted that the final suspension of cells was not a homogeneous mixture. Cells tended to clump together in masses which affected the fluorescence measurements and led to variation in results. The first attempt to solve this issue was to lyse all cells in the suspension to release the nucleic acids and measure the post-lysis fluorescence. These nucleic acids are already bound to SYTOX Green and it was thought that lysis of the cells and the subsequent release of the nucleic acids into solution would result in a more homogeneous mixture and more consistent and accurate fluorescence measurements. Two different cell lysis buffers and their corresponding protocols were used to investigate the problem. The two lysis buffers tried were CyQuant and Triton X-100.

a. Method for cell lysis using CyQuant

The treatment sample was exposed to corona discharge for 10 minutes. This exposure time is not critical for this experiment, however, an exposure time that would guarantee permeabilization, as seen from previous experiments, was chosen. The control sample was left unexposed in the hood. Immediately after exposure, 500 µl of 1 µM SYTOX Green was added to both the control and treatment samples. The petri dishes were incubated for the required time to allow the SYTOX Green molecules to enter the cells. 750 µl of trypsin was added thereafter and the samples were incubated for 10 minutes. 1.5 ml of growth medium

(colourless RPMI + 10 % FBS) was added to each petri dish to counteract the action of trypsin. The cell suspensions were pipetted up and down gently and added to a centrifuge tube (control and treatment). 15 ml PBS was added. The tubes were centrifuged for 7 minutes at 1000 rpm as recommended by the standard protocol. The cells were resuspended in 15 ml PBS. This wash step was repeated three times. The supernatant of first wash and last wash (free DNA) was stored. The fluorescence of the supernatant was measured. The pellets were covered in foil and frozen overnight at -70 °C. The next day, 100 µl of concentrated buffer was combined with 1900 µl de-ionised water. 1 ml of this diluted buffer was added to each pellet. The cells were resuspended by vortexing. The tubes were wrapped in foil and incubated for at least 5 minutes at 37 °C and 5 % CO_2 as recommended by the standard protocol. The fluorescence was then measured in triplicate.

b. Method for cell lysis using Triton X-100

The treatment sample was exposed to corona for 10 minutes while the control sample was left unexposed in the hood. An exposure time of 10 minutes was chosen as in 3.9.3.2.a. Immediately after exposure, 500 µl of 1 µM SYTOX Green was added to both the control and treatment samples and incubated for the required amount of time to allow sufficient time for the SYTOX Green molecules to enter the cells. 750 µl of trypsin was added to both samples and incubated for 10 minutes. The petri dishes were tapped gently to dislodge the cells. 1.5 ml growth medium (colourless RPMI + 10 % FBS) was added to counteract the action of trypsin. The suspension was pipetted up and down gently to break up clumps. The fluorescence of the control and exposed samples were measured in triplicate. The sample was removed from the plate reader and added back to the respective petri dishes. The suspension in the petri dishes was transferred to centrifuge tubes (control and treatment). PBS was then added up to the 15 ml mark. The tubes were centrifuged for 5 minutes at 1500 rpm as recommended by the standard protocol. The wash step was conducted a total of 2 times. The supernatant of both washes was stored. After the final wash, 1 ml of cold deionised water was added and the pellets were broken up. 10 µl of cold Triton X-100 cell lysis buffer was added and the samples were pipetted up and down. The samples were then incubated on ice for 15 minutes as recommended by the standard protocol. The samples were pipetted up and down gently and the fluorescence was measured in triplicate.

Unfortunately, these two methods at measuring post-lysis fluorescence were not successful at solving the cell clumping problem. Cell lysis did not appear to be totally successful as

debris was still observed in the final sample and the resultant suspension was not homogeneous. Further experiments with cell lysis were discontinued.

3.9.3.3 Solving Cell Clumping Problem by Adding Wash Steps

The cell clumping problem was solved by adding wash steps prior to measuring fluorescence to remove as much of the free DNA as possible to reduce cell clumping. The result was the procedure outlined in 3.9.3.3.a, which was used to investigate the variables. An additional modification was included in the procedure, in which the fluorescence of a predetermined number of cells was measured, namely 250 000 cells. This modified and more accurate procedure was used in the investigation of applied voltages and outlined in 3.9.3.3.b.

a. Procedure for optimization of variables

The cell clumping problem was solved by including two wash steps just before fluorescence measurements. This resulted in a more homogeneous cell suspension and therefore, more consistent and accurate fluorescence measurements. The procedure was as follows and was used for the optimization of variables. A fully confluent petri dish was washed 3 times with 1 ml PBS. The required volume of PBS was added to the petri dish and then exposed to corona discharge. Immediately after exposure, 500 µl of 1 µM SYTOX Green solution was added and the petri dish was incubated to allow sufficient time for the stain to enter the cells. 750 µl of trypsin was then added to detach the cells from the growth surface with an incubation time of 10 minutes. Thereafter, 1.5 ml of growth medium was added to negate the effect of trypsin. The sample was transferred to a 15 ml centrifuge tube and washed twice by centrifuging at the standard, recommended 1500 rpm for 5 minutes with 10 ml PBS. The supernatant of the first wash was collected. After the final wash, the cell pellet was re-suspended in 1 ml PBS and the viability and cell concentration were measured. The fluorescence of the cells and supernatant was thereafter measured by adding 200 µl of each sample to a well of a fluorescent plate reader. Fluorescence measurements were made in triplicate. In tandem with each experiment, a corresponding control experiment was conducted. In the control experiment, the full procedure, except exposure to corona discharge, was followed.

b. Procedure for investigation of applied voltages

After the variable optimization experiments were completed the procedure for the final experiments with applied voltages could be established. In this procedure, a more accurate

fluorescence measurement was obtained. The experimental procedure was similar to 3.9.3.3.a. except that the optimal values of the variables were used. Further, to improve accuracy, fluorescence measurements of the cells was conducted on a particular number of cells, namely 250 000. Therefore, 250 000 cells were transferred to a well of a fluorescent plate reader. The volume was then standardised at 200 µl by the addition of PBS. Fluorescence of the cells was then measured, in this manner, in triplicate. Here too, each experiment had a corresponding control in which the full procedure, except exposure to corona discharge, was followed.

3.10 Optimisation of Variables

After numerous preliminary experiments, the variables that had the most profound effect on cell permeabilization were identified. These variables, listed in table 3.1, were exposure time to corona discharge, volume of PBS during exposure, incubation time with SYTOX Green and inter-electrode distance. For the optimisation of these variables, the experimental procedure of 3.9.3.3 a. was used. A detailed explanation of the optimisation of these variables is provided in section 4.6.

Table 3.1: Variables that were optimized

	Condition to be optimized
1	Exposure time to corona discharge
2	Volume of PBS during exposure
3	Incubation time with SYTOX Green
4	Inter-electrode distance

3.11 Investigation of the Influence of Applied Voltage

Once the variables as identified in table 3.1 were optimised, they were used in the investigation of the influence of applied voltage on the level of permeabilization. In our initial experiments, success at cell permeabeabilization was demonstrated with both positive and negative applied voltages. For our final experiments, though, only positive voltages were used. The reason for this was twofold. Firstly, both positive and negative ions have a similar effect on the cell membrane as has been observed by Dobrynin et al. [38]. Secondly, in our experiments, greater magnitudes of corona currents were observed for positive voltages. Therefore, it was decided that, by focusing on only the positive corona, a greater depth of

investigation could be conducted. Other forms of voltage would be investigated during future research. During laboratory experiments, corona discharge, using an ultraviolet camera, was only observed at voltages greater than +3 kV. It was also observed that breakdown occurred at voltages greater than +8 kV. Therefore, positive DC voltages of 4 kV, 5 kV, 6 kV, 7 kV, and 8 kV were investigated. This procedure is detailed in 3.9.3.3 b.

3.12 Corona Discharge Current Analysis

The configuration of the PicoScope was set to a sampling time of 5 GS/s, time per division of 100 µs/div, and 100 pages of data. A sampling rate of 5 GS/s is the maximum for the instrument and ensured a very small sampling interval of 200 ps. The time per division of 100 µs/div allowed each page of data to contain 5 000 000 sampling points spanning a time interval of 1 ms, which ensured the sampling of several current pulses per page. The setting of 100 pages allowed for the capturing of 100 intervals of the waveform each spanning a time period of 1 ms. The data was saved in PicoScope data file format (*.psdata). From this data, a random choice of pages 5, 50, and 90 were chosen to be analyzed for each experiment. These pages were saved in binary format which were imported into Matlab. An example of a single page of data at 6 kV DC, plotted in Matlab, is shown in figure 3.10. The Matlab programme for plotting the discharge current for a single page is included in Appendix XIV.

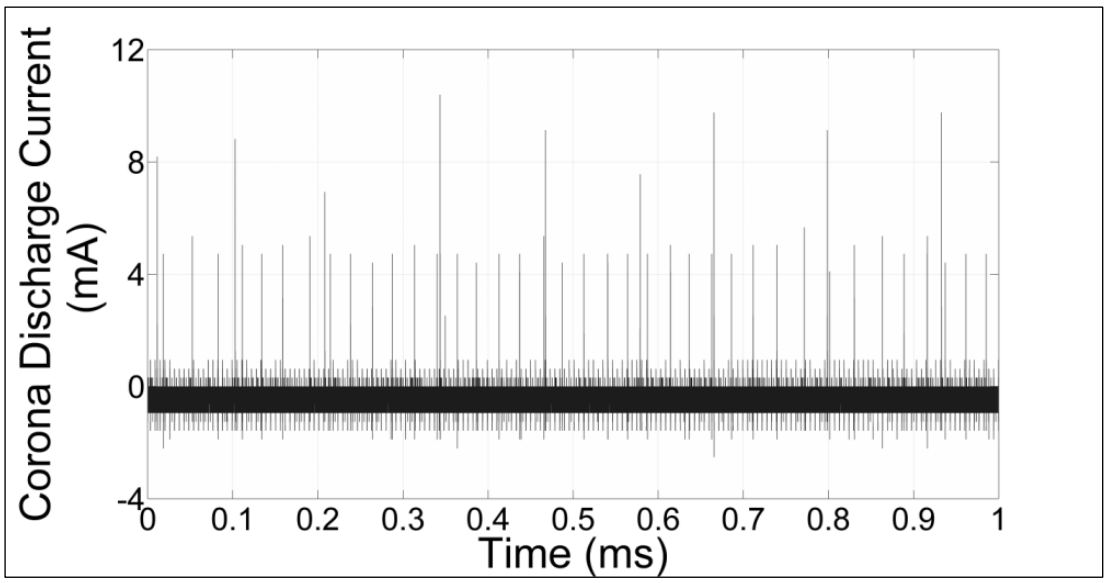

Figure 3.10: Graph of corona discharge current versus time for an applied voltage of 6 kV DC

For permeabilization due to electric fields, the key factor is that it is applied in the form of pulses. For the method of electroporation, the pulse magnitude, pulse width, and number of pulses are all significant characteristics that have a bearing on the efficacy of the procedure. Previous investigations have proven that, for electroporation, pulse width [1, 26, 27, 56, 57, 95], pulse magnitude [27, 62, 95], and the number of pulses [27, 62, 95] all have an effect on permeabilization and cell destruction.

Hoff and co-workers theorized that the ions produced by the corona discharge are responsible for the application of electric fields across the cell membranes [42]. In an attempt to draw parallels between conventional electroporation and corona permeabilization, it is important to note that corona discharge current is composed of a series of nanosecond current pulses. In positive corona, positive ions, formed due to electron avalanches, accumulate in the gap and are responsible for the corona pulses [43]. These pulses, therefore, are as a result of the creation and movement of the ions that are assumed to be responsible for the generation of the electric fields. Just as the characteristics of the applied pulses play an important role in pore formation in the conventional method of electroporation, it is envisaged that so too would the current pulses in the corona discharge method of cell permeabilization. This research investigation, therefore, analyzes the corona discharge pulses of positive DC applied voltages and relates these characteristics to the levels of cell permeabilization and cell destruction. Characteristics of the corona pulses that were analyzed included pulse amplitudes, pulse repetition rates, pulse widths, and pulse rise-times. The characteristic frequencies of single pulses, obtained from the application of a DFFT, were also analyzed. These results are presented and analyzed and those characteristics that affect permeabilization and cell destruction are identified and discussed.

The analysis of the corona pulses was performed using Matlab.

3.12.1 Calculation of Average Rise-time and Average Pulse Width of Corona Discharge Current Pulses

For each applied voltage, 3 pulses were chosen from each of pages 5, 50 and 90. For each of the pulses chosen, a graph of current versus time was displayed as shown in figure 3.11.

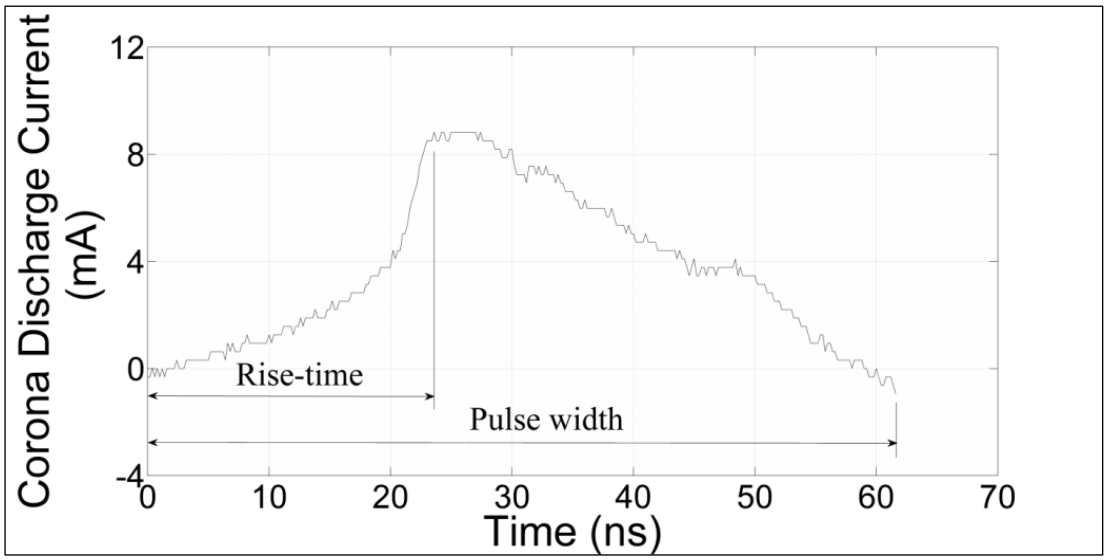

Figure 3.11: Graph of corona discharge current of a single corona pulse versus time for an applied voltage of +6 kV DC

The rise-time and pulse width were recorded. The average of these characteristics for all these pulses was then calculated. Further, since the experiment for each applied voltage was conducted three times, the average of the characteristics for each of the experiments was calculated. In this manner, the average rise-time and pulse width for each of the applied voltages of +4 kV, +5 kV, +6 kV, +7 kV and +8 kV DC was calculated.

The Matlab programme for calculating the pulse width and rise-time is included in Appendix XV.

3.12.2 Calculation of Average Pulse Amplitudes and Average Pulse Spacing

For the chosen pages of data described in section 3.12.1, the peak of each corona pulse was identified and the amplitude of the pulses and the spacing between the peaks were calculated. The average value for these three pages of data was calculated. Thereafter, the average values for all three experiments for each applied voltage were calculated.

The Matlab programme for calculating the average pulse amplitudes and average pulse spacing is included in Appendix XVI.

3.12.3 Calculation of Average Characteristic Frequencies of Each Corona Discharge Current Pulse

For each of the pulses identified, as described in section 3.12.1, a DFFT algorithm was applied to each pulse to identify the characteristic frequencies. Two characteristic frequencies for all experiments were observed, which were termed the primary and secondary characteristic frequencies. These frequencies were recorded. The average of all the characteristic frequencies of the pulses for each applied voltage was calculated. An example of the graph obtained for a single pulse is shown in figure 3.12.

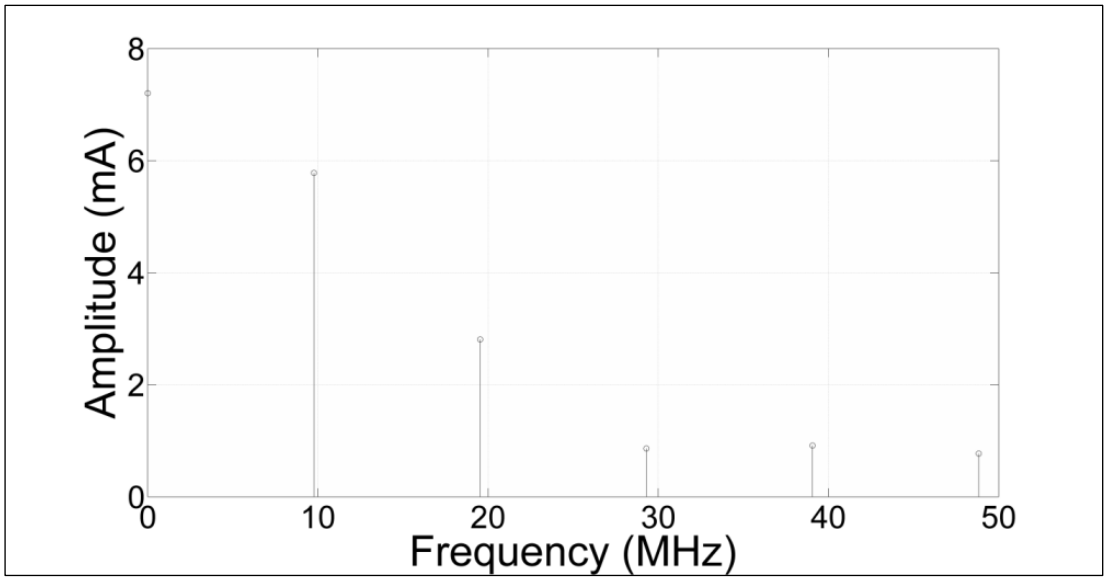

Figure 3.12: Graph of amplitude of characteristic frequencies of a single corona pulse versus frequency for an applied voltage of 6 kV DC

The Matlab programme for calculating the characteristic frequencies is included in Appendix XVII.

3.13 Visual Proof of Cell Permeabilization

Visual proof of cell permeabilization for the devices at various applied voltages was obtained by the preparation of slides that were viewed under a fluorescence microscope. 4',6-diamidino-2-phenylindole (DAPI) stain was applied to the slides to allow for the viewing of all cells, whether permeabilized on not, when viewed under blue light. When viewed under green light, only the permeabilized cells would be visible due to the fluorescence of SYTOX Green.

3.13.1 Slide Preparation

Slides were prepared using Shandon coated double cytoslide by Thermo Scientific. Using the NovoPen, a circle of wax was deposited around each ring on the slide to help contain the added liquid. 120 µl of poly-L-lysine was added slowly to each well until the surface was completely covered. The slides were placed in a container with damp paper towel and incubated for 30 minutes at 37 °C. During the incubation process, 1 ml of each sample was added to labelled 15 ml centrifuge tubes (control and treatment). PBS was added to each tube until the 15 ml mark. The tubes were centrifuged at 1500 rpm for 10 minutes. The supernatant was carefully discarded and the cells were resuspended in 400 µl PBS. After incubation of the slides, the poly-L-lysine was removed from each sample well of slide and the slide was washed twice with PBS. 120 µl of cells, obtained from the centrifuge step above, was added to each sample well of the slide (control and treatment). The slide was placed back in the container on damp paper towel and incubated for 60 minutes at 37 °C. Each sample well of the slide was washed twice with PBS. 120 µl of 4 % paraformaldehyde (PFA) was added to each well and the slide was incubated at 4 °C, in the fridge, for ten minutes. Each sample well was washed twice with PBS. One drop DAPI fluoromounting fluid was added to each sample well. A cover slip was placed over each well. The slides were stored at 4 °C until ready to observe under the fluorescence microscope.

3.14 Conclusion

The choice of the corona-generating device and cell line as well as the experimental procedure that was used for the final experiments were established over the course of numerous trial-and-error experiments.

Details of all the experimental equipment and methodology in this regard are provided. A list of subjects dealt with in this chapter is listed below:

- The equipment used
- The circuit diagrams of the experiments
- The three corona-generating devices
- The three cell lines
- All standard protocols used
- The final experimental procedures
- The analysis of the results

- The preparation of slides

CHAPTER 4

Results and Discussion

4.1 Introduction

This chapter presents the results of all experiments conducted on the three devices and three cell lines and details the evolution of the experimental procedures and protocols. A discussion on all aspects of the results is provided.

Ramachandran et al. [42] have demonstrated the success of delivering molecules to murine cells using corona ions only and not the corona discharge as a whole. There was neither an attempt to characterize the corona discharge nor an attempt to identify the characteristics of the discharge that affect permeabilization or cell destruction. Only the charge deposited on the surface area similar to that of the cell sample was quantified. We, on the other hand, have designed and constructed a different configuration of instrument to utilize the full corona discharge and attempt to identify the characteristics of the corona discharge current pulses that affect molecular delivery and cell destruction. The reason for using the full corona discharge as opposed to just the ions is that corona discharge has many other constituents besides the ions which can have an effect on cell permeabilization and/or cell destruction.

A review of the literature showed that minimal research was previously conducted on molecular delivery to cells using corona discharge. In fact, for our devices and cells, no previous information was found on the experimental procedures. Therefore, the experimental procedure had to be established and refined by trial-and-error over numerous experiments. It was also found that there were many variables that affected the experimental procedure. These variables were first established and then optimized to provide reliable molecular delivery with acceptable levels of cell destruction. Results of the optimisation process is provided in detail in section 4.6. After optimization of the variables, the final experiments on the applied voltage and characteristics of the corona discharge pulses were undertaken. All results obtained over the course of these experiments is provided in detail and discussed. Visual evidence of cell permeabilization was also provided by the preparation of fluorescence slides.

All cell culture and experimental procedures were conducted under sterile conditions in a laminar flow hood.

4.2 Evaluation of the Three Constructed Devices

Three high voltage corona-generating devices, with different configurations and dissimilar characteristics, were constructed.

The three devices that were constructed are:

- A multipoint-to-plane atmospheric-air corona generating device specifically designed and constructed for this research study – Device 1
- An atmospheric-air corona ion generator which is a replica of the device evaluated by Ramachandran et al. [42] – Device 2
- An atmospheric-air point-to-plane corona-generating device with the ground electrode in contact with the sample, specifically designed and constructed for this research study – Device 3

Because of the limited research conducted previously on molecular delivery to cells using corona discharge, the devices tested previously are limited. According to available literature the only atmospheric-air corona-generating device used to test molecular delivery to cells was a corona-ion generator designed by Ramachandran et al. [42]. This device used an indirect method of exposure with the sample placed beyond the ground electrode. In this configuration, cell samples were exposed to the corona ions and not the whole corona discharge. It was proposed that the ions are responsible for the charging of the cell membrane, thereby increasing the transmembrane voltage and resulting in the formation of pores. Therefore, it was decided to design two other devices, which were variations of the corona-ion generator and used to perform the tests. Furthermore, they provided alternative forms of exposure of the cells to corona discharge in which the cells were exposed to the full corona discharge.

4.2.1 Device 1

Device 1, the multipoint-to-plane atmospheric-air corona-generating device specifically designed for this research study, was tested using two different cell lines. The cell lines tested were MT4 and HeLa cells. Numerous experiments under various conditions were conducted. Using device 1, no success was obtained at permeabilizing MT4 cells. MT4 cells are primary mammalian cells which are known to be difficult to transfect [120]. Future research would include investigating MT4 cells further. However, success was obtained with

device 1 and HeLa cells. The table of results of the various experiments under different conditions using this device is shown in Appendix I.

4.2.2 Device 2

Device 2, a replica of the corona-ion generator designed by Ramachandran et al. [42], was tested on three different cell lines, Vero cells, MT4 cells and HeLa cells. Several experiments were conducted under different conditions to attempt to achieve success at molecular delivery to these cell lines.

With this device, as with device 1, success at permeabilization was only obtained with HeLa cells. The table of results showing the various experiments performed with this device is shown in Appendix II.

4.2.3 Device 3

Device 3 was a device specifically designed and constructed for this research in which the cell suspension was in direct contact with the ground electrode. This method allowed the cell suspension to be a more direct part of the corona discharge. Experiments using this device were conducted on MT4 cells. Very few experiments were conducted because it was established that the device was neither practical nor effective on the basis of the following reasons: This device required the ground electrode to be in contact with the cell suspension. From a practical point of view, the device was not suitable since filling, emptying and cleaning the device was complicated. Spillage and leakage of the cell suspension was frequent, which increased the likelihood of cell contamination as well as contamination of the hood, instruments, reagents and personnel. Cell viability was also unacceptably high for the experiments conducted. Further, repeatability of the experiments was a slow process since the instrument and the ground electrode had to be sterilised by autoclaving after each experiment. This was not practical and hampered the experimental process. Due to the above reasons, it was concluded that this configuration was not suitable for experimentation on living cells and further tests with this device were discontinued. The results obtained from experiments using this device are shown in Appendix III.

4.2.4 Choice of Device for the Final Experiments

Due to the unsuitability of device 3, further experiments using this device were suspended early on in the study. Numerous experiments were conducted with the other two devices, device 1 and device 2. Success with molecular delivery to HeLa cells was obtained with both devices. However, it was decided that the final experiments would be conducted with device 1 only, the device specifically designed and constructed for this research study. The main reasons for this were that the apparatus was shown to be effective and the fact that, unlike device 2, it allowed for the exposure of the cells to the full corona discharge and, therefore, allowed for the investigation of the effects of the corona discharge as a whole. The second reason was that device 2, the replica of the instrument used by Ramachandran et al. [42], is a corona ion generator and cells are exposed to mainly the corona ions. Corona discharge has many constituents that can have an effect on cells. The constituents include UV radiation, ions, electrons, excited atoms, reactive gases, radicals, atoms, molecules and ultraviolet radiation [40, 44, 45]. Using device 1, the multipoint-to-plane corona-generating device that was constructed, allowed the investigation of the interaction of the complete corona discharge with cells. This study was important because no previous study, according to available literature, was conducted using the complete corona discharge for molecular delivery to cells.

4.3 Molecular Delivery to Different Cell Lines

Three different cell lines were tested in an attempt to permeabilize each cell line using corona discharge. Two human cell lines and one animal cell line was chosen. The human cell lines were MT4 and HeLa. MT4 is a cell line that is cultured in suspension and the HeLa cell line is cultured as an adherent cell. The choice of these two cell lines was important since it presented an opportunity of testing both an adherent and suspended human cell line. The third cell line is an animal cell line harvested from the kidney of the Green Monkey and was cultured in an adherent form.

4.3.1 Vero Cells

Device 2 was used to test Vero cells for cell permeabilization due to corona discharge. Due to limited time and in the interests of pursuing success on human cell lines, little time was

spent on this cell line. Nevertheless, for the experiments conducted, no success was obtained at permeabilizing Vero cells.

Conditions that were varied in an attempt to obtain successful permeabilization included the applied voltage and the concentration of SYTOX green.

A table of the experimental results for Vero cells is shown in Appendix IV.

Future research can include further investigations into this cell line.

4.3.2 MT4 Cells

Numerous experiments were conducted on the MT4 cell line. All three devices were tested under various conditions with an array of combinations of different factors and variables. No success was obtained at permeabilizing MT4 cells by corona discharge.

Conditions that were varied included inter-electrode distance for device 1 or the distance of the high voltage electrode above the cell suspension surface for devices 2 and 3, exposure time to corona discharge, incubation time with SYTOX Green, the addition of SYTOX Green before or after exposure, volume of medium during exposure, type of medium, the concentration of SYTOX Green, and the nature of the applied voltage.

The results of the experiments and the various conditions are presented in the table in Appendix V.

4.3.3 HeLa Cells

Several experiments were conducted under various conditions on HeLa cells using two devices, device 1 and device 2. Success was obtained at permeabilizing HeLa cells using both these devices. This is a significant development and contribution, since, according to our knowledge, ours is the first successful attempt at delivering molecules to a cell line of human origin using corona discharge. During the course of the experiments, it was apparent that a number of variables affected the success and effectiveness of the procedure. Conditions that were varied included inter-electrode distance or distance of the high voltage electrode from the sample surface, exposure time to corona discharge, incubation time with

SYTOX Green, the addition of SYTOX green before or after exposure, the concentration of SYTOX green and the nature of the applied voltage. The results of the initial experiments for the two devices are shown in Appendix VI.

4.3.4 Choice of Cells for Final Experiments

The choice of cells for the final experiments was a simple one because success was only obtained with one of the cell lines. The HeLa cell line was therefore used for the final experiments. This study investigated molecular delivery to cells with the ultimate goal of transferring drugs and genetic material into the cell interior for the treatment of cancer. The fact that this cell line is a cancer cell of human origin meant that it was appropriate for our study.

4.4 Visual Evidence of Cell Permeabilization

Although positive results were consistently confirmed by the measurement of the fluorescence of exposed cells, it was decided to also demonstrate the success of molecular delivery by preparing slides of various experiments to obtain visual evidence of cell permeabilization. Figures 4.1 - 4.4 are slides of the control and exposed samples of HeLa cells at different voltages with devices 1 and 2.

4.4.1 Device 1

Figures 4.1 - 4.3 provide visual evidence of HeLa cell permeabilization for device 1 at various voltages. Cells are viewed alternately under blue and green light. The blue fluorescence is due to the DAPI stain and highlights all cells that are attached to the slide. The green fluorescence is only visible when SYTOX green enters the cells and binds with the nucleic acids as a result of exposure to corona. In all slides, the control sample shows no appreciable green fluorescence while the cells of exposed samples fluoresces bright green which confirms that the entry of SYTOX Green molecules into the cells only occurs after exposure to corona discharge.

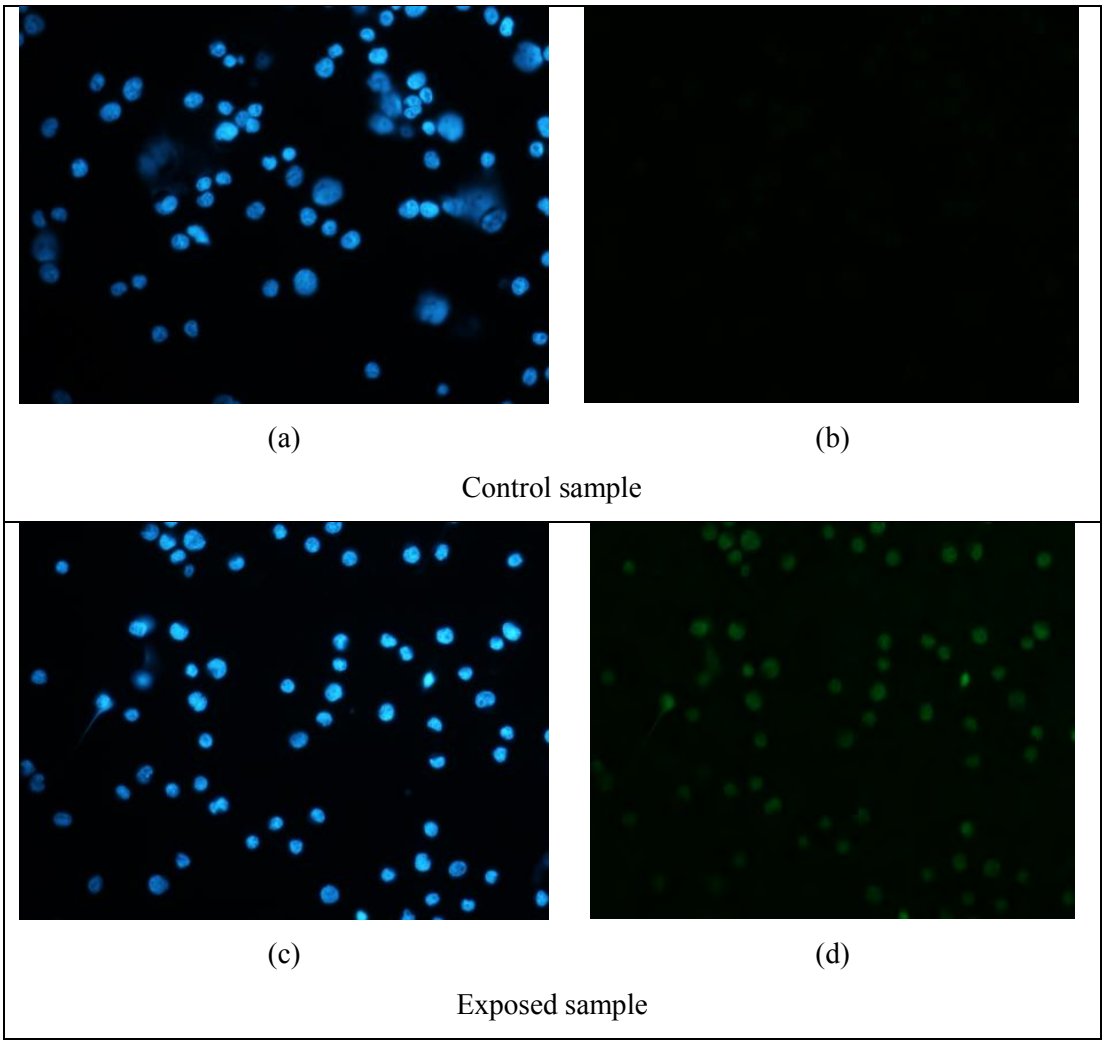

Figure 4.1: Fluorescence slides using device 1 at +5 kV DC on HeLa cells. (a) DAPI fluorescence of cells in control sample (b) SYTOX Green fluorescence of corresponding control cells (c) DAPI fluorescence of cells in exposed sample (d) SYTOX Green fluorescence of corresponding corona-exposed cells

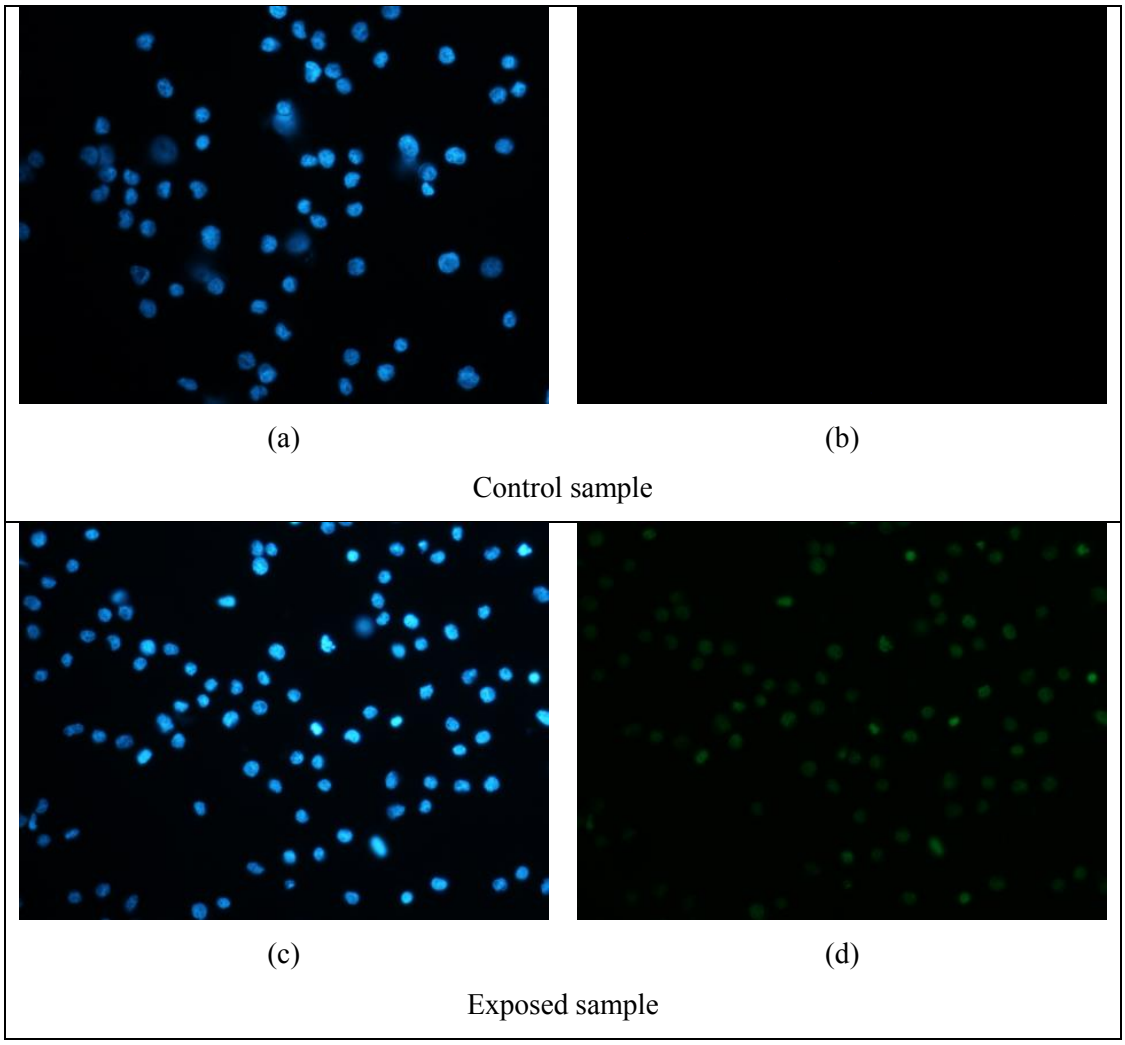

Figure 4.2: Fluorescence slides using device 1 at -5 kV on HeLa cells. (a) DAPI fluorescence of cells in control sample (b) SYTOX Green fluorescence of corresponding control cells (c) DAPI fluorescence of cells in exposed sample (d) SYTOX Green fluorescence of corresponding corona-exposed cells

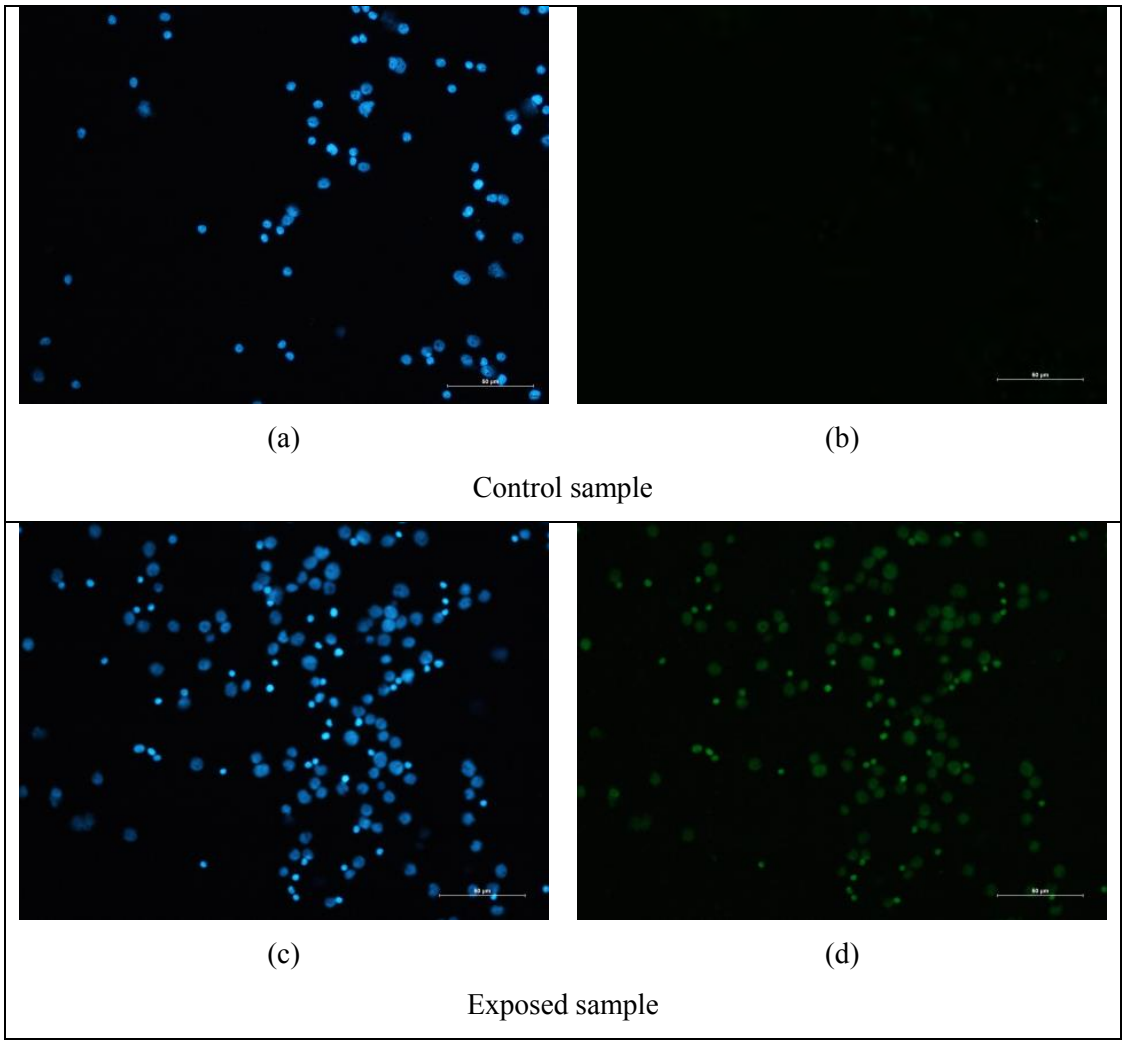

Figure 4.3: Fluorescence slides using device 1 at -7 kV DC on HeLa cells. (a) DAPI fluorescence of cells in control sample (b) SYTOX Green fluorescence of corresponding control cells (c) DAPI fluorescence of cells in exposed sample (d) SYTOX Green fluorescence of corresponding corona-exposed cells

4.4.2 Device 2

Figure 4.4 provides visual evidence of HeLa cell permeabilization for device 2 at a voltage of -7 kV DC. Here again, the green stain only shows fluorescence due to the binding of SYTOX green with nucleic acids as a result of exposure to corona. The blue stain shows all cells stained with DAPI.

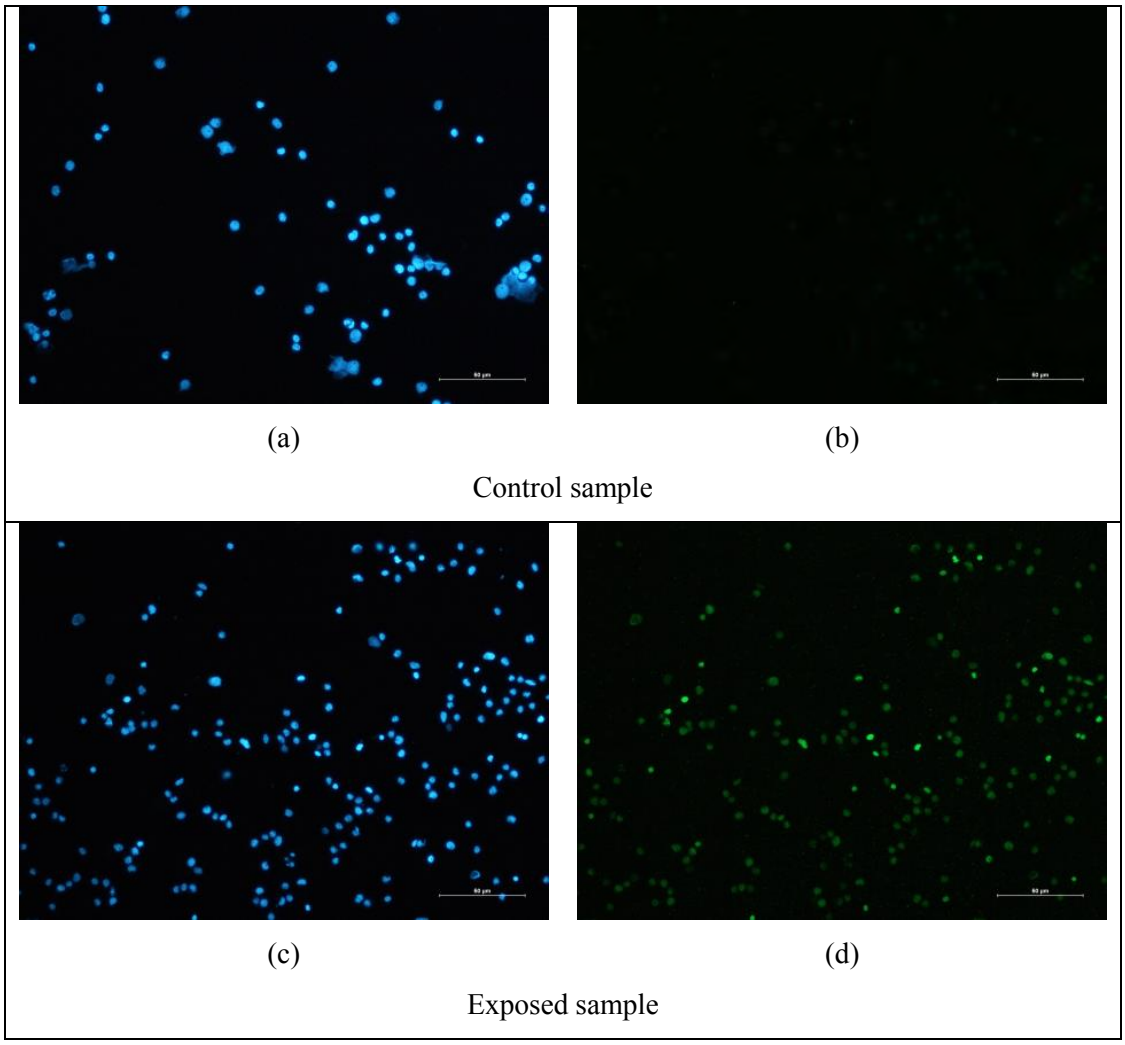

Figure 4.4: Fluorescence slides using device 2 at -7 kV DC on HeLa cells. (a) DAPI fluorescence of cells in control sample (b) SYTOX Green fluorescence of corresponding control cells (c) DAPI fluorescence of cells in exposed sample (d) SYTOX Green fluorescence of corresponding corona-exposed cells

4.4.3 Successful Visual Evidence of Molecular Delivery

It will be recalled that SYTOX Green is unable to pass through the cell membrane of cells that are in their normal physiological states. Therefore, these cells in contact with SYTOX Green will show no fluorescence when viewed under the fluorescence microscope. However, if SYTOX Green is in contact with cells with porated membranes, the molecules will enter the cell, bind with nucleic acids within the nucleus and will fluorescence bright green when excited by the 488 nm line of an argon ion laser and viewed under a microscope. Therefore, after treatment, brightly fluorescing cells imply that the cells have been permeabilized by the

corona discharge and that the SYTOX Green molecules have entered the cells. Therefore, all the slides shown do provide visual evidence of molecular delivery to HeLa cells after exposure to corona discharge with both devices 1 and 2.

4.5 Fluorescence of the Supernatant

A noteworthy phenomenon, which was more evident for higher voltages, was observed when the slides were viewed under a fluorescent microscope. Figures 4.5 - 4.7 show sections of the slide that are fluorescing. It would be expected that green fluorescence would only emanate from permeabilized cells. However, it appears that some regions of the medium actually fluoresce. It can be concluded that, due to the lysis of cells, nucleic acids may appear to have been released into the medium which then bind with SYTOX Green in solution thereby resulting in fluorescence. It is important to note that these lysed cells may not be detected during the cell viability tests using the trypan blue assay [116]. Therefore, this free DNA released by lysed cells and suspended in the medium was detected with SYTOX Green in the supernatant. Thus, a more accurate indication of the destructive effects of corona discharge on cells was obtained by a combination of the cell viability and cell lysis, to which we collectively refer to as cell destruction. This is an important contribution because the method usually used to test the deleterious effects of a procedure on cells is cell viability only using the trypan blue exclusion test. However, as has already been pointed out, using this method only has a major limitation; it does not detect lysed cells. In this study, a new method, not evident in previous literature according to our knowledge, has been devised to assess the destruction of cells.

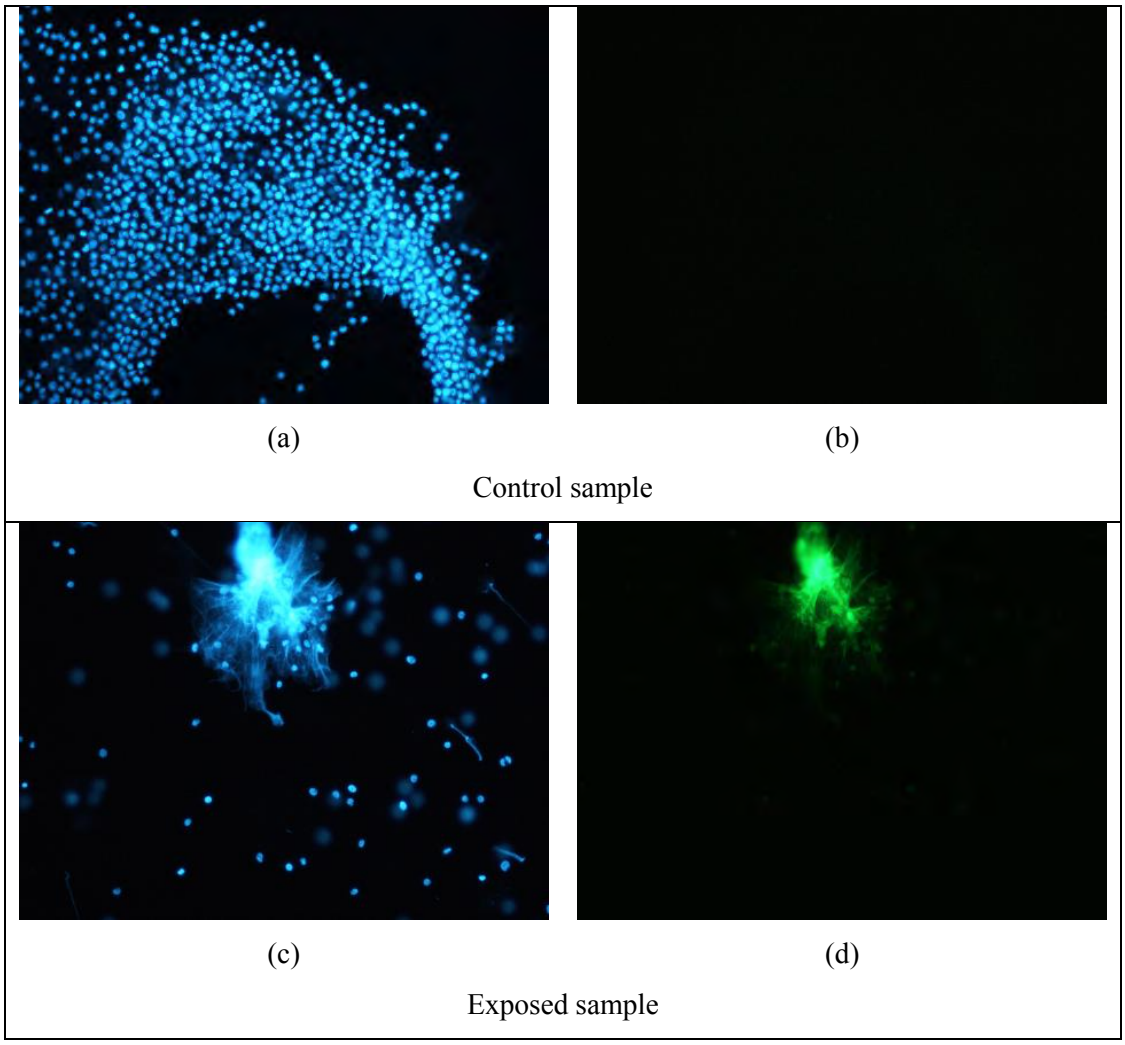

Figure 4.5: Fluorescence slides using device 2 at -6 kV DC on HeLa cells showing free DNA presumed to be due to cell lysis. (a) DAPI fluorescence of cells in control sample (b) SYTOX Green fluorescence of corresponding control cells (c) DAPI fluorescence of cells in exposed sample (d) SYTOX Green fluorescence of corresponding corona-exposed cells

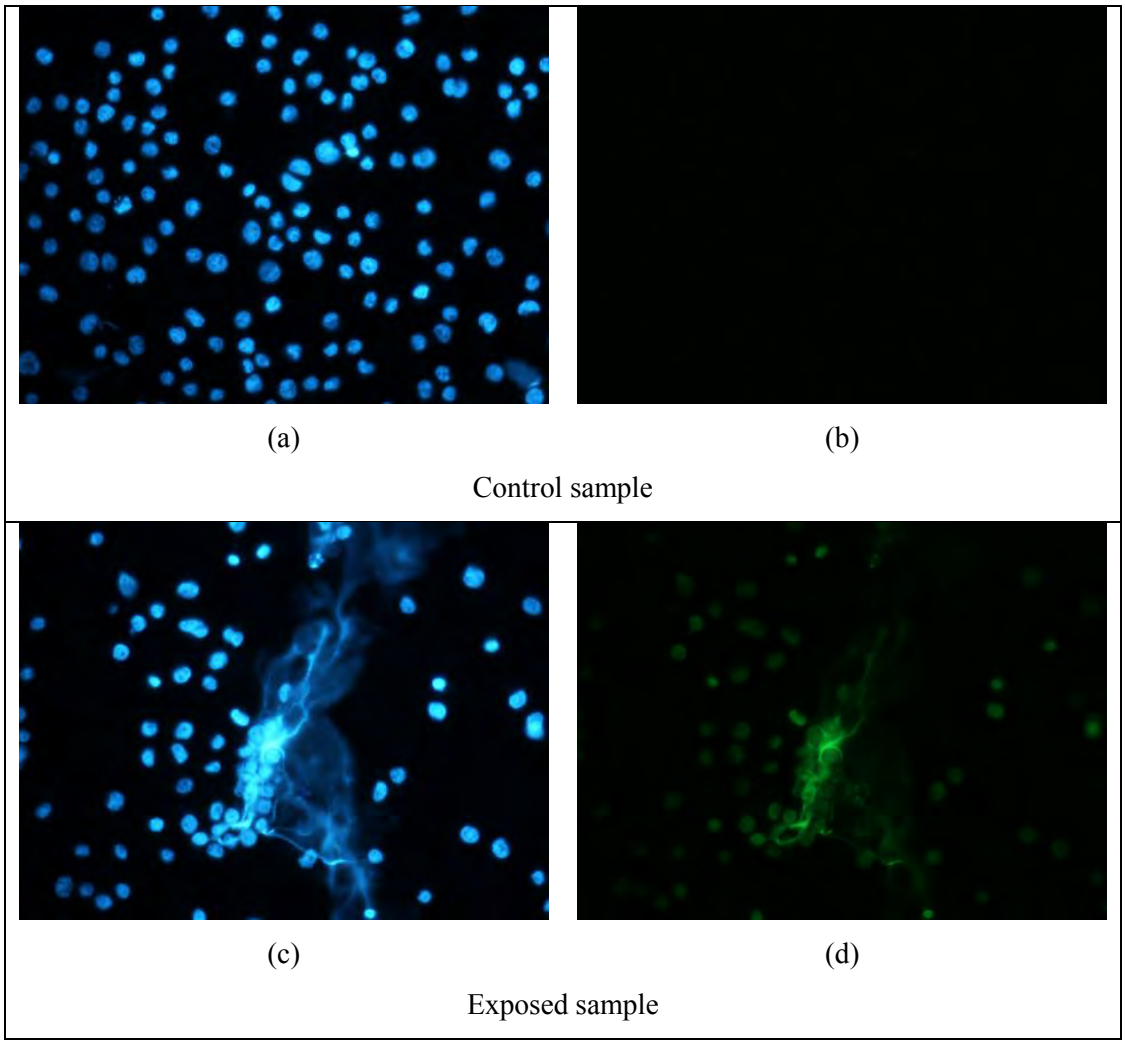

Figure 4.6: Fluorescence slides using device 1 at +7 kV DC on HeLa cells showing free DNA presumed to be due to cell lysis. (a) DAPI fluorescence of cells in control sample (b) SYTOX Green fluorescence of corresponding control cells (c) DAPI fluorescence of cells in exposed sample (d) SYTOX Green fluorescence of corresponding corona-exposed cells

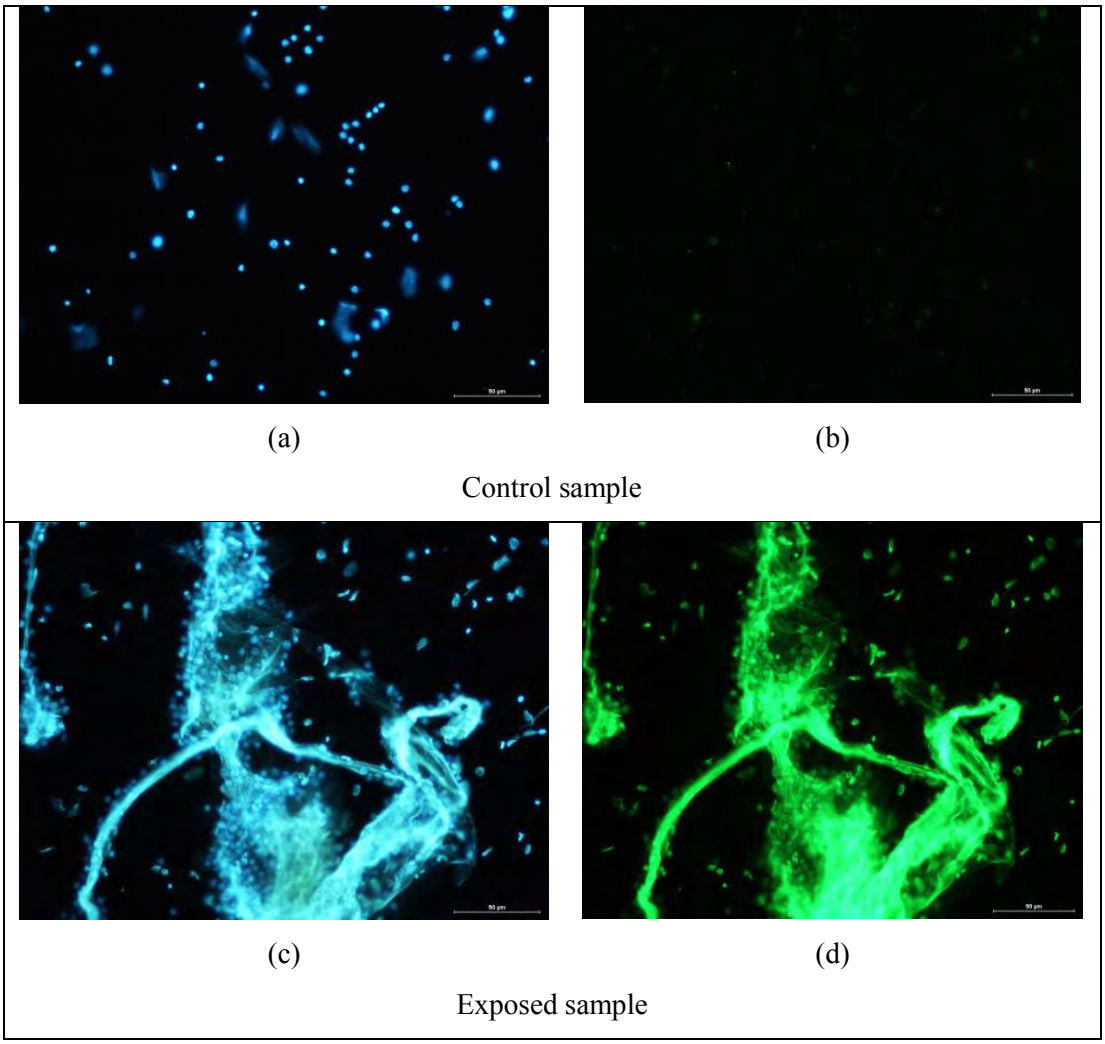

Figure 4.7: Fluorescence slides using device 2 at -7 kV DC on HeLa cells showing free DNA presumed to be due to cell lysis. (a) DAPI fluorescence of cells in control sample (b) SYTOX Green fluorescence of corresponding control cells (c) DAPI fluorescence of cells in exposed sample (d) SYTOX Green fluorescence of corresponding corona-exposed cells

4.6 Optimization of Variables

A necessary goal was to conduct accurate and reproducible experiments on HeLa cells with varying applied voltages since a review of the literature found no information in this regard. To conduct the final experiments, the variables of exposure time to corona discharge, volume of PBS during exposure, incubation time with SYTOX Green and inter-electrode distance were investigated and optimized first. These variables were identified from the trial-and-error experiments conducted previously. Initially, the values of the variables were estimated from previous trial-and-error experiments. As each experiment progressed, the optimal

values established were substituted in the subsequent experiments. For the investigation, each experiment was conducted once with fluorescence measurements made in triplicate. The results of the experiments performed to establish these optimised variables are shown in tables 4.2, 4.4, 4.6, and 4.8.

4.6.1 Exposure Time to Corona Discharge

In order to investigate the exposure time to corona discharge, some of the variables had to be kept constant at a predetermined value. After the initial trial-and-error experiments, it was established that these values produced consistent permeabilization and were therefore appropriate to be used for the optimisation experiments. These values are shown in table 4.1.

Table 4.1: The variables that are kept constant during investigation of exposure time to corona discharge

Inter-electrode Distance	15 mm
Corona Exposure Time	1 minute
Incubation Time with SYTOX Green	10 minutes
Applied Voltage	+ 6 kV DC
Volume of PBS During Exposure	100 µl
SYTOX Green Concentration	0.5 ml of 1µM solution

The results of the experiment are presented in table 4.2 and represented graphically in figures 4.8 - 4.10.

Table 4.2: Fluorescence of cells and supernatant in relation to exposure time to corona discharge

Exposure Time (Minutes)	Fluorescence of Cells (RFU)		Fluorescence of Supernatant (RFU)	
	Control	Treatment	Control	Treatment
1	1593.8	6625.0	1788.3	1998.6
2	1791.6	5594.2	1851.5	1819.3
3	1965.9	3760.7	1208.8	1723.7
4	1735.1	6932.4	1693.5	2336.1
5	1252.0	8432.8	1133.5	1701.3
6	1128.5	7553.5	1051.3	1880.5
7	1236.9	8478.8	1100.0	2015.4
8	1325.9	10058.1	1128.6	2308.6
9	1175.1	12022.3	984.6	1428.5
10	1393.7	10449.7	794.2	2588.1

Each experiment was conducted once with fluorescence measurements in triplicate. Fluorescence is expressed in relative fluorescence units (RFU).

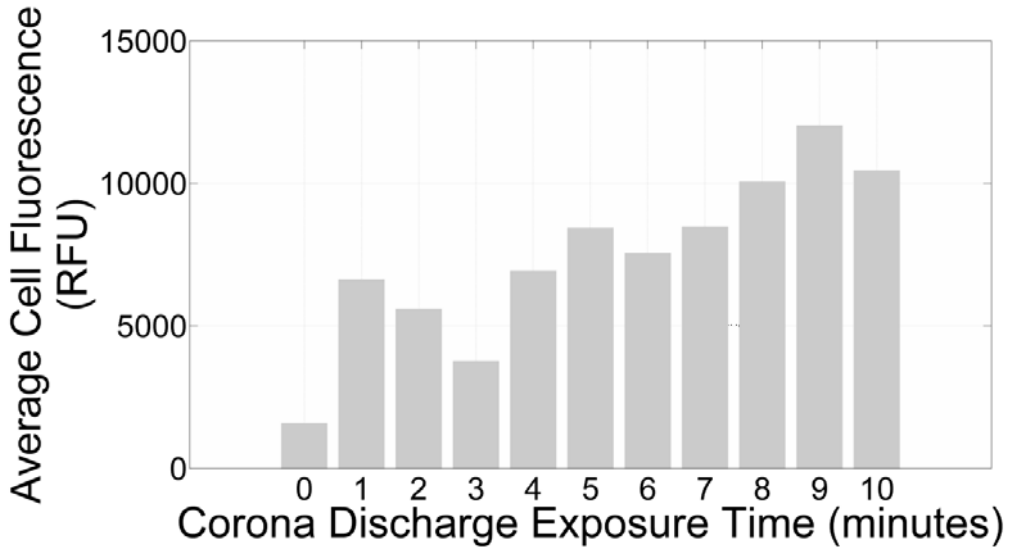

Figure 4.8: Average cell fluorescence versus exposure time

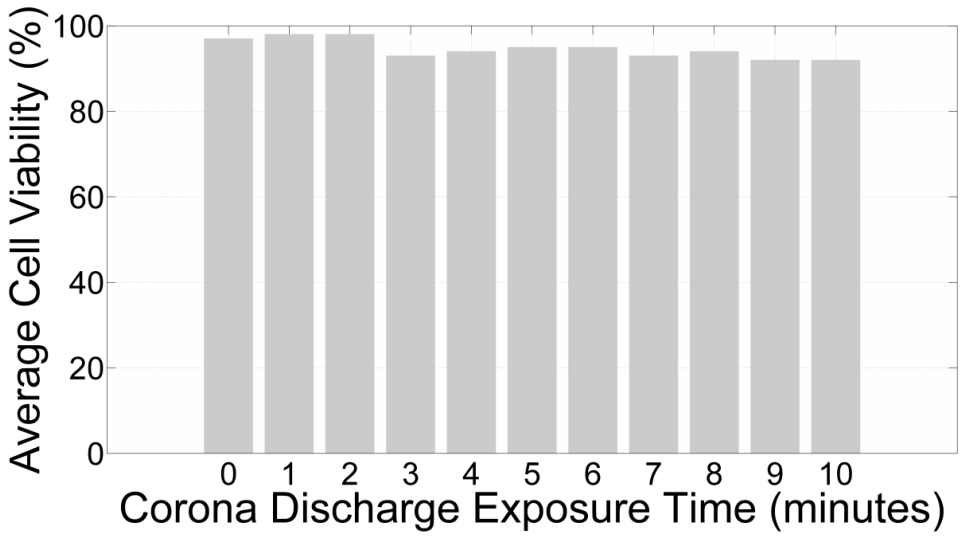

Figure 4.9: Average cell viability versus exposure time

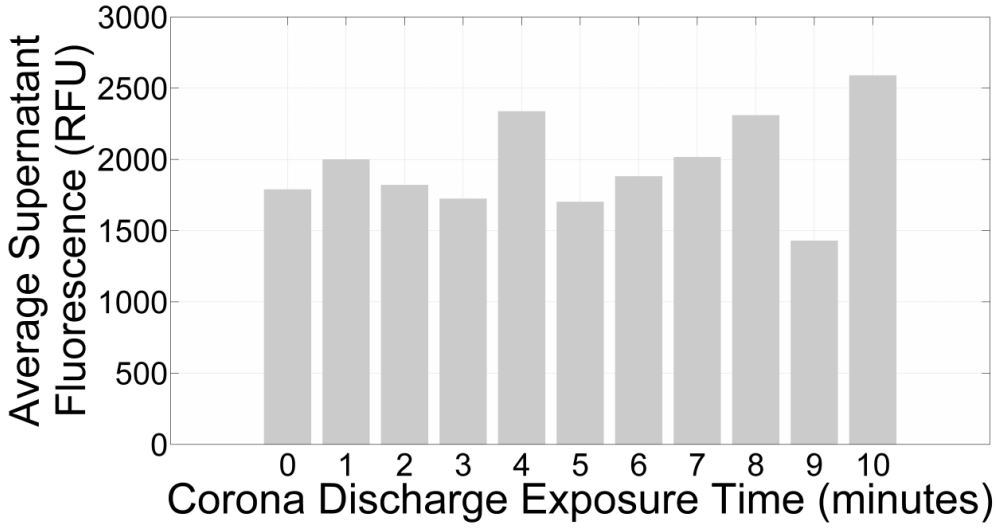

Figure 4.10: Average supernatant fluorescence versus exposure time

The fluorescence shows a tendency to increase with greater exposure times. The reduced supernatant fluorescence at 9 minutes appears to be an anomaly and is therefore treated as such. An exposure time of 7 minutes was therefore deduced, by observation, to be optimal, since, at this point, there is an acceptable balance between permeabilization and cell destruction as shown in figures 4.8 - 4.10. Cell destruction includes both cell viability shown in figure 4.9 and cell lysis shown in figure 4.10. An accurate estimation of the optimal exposure time is difficult to establish however, it is more important that the value chosen is consistent for the rest of the experiments. The complete table of results is included in Appendix VIII.

4.6.2 Volume of PBS during Exposure to Corona Discharge

In order to investigate the volume of PBS during exposure, some of the variables had to be kept constant at a predetermined value. These values were chosen from previous trial-and-error experiments that resulted in reliable cell permeabilization. These values are shown in table 4.3.

Table 4.3: The variables that are kept constant during investigation of volume of PBS

Inter-electrode Distance	15 mm
Corona Exposure Time	1 minute
Incubation Time with SYTOX Green	10 minutes
Applied Voltage	+ 6 kV DC
SYTOX Green Concentration	0.5 ml of 1 μM solution

The results of the experiment are presented in table 4.4 and represented graphically in figures 4.11 - 4.13. Preliminary experiments showed excessive drying of the cell sample and visual evidence of major destruction at volumes lower than 100 μl. Therefore, volumes lower than 100 μl were not considered in the optimisation.

Table 4.4: Fluorescence of cells in relation to volume of PBS during exposure

Volume (μl)	**Fluorescence of Cells (RFU)**		**Fluorescence of Supernatant (RFU)**	
	Control	**Treatment**	**Control**	**Treatment**
100	1593.8	6625.0	1788.3	1998.6
200	1404.0	2097.4	1144.1	1422.0
300	2007.0	1679.8	2069.2	2136.2
400	1819.5	1918.4	1819.5	1918.4

Each experiment was conducted once with fluorescence measurements in triplicate. Fluorescence is expressed in relative fluorescence units (RFU)

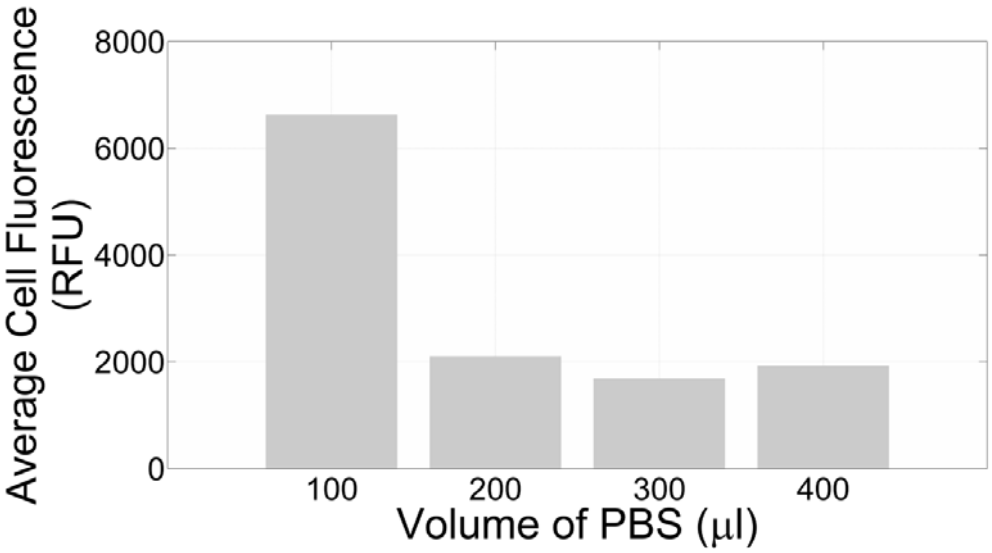

Figure 4.11: Average cell fluorescence versus volume of PBS

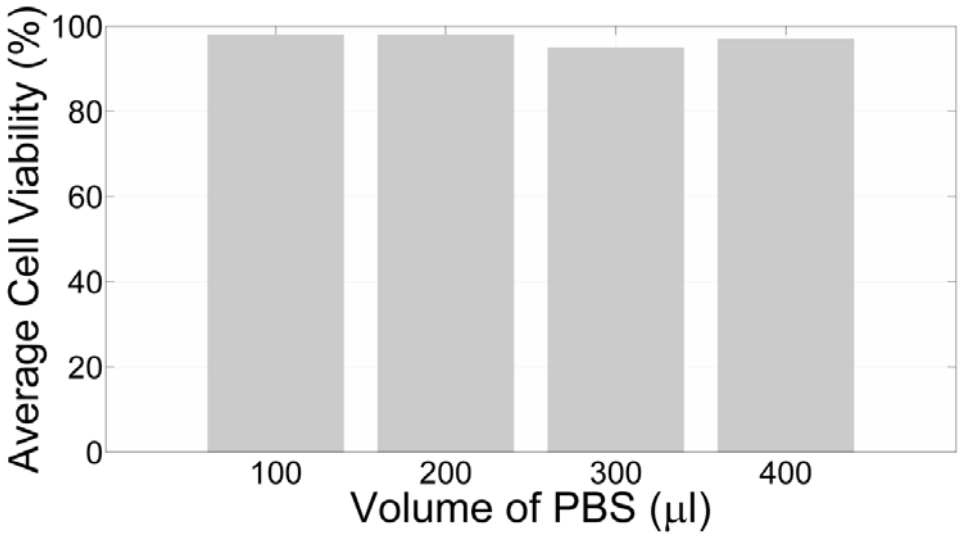

Figure 4.12: Average cell viability versus volume of PBS

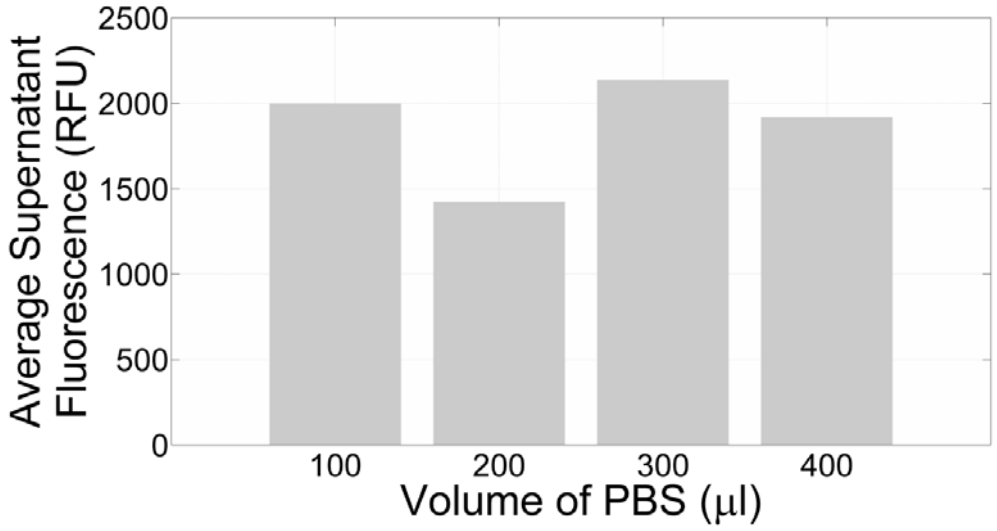

Figure 4.13: Average fluorescence of supernatant versus volume of PBS

From table 4.4 and figure 4.11 it can be seen that the greatest effect is observed at 100 µl. Fluorescence reduces sharply with an increase in volume of PBS. The cell viability and cell lysis are both acceptable at this volume as shown in figures 4.12 and 4.13. Therefore the trade-off between fluorescence and cell destruction is reasonable at 100 µl. The volume of liquid is very important with plasma-cell interactions. A low effect is observed on dry targets or targets with excess liquid while the optimal effect is obtained when the target has very little water and can be classified as just moist [38]. This confirms our findings in these experiments. Therefore, the addition of a volume of 100 µl of PBS to the cell sample before exposure was chosen for the final experiments. This is sufficient volume to just keep the cell monolayer moist. The table of results of these experiments is shown in Appendix IX

4.6.3 Incubation Time with SYTOX Green

In order to investigate the incubation time with SYTOX Green, some of the variables had to be kept constant at a predetermined value. Again, these values were chosen as a result of previous trial-and-error experiments. These values are shown in table 4.5.

Table 4.5: Variables that are kept constant during investigation of incubation time with SYTOX Green

Inter-electrode Distance	15 mm
Corona Exposure Time	1 minute
Applied Voltage	+ 6 kV DC
Volume of PBS During Exposure	100 µl
SYTOX Green Concentration	0.5 ml (1 µl SYTOX Green in 5 ml PBS mixture)

The results of the experiment are presented in table 4.6 and represented graphically in figures 4.14 - 4.16.

Table 4.6: Fluorescence of cells in relation to SYTOX Green incubation time

SYTOX Green Incubation Time (Minutes)	**Fluorescence (RFU)**	
	Control	**Treatment**
2	1600.1	6898.1
4	1562.5	10424.8
6	1445.8	6021.7
8	1536.2	6775.9
10	1297.0	5666.7

Each experiment was conducted once with fluorescence measurements in triplicate. Fluorescence is expressed in relative fluorescence units (RFU)

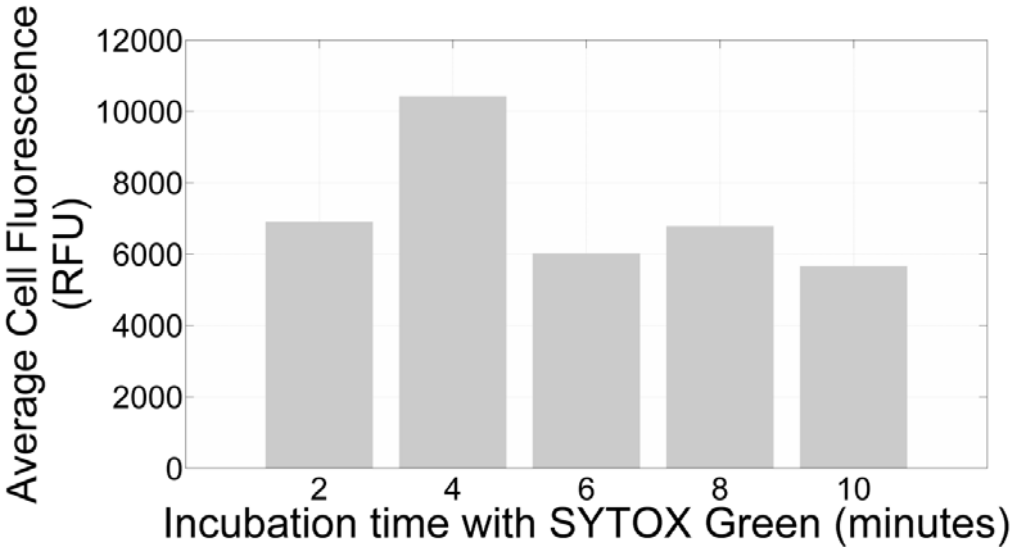

Figure 4.14: Average cell fluorescence versus incubation time with SYTOX Green

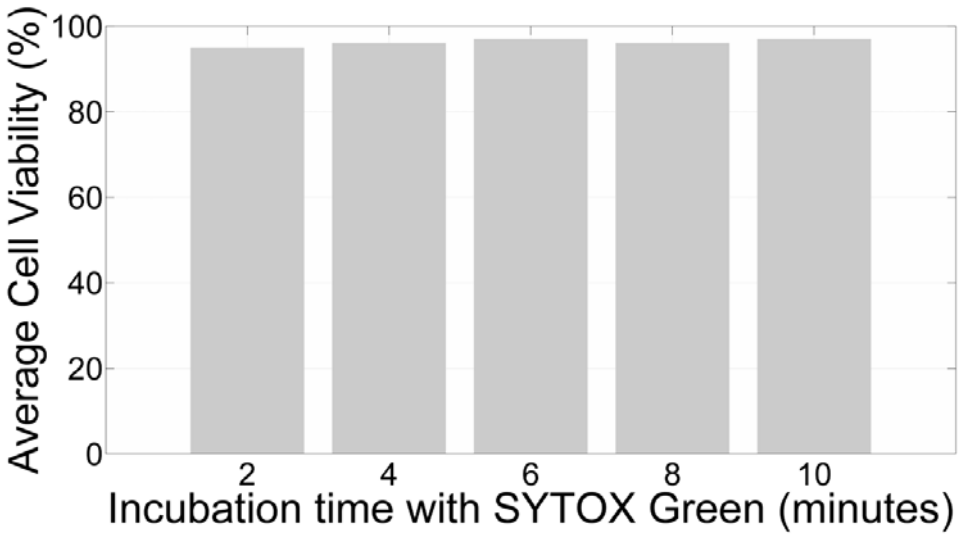

Figure 4.15: Average cell viability versus incubation time with SYTOX Green

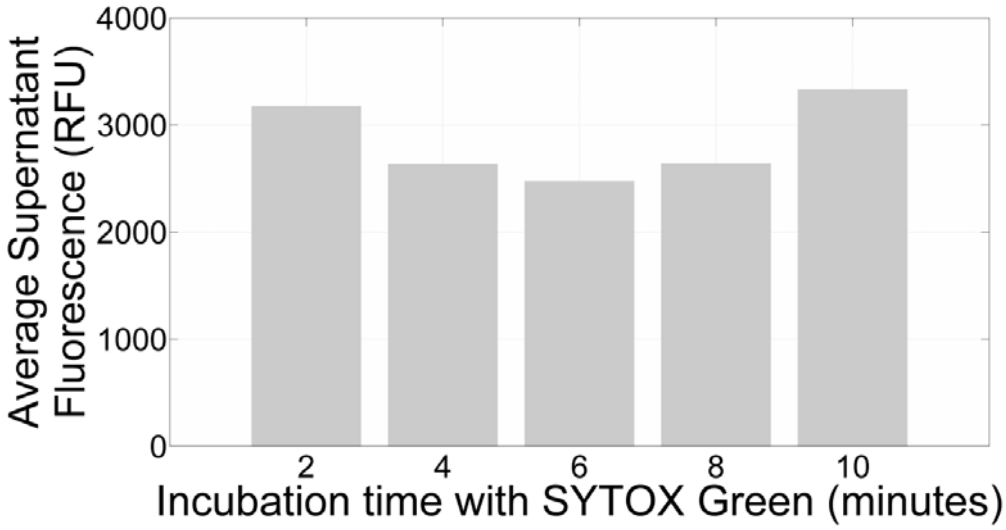

Figure 4.16: Average fluorescence of the supernatant versus incubation time with SYTOX Green

Higher incubation times with SYTOX Green do not have a major effect on cell permeabilization. This is evident from table 4.6 and figure 4.14. The cell viability and cell lysis, as shown in figures 4.15 and 4.16 respectively, are also acceptable for all incubation times. Therefore, an incubation time with SYTOX Green of two minutes was chosen for the final experiments, thereby reducing the experimental time by minimising the incubation time with SYTOX Green. This not only saves time but is also beneficial for the longevity of the cells. The results of experiments are shown in Appendix X.

4.6.4 Inter-electrode Distance

In order to investigate the effect of inter-electrode distance, some of the variables had to be kept constant at a predetermined value. Some of these values were determined from previous trial and error experiments and some were chosen from the established, optimised variables. These values are shown in table 4.7.

Table 4.7: The variables that are kept constant during the investigation of inter-electrode distance

Corona Exposure Time	7 minute
Incubation Time with SYTOX Green	2 minutes
Applied Voltage	+ 6 kV DC
Volume of PBS During Exposure	100 µl
SYTOX Green Concentration	0.5 ml (1 µl SYTOX Green in 5 ml PBS mixture)

The results of the experiment are presented in table 4.8 and represented graphically in figures 4.17 - 4.19.

Table 4.8: Fluorescence of cells in relation to inter-electrode distance

Inter-electrode Distance (mm)	**Fluorescence (RFU)**	
	Control	**Treatment**
13	1678.0	3234.9
15	1600.1	6898.1
17	1367.4	3145.6
19	1766.9	2197.5

Each experiment was conducted once with fluorescence measurements in triplicate.

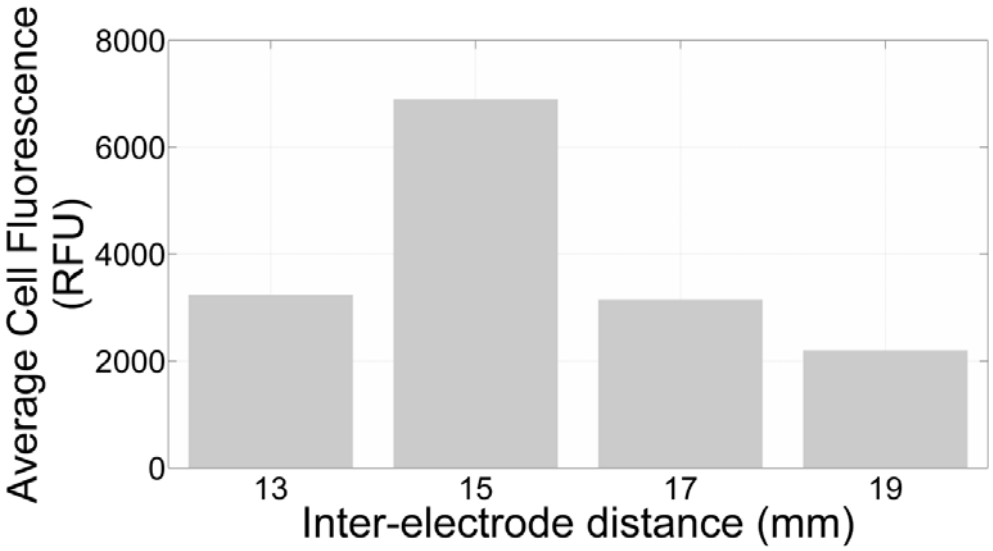

Figure 4.17: Average cell fluorescence versus inter-electrode distance

Therefore, an inter-electrode distance of 15 mm was chosen for the final experiments.

The results of experiments are shown in Appendix XI

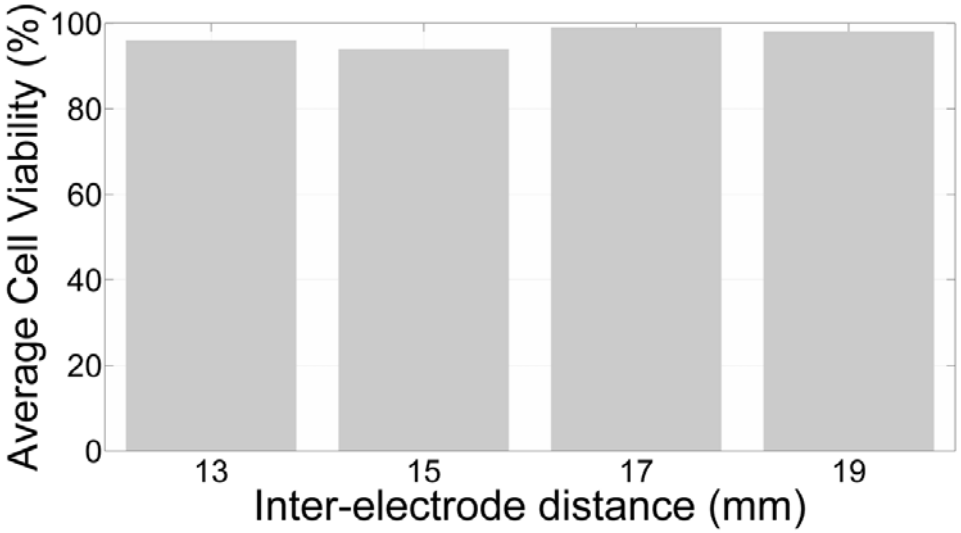

Figure 4.18: Average cell viability versus inter-electrode distance

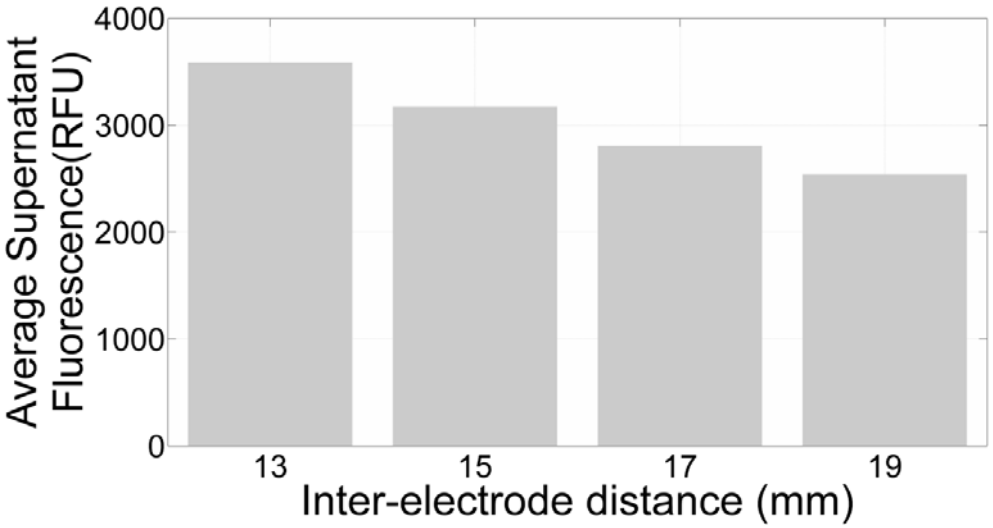

Figure 4.19: Average supernatant fluorescence versus inter-electrode distance

The inter-electrode distance has a major effect on cell permeabilization. The optimal distance for the apparatus was found to be 15 mm. This is evident from table 4.8 and figure 4.17. The cell viability and cell lysis, shown in figures 4.18 and 4.19 respectively, is also acceptable at this inter-electrode distance. Even though the cell lysis is higher at 15 mm than for the wider gaps, the trade-off between permeabilization and cell lysis is acceptable. The results of experiments are shown in Appendix XI.

4.6.5 Optimised Variables

Available literature has shown that there is limited research involving cell permeabilization with corona discharge and non-existent for this type of device and HeLa cells. It was therefore necessary to first establish and optimise the salient variables that have a major influence on the success of the experiments before continuing with the final experiments. The optimised variables, shown in table 4.9, provide a reasonable trade-off between cell permeabilization and cell destruction and these values are chosen as the optimised values to be used for future experiments.

Table 4.9: Optimised variables

Variable	Optimal Value
Exposure time to corona discharge	7 minutes
Volume of PBS during exposure	100 μl
Incubation time with SYTOX Green	2 minutes
Inter-electrode distance	15 mm

4.7 Level of Permeabilization and Cell Destruction in Relation to Applied Voltage

After the variable conditions were optimized, experiments were conducted on applied voltages of +4 kV, +5 kV, +6 KV, +7 kV and +8 kV DC. The level of permeabilization and cell destruction was investigated for these applied voltages. All experiments were conducted in triplicate and the results averaged. Fluorescence measurements for each experiment were conducted in triplicate and averaged.

Figure 4.20 shows that the general trend is an increase in cell permeabilization with an increase in applied voltage. However there is also an increase in cell destruction as proven by figures 4.21 and 4.22 which shows a decrease in cell viability and an increase in cell lysis. The table of experimental results is shown in Appendix XIII.

4.7.1 Fluorescence of Cells versus Applied Voltage

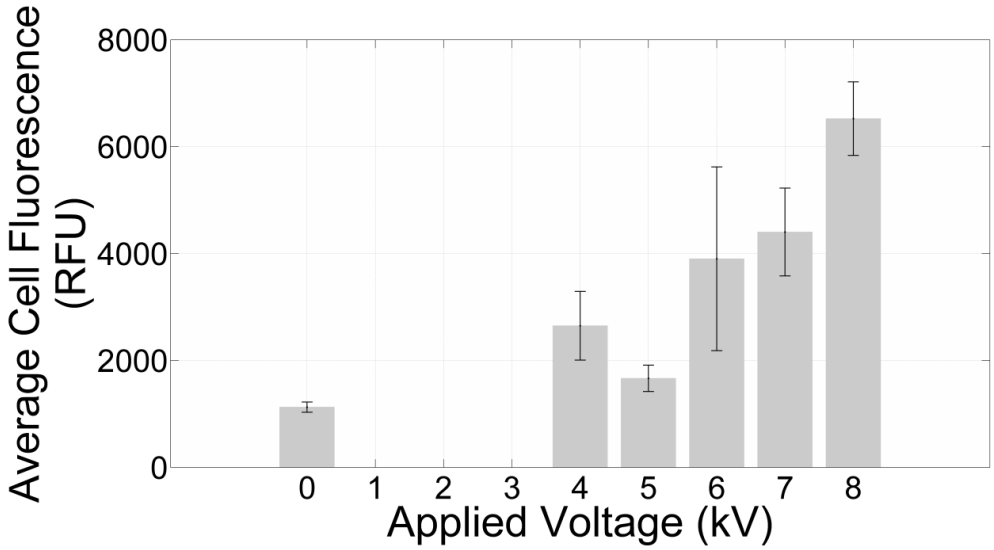

Figure 4.20: Graph of fluorescence per 250 000 cells versus applied voltage.

Each experiment was conducted three times and each bar represents the average fluorescence of three experiments. Fluorescence was measured in triplicate for each experiment. The error bars represent the standard error of the mean. Fluorescence is expressed in relative fluorescence units (RFU).

4.7.2 Cell Viability versus Applied Voltage

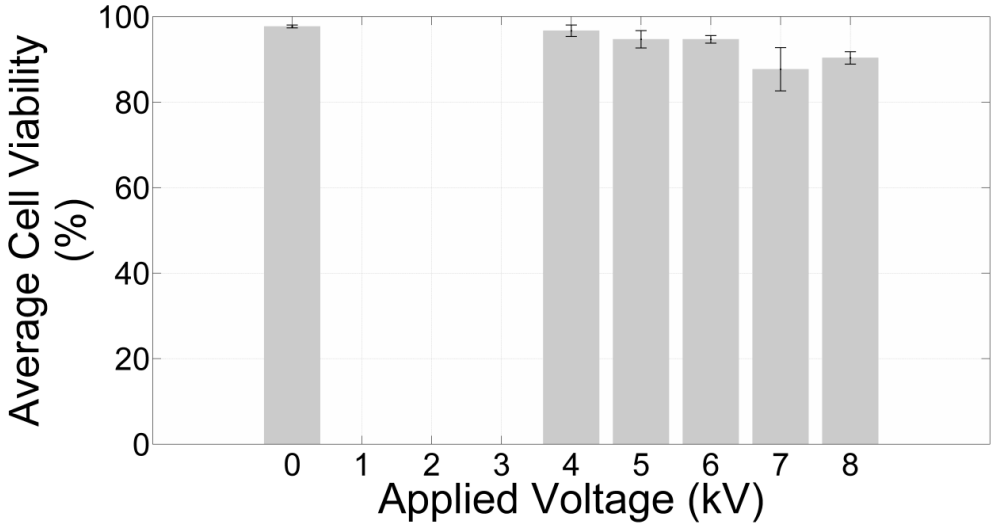

Figure 4.21: Graph of cell viability using the trypan blue assay versus applied voltage.

Each experiment was conducted three times and each bar represents the average fluorescence of three experiments. Fluorescence was measured in triplicate for each experiment. The error bars represent the standard error of the mean. Average cell viability is represented as a percentage of total cells.

4.7.3 Cell Lysis Versus Applied Voltage

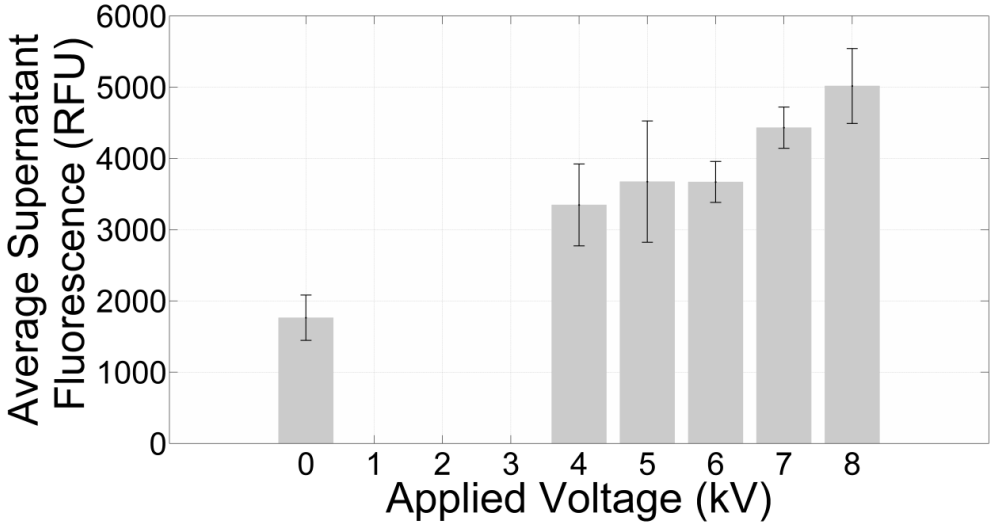

Figure 4.22: Average supernatant fluorescence versus applied voltage.

Each experiment was conducted three times and each bar represents the average fluorescence of three experiments. Fluorescence was measured in triplicate for each experiment. The error bars represent the standard error of the mean. Fluorescence is expressed in relative fluorescence units (RFU).

4.8 Analysis of the Corona Discharge Current Pulse Characteristics

This section presents an analysis of the corona discharge current pulses and attempts to find associations between these characteristics and the levels of permeabilization and cell destruction. The characteristics that were analyzed include pulse widths, pulse rise-times, pulse peak amplitudes, and pulse spacing. The characteristic frequencies of individual pulses were also calculated using the DFFT and analyzed.

4.8.1 Dependence of the Average Characteristic Frequencies of the Corona Discharge Current Pulses on Applied Voltage

Table 4.10 shows that for each applied voltage and each experiment, two characteristic frequencies of the pulses were found. These two frequencies were 9.8 MHz and 19.5 MHz. The characteristic frequencies were the same for each pulse for all applied voltages. It was concluded that the characteristic frequencies of the corona discharge current pulses did not vary with applied voltage and, therefore, did not have any effect on the levels of permeabilization and cell destruction over the range of voltages tested.

Table 4.10: Average primary and secondary characteristic frequencies for each applied voltage

Applied Voltage (kV)	Primary Characteristic Frequency (MHz)	Secondary Characteristic Frequency (MHz)
4	9.8	19.5
5	9.8	19.5
6	9.8	19.5
7	9.8	19.5
8	9.8	19.5

4.8.2 Dependence of the Average Widths of the Corona Discharge Current Pulses on Applied Voltage

Figure 4.23 illustrates the average corona pulse width for varying applied voltages. The results reveal that the average corona pulse width is fairly constant as the applied voltage increases and there is no significant dependence of the pulse width on applied voltage. Therefore, it was concluded that the average widths of the corona discharge current pulses did not have a major effect on the levels of permeabilization and cell destruction over the range of voltages tested. This observation is consistent with the findings of 4.8.1, in which it was found that the characteristics frequencies of the pulses is constant and therefore has no effect on cell permeabilization.

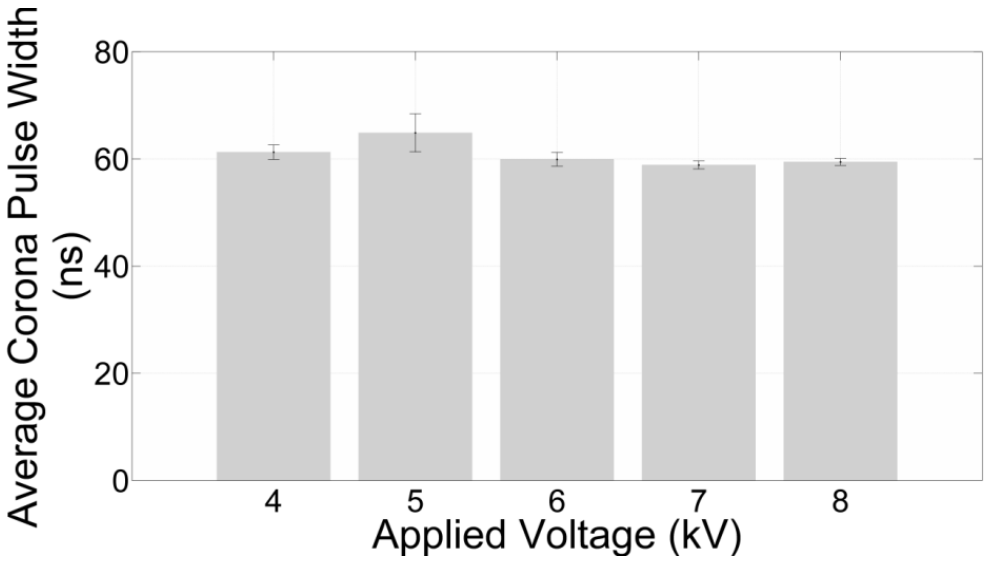

Figure 4.23: Average corona discharge current pulse width versus applied voltage.

The error bars represent the standard error of the mean. The table of experimental results are shown in Appendix XVIII

4.8.3 Dependence of the Average Rise-times of the Corona Discharge Current Pulses on Applied Voltage

Figure 4.24 illustrates the average corona pulse rise-time for varying applied voltages. The results reveal that the relationship between the corona pulse rise-time and applied voltage is relatively constant and proves that the rise-time of the pulses is not dependent on the applied voltage. Therefore, it was concluded that the average rise-times of the corona discharge

current pulses did not have any appreciable effect on the levels of permeabilization and cell destruction over the range of voltages tested.

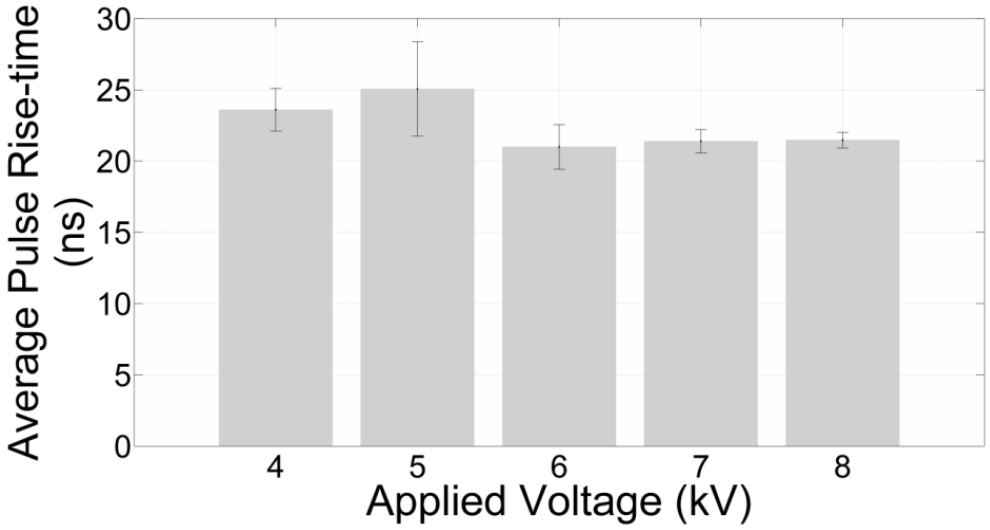

Figure 4.24: Average corona discharge current pulse rise-time versus applied voltage.

The error bars represent the standard error of the mean. The table of experimental results are shown in Appendix XVIII.

4.8.4 Dependence of the Average Peak Amplitudes of the Corona Discharge Current Pulses on Applied Voltage

Figure 4.25 illustrates the average corona pulse peak amplitude for varying applied voltages. The results reveal that, for our experiments, and for the voltages tested, even though there is noticeable variation, there is no dependence of the average pulse magnitude on the applied voltage. It was therefore concluded that the average peak amplitudes of the corona discharge current pulses did not have a significant effect on the levels of permeabilization and cell destruction over the range of voltages tested.

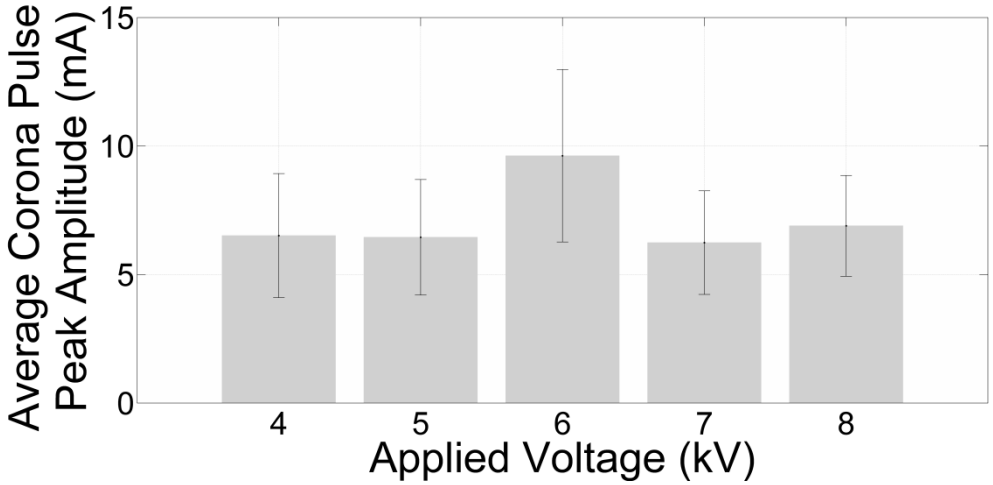

Figure 4.25: Average corona discharge current pulse peak amplitude versus applied voltage.

The error bars represent the standard error of the mean.

The table of experimental results is shown in Appendix XIX.

4.8.5 Dependence of the Average Spacing of the Corona Discharge Current Pulses on Applied Voltage

Figure 4.26 illustrates the average corona pulse spacing for varying applied voltages. The results reveal that the spacing between corona pulses varies appreciably with applied voltage. Except for applied voltages of 5 kV, which might be an anomaly, the general trend is a decrease in the corona pulse spacing as applied voltage increases. It was therefore concluded that the average spacing of the corona discharge current pulses was the only analyzed characteristic that was found to have a significant effect on the levels of permeabilization and cell destruction over the range of voltages tested.

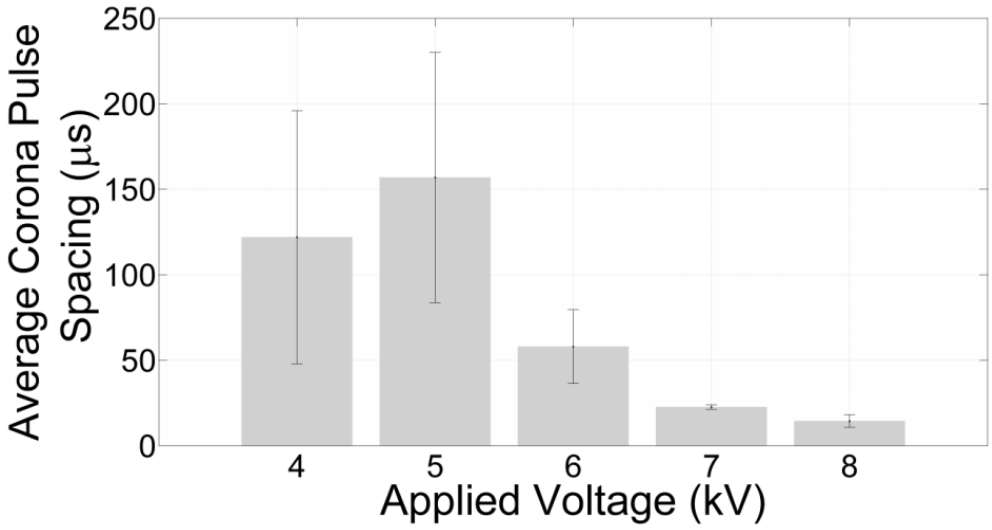

Figure 4.26: Average corona discharge current pulse spacing versus applied voltage.

The error bars represent the standard error of the mean. The table of experimental results is shown in Appendix XIX.

4.8.6 Dependence of the Level of Permeabilization on the Average Spacing of the Corona Discharge Current Pulses

As mentioned in 4.8.5, the only characteristic of the corona discharge current pulses found to vary appreciably with applied voltage was the pulse spacing. Therefore, an attempt was made to establish a relationship between this characteristic and the levels of cell permeabilization and cell destruction. Figure 4.27 is a graph of the average cell fluorescence versus average corona discharge pulse spacing. It is clear that the level of molecular delivery to cells is dependent on the corona discharge current pulse spacing. The smaller the pulse spacing (that is, a greater frequency of the pulses), then the greater the level of molecular delivery to cells.

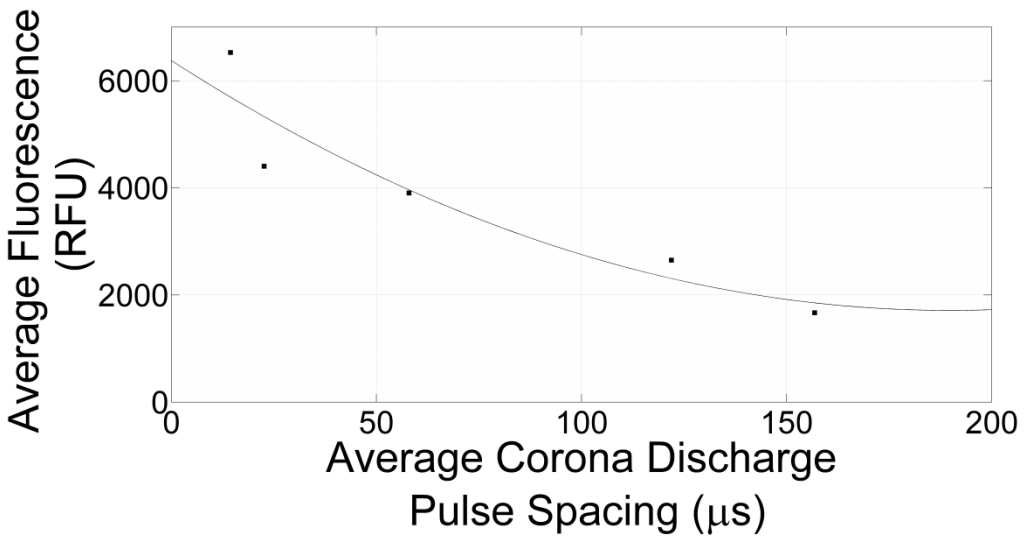

Figure 4.27: Dependence of average cell fluorescence on the average corona discharge current pulse spacing.

A second order polynomial curve is fitted through the points for best fit. This relationship can be important for calibration of corona-generating instruments. Depending on the application, different concentrations of molecules are required to be transferred to cells. For example, different drugs might require to be administered in different concentrations for optimal effect

4.8.7 Dependence of the Level of Cell Destruction on the Average Spacing of the Corona Discharge Current Pulses

Figure 4.28 shows that the cell viability decreases with smaller average corona discharge pulse spacing. The figure also shows that cell lysis increases with smaller average corona discharge pulse spacing as evident by increasing fluorescence of the supernatant. Therefore, it can be concluded that the smaller the pulse spacing (that is, a greater number of pulses per unit time), then the greater the level of cell destruction.

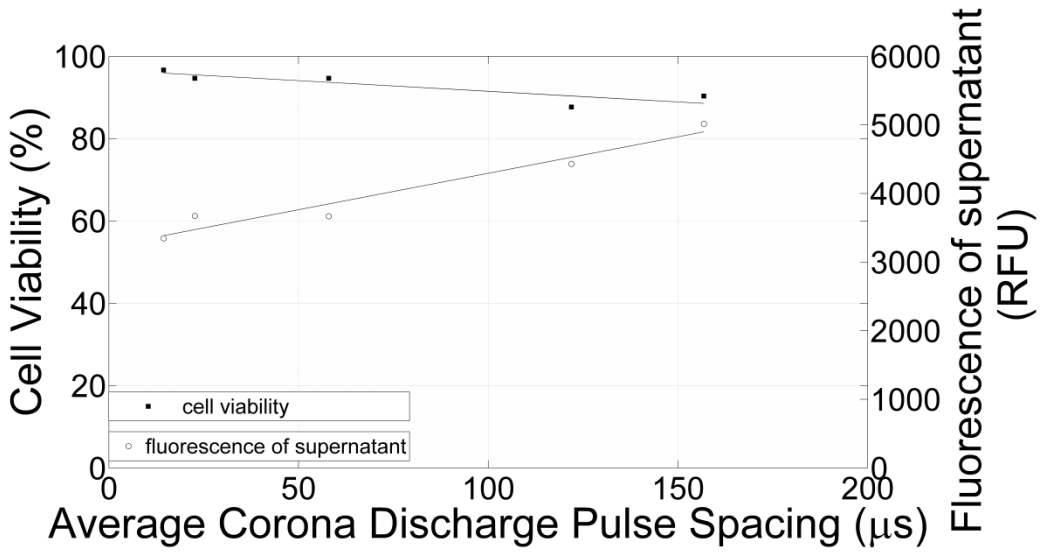

Figure 4.28: Dependence of cell viability and cell lysis on the average corona discharge pulse spacing.

Straight lines are fitted through the points for best fit. These linear relationships are also important in calibrating corona-generating instruments. Certain applications are more stringent and require lower levels of cell destruction. For example, in cancer treatment, minimal damage to healthy cells is required whereas, in some genetic engineering applications, only a small number of permeabilized cells are required and little attention is paid to the destroyed cells.

4.8.8 Discussion on the Analysis of the Corona Discharge Current Pulses

It has been observed that the levels of molecular transfer and cell destruction tend to increase with increasing applied voltage as demonstrated by the experimental results. The corona discharge current pulse characteristics were analyzed in an attempt to identify the characteristics that are related to the levels of permeabilization and cell destruction for the chosen cell line and the instrument that was designed and constructed. Guided by a review of the literature on conventional electroporation, the characteristics of the corona discharge current pulses that were investigated were the average pulse widths, average pulse rise-times, average pulse amplitudes, average pulse spacing, and average characteristic frequencies of single pulses. The analysis shows that, for our atmospheric-air corona-producing device and for the voltages investigated, the only characteristic that varied significantly with the applied voltage was the average corona discharge current pulse spacing. There is a direct relationship between molecular delivery to cells, and the average corona discharge pulse spacing. Smaller

pulse spacing, which means a greater pulse repetition rate, favours a greater degree of cell permeabilization. Furthermore, a greater pulse repetition rate is related to a lower cell viability and greater cell lysis which, combined, relate to a higher level of cell destruction.

Literature on the conventional form of electroporation proves that the number of applied pulses directly affects the permeabilization and destruction of cells [27, 62, 95]. We have established that the repetition rate of the corona pulses in a corona discharge has a direct bearing on the degree of cell permeabilization and cell destruction which is an important contribution to knowledge. The importance of this fact is that, for a particular corona-generating instrument and application it is more reliable and accurate to utilize the characteristics of the corona discharge current pulses to tune the device to suit a particular application. In our case, the characteristic that was found to have the greatest effect was the repetition rate of the pulses.

4.9 Proposed Theory on the Mechanism of DC Corona Electroporation

One of the contributions of this study is the proposal of a theory of the mechanism of DC corona electroporation.

For the conventional form of electroporation, pore formation in the membrane due to an electrical impulse is as a result of the influence of the electric field on the charges and dipoles of the membrane lipid molecules. Each lipid molecule in the cell membrane has a polar and a non-polar part [85]. The electric field reconfigures the charges and dipoles in the lipid molecules, thereby increasing dipole moments in the direction of the field [67]. A polarisation mechanism is therefore assumed to be responsible for the change in permeability of the membrane [92]. As a result, rearrangement of the lipid molecules occurs, which results in the formation of pores in the membrane [67]. Neumann et al. [67] found that the polar head was capable of independent movement, a result also confirmed by Stulen [121] and Lopez et al. [122]. This independent movement of the polar head due to the applied electric field and the subsequent reorientation of the lipid molecules results in the formation of pores which is illustrated in figure 4.29

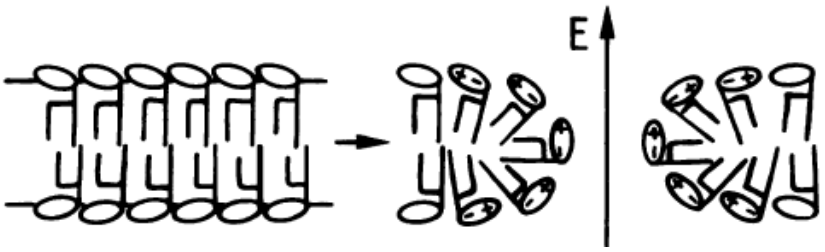

Figure 4.29: Pore formation in the cell membrane [67]

This theory of the interaction of the electric fields with the lipid molecules can be extended to corona discharge. Of all the species produced in the plasma, it was speculated that the ions play a major role in the interaction of plasmas with cells and their main effect is on the cell membrane [38]. Ramachandran et al. [42] briefly proposed two possible methods of the interaction of the ions with the cell membrane. First, it was thought that, due to the deposition of ions on the sample, an electric field results in the conductive culture medium which results in pore formation in the cell membranes. The second theory is that when the ionic current flows through the culture media, the ions exchange charge with the cell membrane, thereby resulting in pore formation in the cell membrane.

One of the main findings of our research was that the level of cell permeabilization is dependent on the repetition rate of the corona discharge pulses. The larger the applied voltage, the greater the repetition rate of the corona discharge pulses. In positive corona, positive ions, produced as a result of electron avalanches, accumulate in the gap and are responsible for the corona current pulses [43]. A greater corona current pulse repetition rate results in a greater concentration of ions. It can therefore be concluded, as a result of our experimental results, that the effect on cell membranes due to corona discharge is largely as a result of the action of the ions that are produced. Since pore formation in cell membranes is due to the effects of electric fields, it is a reasonable assumption that the ions produced result in an increased transmembrane electric field. A plausible theory for cell membrane permeabilization due to corona discharge is that, for positive corona discharge, as used in our investigation, positive ions settle onto the adherent monolayer of HeLa cells. A single cell within a corona discharge is shown in figure 4.30. This is a reasonable assumption because the cells are not submerged in the liquid. Only 100 μl of PBS was added, just enough to keep the cell monolayer moist.

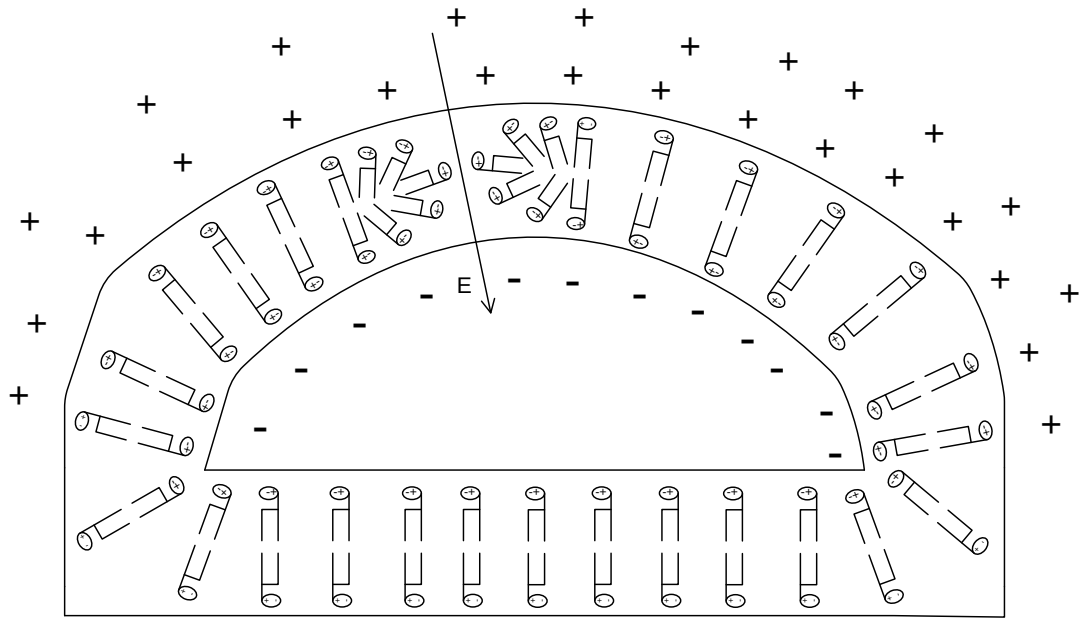

Figure 4.30: Distribution of ions on cell surface and within the cell

The positive corona ions on the surface of the cell attract the negative ions within the intracellular electrolyte towards the cell membrane, thereby creating a transmembrane electric field. This resultant field interacts with the dipoles of the phospholipids in a mechanism similar to that of electroporation, causing them to move, forming pores.

4.10 Conclusion

Because the exact procedure and protocols required for these devices and cell lines were unknown, numerous experiments, under different conditions, were conducted in which the procedures and protocols were modified and improved until a concise, efficient and accurate method was established. The evolution of the experimental technique was documented. A discussion of the choice of device and cell line used during the final experiments is also provided.

The course of these experiments also identified the salient variables that had an influence on the success of the procedure, which were unknown at the commencement of the study. These variables were also optimised to provide reliable molecular delivery with minimal cell

destruction. The variables that were identified and optimised were exposure time to corona discharge, volume of PBS during exposure, Incubation time with SYTOX Green, and inter-electrode distance. Thereafter, the analysis of the corona discharge current pulses is discussed in detail. The characteristics of the corona discharge current pulses that have a profound effect on the levels of molecular delivery and cell destruction are identified and discussed. It was established that, for our corona-generating device, the only characteristic of the corona discharge current pulses that varied with increasing applied voltage was the repetition rate of the pulses. It was further demonstrated that, as the applied voltage increased, so too did the repetition rate of the current pulses. An increasing repetition rate resulted in increasing molecular delivery as well as an increasing associated cell destruction.

Fluorescent slides of cell samples after experiments were also prepared and presented. These slides provided visual proof of cell permeabilization after exposure to corona discharge. In all cases, only cells exposed to corona discharge were penetrated by the SYTOX Green molecules.

Finally, a theory of the mechanism of positive DC corona electroporation is also proposed in which it is proffered that the ions created during the corona discharge current pulses induce a pulsed electric field across the cell membrane, thereby interacting with the dipoles of the lipid molecules and resulting in pore formation in the membrane.

CHAPTER 5

Conclusions and Recommendations for Future Work

5.1 Introduction

Cancer is one of the leading causes of mortality worldwide and there exists great motivation to devise effective treatments and cures. The methods of cancer treatment include the two methods, electrochemotherapy and gene therapy, that are being increasingly utilised. A technique called electroporation is a necessary part of electrochemotherapy and is being increasingly used in gene therapy. Electroporation is a procedure that uses high voltage electrodes applied directly to the treatment area. As a result, electric fields are applied across the cell membrane resulting in the formation of pores through which molecules can pass. It is a well-established and accepted technique and is often used to transfer molecules like drugs and genetic material to cells for therapeutic applications. This technique, however, has some disadvantages. A viable alternative of applying the electric fields, in our opinion, is the use of corona discharge which is non-contact and has low associated current. The available literature shows very little research has been undertaken in this regard previously and the results of our investigation is an important step in leading to further research in the field of DC corona electroporation, possibly evolving it into an accepted technique.

In an attempt to prove the feasibility of this technique, the research questions that we attempted to answer in this investigation were:

- What are the characteristics of the corona discharge current pulses that affect both molecular delivery to cells and the associated cell destruction?
- What is the mechanism behind the interaction of the corona discharge with the cell membrane?

To answer these questions, a multipoint-to-plane atmospheric-air corona-generating device was designed and constructed to investigate permeabilization of cells. The results of this study are applicable to this corona-generating device and cell lines used.

5.2 Conclusions

5.2.1 Successful Permeabilization of a Cell Line of Human Origin

This investigation was successful at demonstrating molecular delivery to a cell line of human origin. The molecular delivery was proven by both the measurement of increased fluorescence of SYTOX Green as well as visual observation of this increased fluorescence using fluorescent microscopy. According to our knowledge and supported by a review of the literature, molecular delivery to a cell line of human origin due to exposure to corona discharge has not been demonstrated before.

5.2.2 Different Cell Lines

It was established that the success of this procedure is dependent on the cell line, as has been demonstrated by our experiments. Three different cell lines were tested; Vero cells, MT4 cells and HeLa cells. Vero cells are an animal cell line harvested from the kidney of a green monkey while MT4 and HeLa cells are of human origin. The MT4 cell is a T-lymphocyte cell while the HeLa cell line is an immortalised, cervical cancer cell. Numerous experiments on these cell lines have yielded positive results for the HeLa cell line only. This shows that corona discharge is selective at permeabilizing different cell lines. Future research might possibly produce a variation in the method and/or configuration of the instrument that might result in success at permeabilizing the other cell lines.

5.2.3 Identification and Optimisation of Variables

In a multipoint-to-plane configuration, there are different variables that affect the levels of permeabilization and cell destruction. Our laboratory experiments have identified these variables as exposure time to corona discharge, incubation time with SYTOX Green, volume of liquid during exposure, and inter-electrode distance. Further experiments have assessed the optimal values of these variables. These optimized variables resulted in reliable cell permeabilization with minimal damage to cells.

5.2.4 Effect of Magnitude of Applied Voltage

Once the optimized conditions were obtained, the effect of different applied voltages on the

level of cell permeabilization and the short-term destructive effects on cells were investigated. The general trend is an increase in fluorescence and therefore, permeabilization, with an increase in applied voltage. Even though higher levels of permeabilization were obtained with an increase in applied voltage, this increase in voltage also resulted in greater cell destruction. It is therefore important that, when employing the method of atmospheric-air corona discharge for cell permeabilization, the optimal set of variables are established thereby ensuring a reasonable trade-off between cell permeabilization and cell destruction. This would allow for greater efficiency when the technique is adapted and utilized for molecular delivery applications like drug delivery and genetic engineering.

5.2.5 Effect of the Characteristics of the Corona Discharge Current Pulses

The corona discharge current pulses were also analyzed in an attempt to identify the characteristics of the pulses that were related to the levels of permeabilization and destruction. These characteristics of the corona pulses included amplitudes, repetition rates, widths, and rise-times. The characteristic frequency of single pulses, obtained from the application of a DFFT, was also analyzed. The analysis shows that, for our corona-generating device and for the voltages chosen, the only characteristic that varied significantly with the applied voltage is the average corona discharge current pulse spacing. There is a direct relationship between both cell permeabilization and cell destruction, and the average corona discharge pulse spacing. Smaller pulse spacing, and therefore, a greater pulse repetition rate favours a greater degree of cell permeabilization. Furthermore, a greater pulse repetition rate is related to a greater level of cell destruction. A higher pulse repetition rate would result in a greater total pulsed electric field applied across the cell membrane per unit time. It is therefore surmised that this would result in a higher degree of cell permeabilization and cell destruction.

When setting the parameters for a particular corona-generating instrument and application, one cannot rely on using the magnitude of the applied voltage as a means of controlling cell permeabilization and destruction since the characteristics of the corona discharge tends to vary. It is more reliable to utilize the characteristics of the corona discharge pulses to tune the device to suit a particular application.

5.2.6 A New Method of Assessing Cell Destruction

Another important contribution of this study is that previous research studies reported cell viability with standard protocols like the trypan blue exclusion assay. It is insufficient to report on cell viability measured in this manner only since these methods measure the viability of clearly defined cells. During exposure to corona discharge, it appears that some of the cells were lysed because there was a noticeable increase in the fluorescence of the supernatant. This increase in fluorescence may be attributed to the release of DNA due to cell lysis. A relationship between the fluorescence of the supernatant and the applied voltage has therefore been presented as a marker for cell lysis. A more accurate indication of cell destruction is therefore obtained from a combination of cell viability and cell lysis. Cell viability tends to decrease with increasing applied voltage and cell lysis tends to increase with increasing applied voltage. This implies that cell destruction due to exposure to corona discharge tended to increase with increasing applied voltage.

5.2.7 Proposed Theory of the Interaction of Corona Discharge with the Cell Membrane

A theory behind the mechanism of DC corona electroporation is also proposed. In essence, the basic theory is that the corona pulses produce ions during their existence, which result in a pulsed electric field across the cell membrane. Just as in the conventional form of electroporation, this electric field interacts with the dipoles of the lipid molecules causing their reorientation and therefore resulting in the formation of pores in the membrane.

5.3 Recommendations for Future Work

5.3.1 Different Cell Lines

In this investigation, three different cell lines were tried but success was only obtained with one, the HeLa cell line. This alludes to the fact that corona discharge is selective at permeabilizing different cell lines. However, further investigation in this area is warranted to either discover the reason why or to reattempt permeabilization by varying the conditions and/or configuration of the device.

5.3.2 Nature of Applied Voltage

In initial investigations, different voltages were attempted which included positive DC, negative DC, and positive and negative square waves. However, due to time constraints, the final experiments were conducted using positive DC only. Further experimentation should include investigations of negative DC as well as square waves. These voltages might offer improved corona electroporation.

5.3.3 Larger Molecules

In our investigation, we have used SYTOX Green molecules which are relatively small. Genetic material like DNA and RNA are somewhat larger molecules and therefore, it would be necessary for future work to include molecular delivery of larger molecules like nucleic acids.

5.3.4 Equivalent Circuit Analysis

Accurate determination of the electrical parameters of a cell is important for investigations on the interaction of cell membranes with electric fields. Future work would include the determination of an equivalent circuit of a cell sample within a corona discharge. Experimental measurements of the total impedance of the device under test can be determined which can then be used to approximate the parameters of the equivalent circuit thereby approximating the two important electrical characteristics of the cell; the cell membrane capacitance and the resistance of the intracellular fluid. An iterative computer programme will be written to approximate the parameters of the circuit from measured impedance values.

REFERENCES

[1] J. C. Weaver, “Electroporation - a General Phenomenon for Manipulating Cells and Tissues,” *J. Cell. Biochem.,* vol. 51, no. 4, pp. 426-435, Apr, 1993.

[2] G. A. Hughes, “Nanostructure-mediated drug delivery,” *Nanomedicine: NBM,* vol. 1, pp. 9, 2005.

[3] "Global Markets and technologies for Advanced Drug Delivery Systems," 18 November, 2015; http://www.bccresearch.com/market-research/pharmaceuticals/advanced-drug-delivery-markets-phm006j.html/.

[4] T. Sobh, and K. Elleithy, "Emerging Trends in Computing, Informatics, Systems Sciences, and Engineering," New York: Springer, 2013.

[5] J. Gehl, "Drug and Gene Electrotransfer in Cancer Therapy," *Somatic Genome Manipulation*, X.-Q. Li, D. J. Donnelly and T. G. Jensen, eds., pp. 3-15: Springer New York, 2015.

[6] "Fact Sheet No. 297," 18 November 2015; http://www.who.int/mediacentre/factsheets/fs297/en/.

[7] A. Gothelf, L. M. Mir, and J. Gehl, “Electrochemotherapy: results of cancer treatment using enhanced delivery of bleomycin by electroporation,” *Cancer Treat. Rev.,* vol. 29, no. 5, pp. 371-387, Oct, 2003.

[8] M. L. Yarmush, A. Golberg, G. Sersa, T. Kotnik, and D. Miklavcic, “Electroporation-based technologies for medicine: principles, applications, and challenges,” *Annu. Rev. Biomed. Eng.,* vol. 16, pp. 295-320, Jul 11, 2014.

[9] J. A. Roth, and R. J. Cristiano, “Gene therapy for cancer: what have we done and where are we going?,” *J. Natl. Cancer Inst.,* vol. 89, no. 1, pp. 21-39, 1997.

[10] D. Cross, and J. K. Burmester, “Gene therapy for cancer treatment: past, present and future,” *Clin. Med. Res.,* vol. 4, no. 3, pp. 218-227, 2006.

[11] M. S. Markov, *Electromagnetic Fields in Biology and Medicine*: CRC Press, 2015.

[12] D. Miklavcic, G. Sersa, E. Brecelj, J. Gehl, D. Soden, G. Bianchi, P. Ruggieri, C. R. Rossi, L. G. Campana, and T. Jarm, “Electrochemotherapy: technological advancements for efficient electroporation-based treatment of internal tumors,” *Med. Biol. Eng. Comput.,* vol. 50, no. 12, pp. 1213-25, Dec, 2012.

[13] G. Sersa, D. Miklavcic, M. Cemazar, Z. Rudolf, G. Pucihar, and M. Snoj, “Electrochemotherapy in treatment of tumours,” *Eur. J. Surg. Oncol.,* vol. 34, no. 2, pp. 232-40, Feb, 2008.

[14] S. Li, "Electroporation for drug and gene delivery in the clinic: doctors go electric," *Electroporation Protocols: Preclinical and clinical Gene Medicine in Methods in Molecular Biology*, J. Gehl, ed.: Humana Press, 2008.

[15] S. Sasaki, M. Kanzaki, and T. Kaneko, "Highly efficient and minimally invasive transfection using time-controlled irradiation of atmospheric-pressure plasma," *Appl. Phys. Express,* vol. 7, 2014.

[16] D. Ibrahhem, Elaissari, A., and Fessi, H., "Gene therapy and DNA delivery systems," *Int. J. Pharm.,* vol. 459, pp. 70-83, 2014, 2014.

[17] K. Kamimura, T. Suda, D. Zhang, and D. Liu, "Advances in Gene Delivery Systems," *Pharm. Med.,* vol. 25, no. 5, pp. 293-306, 2011.

[18] Y. Sakai, V. Khajoee, Y. Ogawa, K. Kusuhara, Y. Katayama, and T. Hara, "A novel transfection method for mammalian cells using gas plasma," *J. Biotechnol.,* vol. 121, 2006.

[19] F. Andre, and L. M. Mir, "DNA electrotransfer: its principles and an updated review of its therapeutic applications," *Gene Ther.,* vol. 11 Suppl 1, pp. S33-42, Oct, 2004.

[20] J. Gehl, "Electroporation for drug and gene delivery in the clinic: doctors go electric," *Methods Mol. Biol.,* vol. 423, pp. 351-9, 2008, 2008.

[21] X. Gao, K.-S. Kim, and D. Liu, "Nonviral gene delivery: What we know and what is next," *AAPS J.,* vol. 9, no. 1, pp. E92-E104, 2007/03/01, 2007.

[22] D. Wells, "Gene therapy progress and prospects: electroporation and other physical methods," *Gene Ther.,* vol. 11, no. 18, pp. 1363-1369, 2004.

[23] J. Gehl, "Electroporation: theory and methods, perspectives for drug delivery, gene therapy and research," *Acta Physiol. Scand.,* vol. 177, no. 4, pp. 437-47, Apr, 2003.

[24] J. C. Weaver, "Electroporation of cells and tissues," *IEEE Trans. on Plasma Sci.,* vol. 28, no. 1, pp. 24-33, Feb, 2000.

[25] T. Y. Tsong, "Electroporation of Cell-Membranes," *Biophys. J.,* vol. 60, no. 2, pp. 297-306, Aug, 1991.

[26] R. Benz, F. Beckers, and U. Zimmermann, "Reversible electrical breakdown of lipid bilayer membranes: a charge-pulse relaxation study," *J. Membr. Biol.,* vol. 48, no. 2, pp. 181-204, Jul 16, 1979.

[27] T. K. Wong, and E. Neumann, "Electric field mediated gene transfer," *Biochem. Biophys. Res. Commun.,* vol. 107, no. 2, pp. 584-7, Jul 30, 1982.

[28] L. Mir, "Electroporation-Based Gene Therapy: Recent Evolution in the Mechanism Description and Technology Developments," *Electroporation Protocols*, Methods in

Molecular Biology S. Li, J. Cutrera, R. Heller and J. Teissie, eds., pp. 3-23: Springer New York, 2014.

[29] T. Kotnik, W. Frey, M. Sack, S. H. Meglič, M. Peterka, and D. Miklavčič, "Electroporation-based applications in biotechnology," *Trends Biotechnol.,* vol. 33, no. 8, pp. 480-488, 2015.

[30] R. Vanbever, and V. V. Preat, "In vivo efficacy and safety of skin electroporation," *Adv. Drug Deliv. Rev.,* vol. 35, no. 1, pp. 77-88, Jan 4, 1999.

[31] L. Zhang, and D. Rabussay, "Clinical evaluation of safety and human tolerance of electrical sensation induced by electric fields with non-invasive electrodes," *Bioelectrochemistry,* vol. 56, no. 1, pp. 233-236, 2002.

[32] M. Wallace, B. Evans, S. Woods, R. Mogg, L. Zhang, A. C. Finnefrock, D. Rabussay, M. Fons, J. Mallee, and D. Mehrotra, "Tolerability of two sequential electroporation treatments using MedPulser DNA delivery system (DDS) in healthy adults," *Mol. Ther.,* vol. 17, no. 5, pp. 922-928, 2009.

[33] M. R. Prausnitz, "The effects of electric current applied to skin: a review for transdermal drug delivery," *Adv. Drug Delivery Rev.,* vol. 18, no. 3, pp. 395-425, 1996.

[34] I. Mathiesen, "Electropermeabilization of skeletal muscle enhances gene transfer in vivo," *Gene Ther.,* vol. 6, no. 4, pp. 508-514, Apr, 1999.

[35] P. Lefesvre, J. Attema, and D. van Bekkum, "A comparison of efficacy and toxicity between electroporation and adenoviral gene transfer," *BMC Mol. Biol.,* vol. 3, no. 1, pp. 12, Aug 13, 2002.

[36] W. S. Meaking, J. Edgerton, C. W. Wharton, and R. A. Meldrum, "Electroporation-induced damage in mammalian cell DNA," *(BBA)-Gene Structure and Expression,* vol. 1264, no. 3, pp. 357-362, Dec 27, 1995.

[37] J. Pinero, M. Lopez-Baena, T. Ortiz, and F. Cortes, "Apoptotic and necrotic cell death are both induced by electroporation in HL60 human Promyeloid leukemia cells," *Apoptosis,* vol. 2, no. 3, pp. 330-336, May, 1997.

[38] D. Dobrynin, G. Fridman, G. Friedman, and A. Fridman, "Physical and biological mechanisms of direct plasma interaction with living tissue," *New J. Phys.,* vol. 11, Nov 26, 2009.

[39] G. Fridman, G. Friedman, A. Gutsol, A. B. Shekhter, V. N. Vasilets, and A. Fridman, "Applied plasma medicine," *Plasma Processes Polym.,* vol. 5, no. 6, pp. 503-533, Aug 15, 2008.

[40] M. G. Kong, G. Kroesen, G. Morfill, T. Nosenko, T. Shimizu, J. van Dijk, and J. L. Zimmermann, "Plasma medicine: an introductory review," *New J. Phys.,* vol. 11, Nov 26, 2009.

[41] R. J. Connolly, G. A. Lopez, A. M. Hoff, and M. J. Jaroszeski, "Characterization of plasma mediated molecular delivery to cells in vitro," *Int. J. Pharm.,* vol. 389, no. 1-2, pp. 53-57, Apr 15, 2010.

[42] N. Ramachandran, M. Jaroszeski, and A. M. Hoff, "Molecular delivery to cells facilitated by corona ion deposition," *IEEE Trans. NanoBiosci.,* vol. 7, no. 3, pp. 233-239, Sep, 2008.

[43] W. N. English, "Positive and Negative Point-to-Plane Corona in Air," *Phys. Rev.,* vol. 74, no. 2, pp. 170-178, Jul, 1948.

[44] M. Yousfi, A. Bekstein, N. Merbahi, O. Eichwald, O. Ducasse, M. Benhenni, and J. P. Gardou, "Basic data for atmospheric pressure non-thermal plasma investigations in environmental and biomedical applications," *Plasma Sources Sci. Technol.,* vol. 19, no. 3, Jun, 2010.

[45] M. Yousfi, N. Merbahi, A. Pathak, and O. Eichwald, "Low-temperature plasmas at atmospheric pressure: toward new pharmaceutical treatments in medicine," *Fundam. Clin. Pharmacol.,* vol. 28, no. 2, pp. 123-135, Apr, 2014.

[46] N. Ramachandran, "Corona Ion Deposition: A Novel Non-Contact Method for Drug and Gene Delivery to Living Systems," Department of Chemical & Biomedical Engineering, University of South Florida, 2008.

[47] A. Abou-Ghazala, S. Katsuki, K. H. Schoenbach, F. Dobbs, and K. Moreira, "Bacterial decontamination of water by means of pulsed-corona discharges," *IEEE Trans. Plasma Sci.,* vol. 30, no. 4, pp. 1449-1453, August, 2002.

[48] M. Korachi, Z. Turan, K. Senturk, F. Sahin, and N. Aslan, "An investigation into the biocidal effect of high voltage AC/DC atmospheric corona discharges on bacteria, yeasts, fungi and algae," *J. Electrostat.,* vol. 67, no. 4, pp. 678-685, Jul, 2009.

[49] D. Dobrynin, G. Friedman, A. Fridman, and A. Starikovskiy, "Inactivation of bacteria using dc corona discharge: role of ions and humidity," *New J. Phys.,* vol. 13, Oct 24, 2011.

[50] N. Goodman, and J. F. Hughes, "The effect of corona discharge on dust mite and cat allergens," *J. Electrostat.,* vol. 60, no. 1, pp. 69-91, Jan, 2004.

[51] R. Cramariuc, A. Tudorache, M. Popa, E. Branduse, L. Nisiparu, A. Mitelut, M. Turtoi, and L. Fotescu, "Corona discharge in electroporation of cell membranes," in Journal of Physics: Conference Series, 2008, pp. 012062.

[52] T. Kotnik, P. Kramar, G. Pucihar, D. Miklavcic, and M. Tarek, "Cell Membrane Electroporation-Part 1: The Phenomenon," *IEEE Electr. Insul. Mag.,* vol. 28, no. 5, pp. 14-23, Sep-Oct, 2012.

[53] G. L. Prasanna, and T. Panda, "Electroporation: Basic principles, practical considerations and applications in molecular biology," *Bioprocess. Eng.,* vol. 16, no. 5, pp. 261-264, Apr, 1997.

[54] J. C. Weaver, and Y. A. Chizmadzhev, "Theory of electroporation: a review," *Bioelectrochem. Bioenerg.,* vol. 41, no. 2, pp. 135-160, Dec, 1996.

[55] F. Apollonio, M. Liberti, P. Marracino, and L. Mir, "Electroporation mechanism: Review of molecular models based on computer simulation," in Antennas and Propagation (EUCAP), 2012 6th European Conference on, 2012, pp. 356-358.

[56] E. H. Serpersu, K. Kinosita, Jr., and T. Y. Tsong, "Reversible and irreversible modification of erythrocyte membrane permeability by electric field," *(BBA)-Biomembranes,* vol. 812, no. 3, pp. 779-85, Feb 14, 1985.

[57] U. Zimmermann, and R. Benz, "Dependence of the Electrical Breakdown Voltage on the Charging Time in Valonia-Utricularis," *J. Membr. Biol.,* vol. 53, no. 1, pp. 33-43, Feb, 1980.

[58] H. G. L. Coster, "A Quantitative Analysis of Voltage-Current Relationships of Fixed Charge Membranes and Associated Property of Punch-Through," *Biophys. J.,* vol. 5, no. 5, pp. 669-&, 1965.

[59] H. G. L. Coster, and U. Zimmermann, "Mechanism of Electrical Breakdown in Membranes of Valonia-Utricularis," *J. Membr. Biol.,* vol. 22, no. 1, pp. 73-90, Dec, 1975.

[60] A. Sale, and W. Hamilton, "Effects of high electric fields on microorganismsI. Killing of bacteria and yeasts," *(BBA) - General Subjects,* vol. 148, no. 3, pp. 781-788, Dec, 1967.

[61] A. J. Sale, and W. A. Hamilton, "Effects of high electric fields on micro-organisms. 3. Lysis of erythrocytes and protoplasts," *(BBA) - Biomembranes,* vol. 163, no. 1, pp. 37-43, Aug, 1968.

[62] Y. Mouneimne, P. F. Tosi, Y. Gazitt, and C. Nicolau, "Electro-Insertion of Xeno-Glycophorin into the Red Blood-Cell Membrane," *Biochem. Biophys. Res. Commun.,* vol. 159, no. 1, pp. 34-40, Feb 28, 1989.

[63] R. Vanbever, N. Lecouturier, and V. Preat, "Transdermal delivery of metoprolol by electroporation," *Pharm. Res.,* vol. 11, no. 11, pp. 1657-62, Nov, 1994.

[64] M. Fromm, L. P. Taylor, and V. Walbot, "Expression of Genes Transferred into Monocot and Dicot Plant-Cells by Electroporation," *Proc. Natl. Acad. Sci. U. S. A.,* vol. 82, no. 17, pp. 5824-5828, September, 1985.

[65] T.-M. Ou-Lee, R. Turgeon, and R. Wu, "Expression of a foreign gene linked to either a plant-virus or a Drosophila promoter, after electroporation of protoplasts of rice, wheat, and sorghum," *Proc. Nat. Acad. Sci. U.S.A.,* vol. 83, no. 18, pp. 6815-6819, Sep, 1986.

[66] D. W. Ow, J. D. E. Wet, D. R. Helinski, S. H. Howell, K. V. Wood, and M. Deluca, "Transient and stable expression of the firefly luciferase gene in plant cells and transgenic plants," *Science,* vol. 234, no. 4778, pp. 856-9, Nov 14, 1986.

[67] E. Neumann, M. Schaeferridder, Y. Wang, and P. H. Hofschneider, "Gene-Transfer into Mouse Lyoma Cells by Electroporation in High Electric-Fields," *EMBO J.,* vol. 1, no. 7, pp. 841-845, 1982.

[68] R. Heller, M. Jaroszeski, A. Atkin, D. Moradpour, R. Gilbert, J. Wands, and C. Nicolau, "In vivo gene electroinjection and expression in rat liver," *FEBS Lett.,* vol. 389, no. 3, pp. 225-228, Jul 8, 1996.

[69] R. Bergan, Y. Connell, B. Fahmy, and L. Neckers, "Electroporation Enhances C-Myc Antisense Oligodeoxynucleotide Efficacy," *Nucleic Acids Res.,* vol. 21, no. 15, pp. 3567-3573, Jul 25, 1993.

[70] H. Aihara, and J. Miyazaki, "Gene transfer into muscle by electroporation in vivo," *Nat. Biotechnol.,* vol. 16, no. 9, pp. 867-70, Sep, 1998.

[71] R. L. Harrison, B. J. Byrne, and L. Tung, "Electroporation-mediated gene transfer in cardiac tissue," *FEBS Lett.,* vol. 435, no. 1, pp. 1-5, Sep 11, 1998.

[72] G. Chu, H. Hayakawa, and P. Berg, "Electroporation for the efficient transfection of mammalian cells with DNA," *Nucleic Acids Res.,* vol. 15, no. 3, pp. 1311-26, Feb 11, 1987.

[73] Y. Zhao, Z. Zheng, C. J. Cohen, L. Gattinoni, D. C. Palmer, N. P. Restifo, A. Rosenberg, and R. A. Morgan, "High-efficiency Transfection of Primary Human and Mouse T Lymphocytes Using RNA Electroporation," *Mol. Ther.,* vol. 13, no. 1, pp. 151-159, Jan, 2006.

[74] Q. A. Zheng, and D. C. Chang, "High-efficiency gene transfection by in situ electroporation of cultured cells," *Biochim. Biophys. Acta,* vol. 1088, no. 1, pp. 104-10, Jan 17, 1991.

[75] M. Okino, and H. Mohri, "Effects of a High-Voltage Electrical Impulse and an Anticancer Drug on Invivo Growing Tumors," *Jpn. J. Cancer Res.,* vol. 78, no. 12, pp. 1319-1321, Dec, 1987.

[76] L. M. Mir, S. Orlowski, J. Belehradek, and C. Paoletti, "Electrochemotherapy Potentiation of Antitumor Effect of Bleomycin by Local Electric Pulses," *Eur. J. Cancer,* vol. 27, no. 1, pp. 68-72, 1991.

[77] M. Hyacinthe, M. J. Jaroszeski, V. V. Dang, D. Coppola, R. C. Karl, R. A. Gilbert, and R. Heller, "Electrically enhanced drug delivery for the treatment of soft tissue sarcoma," *Cancer,* vol. 85, no. 2, pp. 409-417, Jan 15, 1999.

[78] L. H. Ramirez, S. Orlowski, D. An, G. Bindoula, R. Dzodic, P. Ardouin, C. Bognel, J. Belehradek, J. N. Munck, and L. M. Mir, "Electrochemotherapy on liver tumours in rabbits," *Br. J. Cancer,* vol. 77, no. 12, pp. 2104-2111, Jun, 1998.

[79] S. Orlowski, J. Belehralek Jr., C. Paoletti, and L. M. Mir, "Transient Electropermeabilization of Cells in Culture: increase in cytotoxicity of anticancer drugs," *Biochem. Pharmacol.,* vol. 37, no. 24, pp. 4727-4733, Dec, 1988.

[80] M. Marty, G. Sersa, J. R. Garbay, J. Gehl, C. G. Collins, M. Snoj, V. Billard, P. F. Geertsen, J. O. Larkin, D. Miklavcic, I. Pavlovic, S. M. Paulin-Kosir, M. Cemazar, N. Morsli, D. M. Soden, Z. Rudolf, C. Robert, G. C. O'Sullivan, and L. M. Mir, "Electrochemotherapy-An easy, highly effective and safe treatment of cutaneous and subcutaneous metastases: Results of ESOPE(European Standard Operating Procedures of Electrochemotherapy) study," *EJC Suppl.,* vol. 4, no. 11, pp. 3-13, Nov, 2006.

[81] T. K. Kim, and J. H. Eberwine, "Mammalian cell transfection: the present and the future," *Anal. Bioanal. Chem.,* vol. 397, no. 8, pp. 3173-8, Aug, 2010.

[82] C. Chen, S. W. Smye, M. P. Robinson, and J. A. Evans, "Membrane electroporation theories: a review," *Med. Biol. Eng. Comput.,* vol. 44, no. 1-2, pp. 5-14, Mar, 2006.

[83] R. Pethig, "Dielectric properties of biological materials: Biophysical and medical applications," *IEEE Trans. on Electr. Insul.*, no. 5, pp. 453-474, 1984.

[84] J. C. Weaver, and K. H. Schoenbach, "Biodielectrics," *IEEE Trans. Dielectr. Electr. Insul.,* vol. 10, no. 5, pp. 715-716, Oct, 2003.

[85] R. W. Glaser, S. L. Leikin, L. V. Chernomordik, V. F. Pastushenko, and A. I. Sokirko, "Reversible Electrical Breakdown of Lipid Bilayers - Formation and Evolution of Pores," *Biochim. Biophys. Acta,* vol. 940, no. 2, pp. 275-287, May 24, 1988.

[86] J. Teissie, and T. Y. Tsong, "Evidence of Voltage-Induced Channel Opening in Na-K Atpase of Human-Erythrocyte Membrane," *J. Membr. Biol.,* vol. 55, no. 2, pp. 133-140, 1980.

[87] J. Teissie, and M. P. Rols, "An Experimental Evaluation of the Critical Potential Difference Inducing Cell-Membrane Electropermeabilization," *Biophys. J.,* vol. 65, no. 1, pp. 409-413, Jul, 1993.

[88] M. Hibino, M. Shigemori, H. Itoh, K. Nagayama, and K. Kinosita, Jr., "Membrane conductance of an electroporated cell analyzed by submicrosecond imaging of transmembrane potential," *Biophys. J.,* vol. 59, no. 1, pp. 209-20, Jan, 1991.

[89] K. Kinosita, Jr., and T. T. Tsong, "Hemolysis of human erythrocytes by transient electric field," *Proc. Natl. Acad. Sci. U. S. A.,* vol. 74, no. 5, pp. 1923-7, May, 1977.

[90] H. G. L. Coster, and U. Zimmermann, "Direct Demonstration of Dielectric-Breakdown in Membranes of Valonia-Utricularis," *Z. Naturforsch.,* vol. C 30, no. 1, pp. 77-79, 1975.

[91] T. Y. Tsong, "Electric Modification of Membrane-Permeability for Drug Loading into Living Cells," *Methods Enzymol.,* vol. 149, pp. 248-259, 1987.

[92] E. Neumann, and K. Rosenheck, "Permeability changes induced by electric impulses in vesicular membranes," *J. Membr. Biol.,* vol. 10, no. 3, pp. 279-90, Dec 29, 1972.

[93] K. Kinosita, Jr., I. Ashikawa, N. Saita, H. Yoshimura, H. Itoh, K. Nagayama, and A. Ikegami, "Electroporation of cell membrane visualized under a pulsed-laser fluorescence microscope," *Biophys. J.,* vol. 53, no. 6, pp. 1015-9, Jun, 1988.

[94] L. V. Chernomordik, S. I. Sukharev, S. V. Popov, V. F. Pastushenko, A. V. Sokirko, I. G. Abidor, and Y. A. Chizmadzhev, "The Electrical Breakdown of Cell and Lipid-Membranes - the Similarity of Phenomenologies," *Biochim. Biophys. Acta,* vol. 902, no. 3, pp. 360-373, Sep 3, 1987.

[95] M. P. Rols, and J. Teissie, "Electropermeabilization of mammalian cells to macromolecules: Control by pulse duration," *Biophys. J.,* vol. 75, no. 3, pp. 1415-1423, Sep, 1998.

[96] F. F. Chen, *Introduction to plasma physics and controlled fusion*, 2nd ed., New York: Plenum Press, 1984.

[97] J. S. Townsend, *Electricity in gases*: Oxford University Press, 1915.

[98] J. S. Chang, P. A. Lawless, and T. Yamamoto, "Corona Discharge Processes," *IEEE Trans. Plasma Sci.,* vol. 19, no. 6, pp. 1152-1166, Dec, 1991.

[99] T. Gonen, *Electric Power Transmission System Engineering Analysis and Design*, Boca raton: CRC Press, 2009.

[100] M. Abdel-Salam, *High-Voltage Engineering: Theory and Practice, Revised and Expanded*, Second ed., New York: Marcel Dekker, Inc., 2000.

[101] J. M. Meek, and J. D. Craggs, *Electrical Breakdown of Gases*: Oxford University Press, London, England, 1953.

[102] P. S. Maruvada, "Corona-Generated Space Charge Environment in the Vicinity of HVDC Transmission Lines," *ITEI,* vol. EI-17, no. 2, pp. 125-130, April, 1982.

[103] O. G. M. Khan, and A. H. El-Hag, "Biological cell electroporation using nanosecond electrical pulses," in Biomedical Engineering (MECBME), 2011 1st Middle East Conference on, 2011, pp. 28-31.

[104] A. Fridman, A. Chirokov, and A. Gutsol, "Non-thermal atmospheric pressure discharges," *J. Phys. D: Appl. Phys.,* vol. 38, no. 2, pp. R1-R24, Jan 21, 2005.

[105] M. Goldman, A. Goldman, and R. S. Sigmond, "The Corona Discharge, Its Properties and Specific Uses," *Pure Appl. Chem.,* vol. 57, no. 9, pp. 1353-1362, 1985.

[106] E. Nasser, *Fundamentals of gaseous ionization and plasma electronics*: Wiley-Interscience, 1971.

[107] B. Chesebro, and K. Wehrly, "Development of a sensitive quantitative focal assay for human immunodeficiency virus infectivity," *J. Virol.,* vol. 62, no. 10, pp. 3779-88, Oct, 1988.

[108] B. Chesebro, R. Buller, J. Portis, and K. Wehrly, "Failure of human immunodeficiency virus entry and infection in CD4-positive human brain and skin cells," *J. Virol.,* vol. 64, no. 1, pp. 215-21, Jan, 1990.

[109] B. Chesebro, K. Wehrly, J. Metcalf, and D. E. Griffin, "Use of a new CD4-positive HeLa cell clone for direct quantitation of infectious human immunodeficiency virus from blood cells of AIDS patients," *J. Infect. Dis.,* vol. 163, no. 1, pp. 64-70, Jan, 1991.

[110] A. Mraihi, N. Merbahi, M. Yousfi, A. Abahazem, and O. Eichwald, "Electrical and spectroscopic analysis of mono- and multi-tip pulsed corona discharges in air at atmospheric pressure," *Plasma Sources Sci. Technol.,* vol. 20, no. 6, Dec, 2011.

[111] B. L. Roth, M. Poot, S. T. Yue, and P. J. Millard, "Bacterial viability and antibiotic susceptibility testing with SYTOX Green nucleic acid stain," *Appl. Environ. Microbiol.,* vol. 63, no. 6, pp. 2421-2431, Jun, 1997.

[112] K. Thevissen, F. R. G. Terras, and W. F. Broekaert, "Permeabilization of fungal membranes by plant defensins inhibits fungal growth," *Appl. Environ. Microbiol.,* vol. 65, no. 12, pp. 5451-5458, Dec, 1999.

[113] S. Homhuan, B. Zhang, F. S. Sheu, A. A. Bettiol, and F. Watt, "Single-cell electroporation using proton beam fabricated biochips," *Biomed. Microdevices,* vol. 14, no. 3, pp. 533-540, Jun, 2012.

[114] H. Y. Wang, and C. Lu, "Microfluidic electroporation for delivery of small molecules and genes into cells using a common DC power supply," *Biotechnol. Bioeng.,* vol. 100, no. 3, pp. 579-586, Jun 15, 2008.

[115] J. Wang, M. J. Stine, and C. Lu, "Microfluidic cell electroporation using a mechanical valve," *Anal. Chem.,* vol. 79, no. 24, pp. 9584-9587, Dec 15, 2007.

[116] K. H. Jones, and J. A. Senft, "An improved method to determine cell viability by simultaneous staining with fluorescein diacetate-propidium iodide," *J. Histochem. Cytochem.,* vol. 33, no. 1, pp. 77-9, Jan, 1985.

[117] M. Meijer, M. P. Pruchniak, M. Arazna, and U. Demkow, "Extracellular traps: how to isolate and quantify extracellular DNA (ET-DNA)," *Cen. Eur. J. Immunol.,* vol. 37, no. 4, pp. 321-325, Dec, 2012.

[118] A. K. Gupta, P. Hasler, W. Holzgreve, S. Gebhardt, and S. Hahn, "Induction of neutrophil extracellular DNA lattices by placental microparticles and IL-8 and their presence in preeclampsia," *Hum. Immunol.,* vol. 66, no. 11, pp. 1146-1154, Nov, 2005.

[119] M. J. Stoddart, *Mammalian cell viability : methods and protocols*, New York: Humana Press/Springer, 2011.

[120] J. L. Hartley, *Protein expression in mammalian cells: methods and protocols*: Humana Press, 2012.

[121] G. Stulen, "Electric field effects on lipid membrane structure," *(BBA)-Biomembranes,* vol. 640, no. 3, pp. 621-627, 1981.

[122] A. Lopez, M. Rols, and J. Teissie, "Phosphorus-31 NMR analysis of membrane phospholipid organization in viable, reversibly electropermeabilized Chinese hamster ovary cells," *Biochemistry,* vol. 27, no. 4, pp. 1222-1228, 1988.

APPENDIX I

All results with device 1

(A) MT4 cells

Inter-electrode Distance (mm)	Corona Exposure Time (minutes)	SYTOX Green Incubation Time (minutes)	Cell Concentration (cells/ml)	Medium	Addition of SYTOX Green	Concentration of SYTOX Green	Applied Voltage	Fluorescence (RFU)		Viability Before (%)	Viability After (%)	
								Control	Treatment	Treatment	Control	Treatment
15	10	10	5.00E+06	RPMI,FBS, 1.4 ml	before	1µl in 3 ml	-3 kV DC	59697.2	98990.2			
20	10	10	2.50E+06	RPMI,FBS, 1.4 ml	before	0.6µl in 3 ml	8 kV, ±, 25 Hz square	102100	84720		94%	95%
20	1.5	10	2.50E+06	RPMI,FBS, 1.4 ml	before	1µl in 3.2 ml	8 kV, ±, 25 Hz square	92330.00	95610.00	99%	95%	96%
20	10	10	2.50E+06	PBS, 1.4 ml	before	1µl in 3.2 ml	8 kV, ±, 25 Hz square	296400.00	69490.00	93%	16%	11%
20	10	10	2.50E+06	RPMI,FBS, 1.4 ml	before	1µl in 3.2 ml	-5 kV DC	149900.00	146400.00	93%	84%	80%
20	10	10	2.50E+06	PBS, 1.4 ml	before	1µl in 3.2 ml	8 kV, ±, 25 Hz square	264100.00	63260.00	93%	37%	9%
15	10	10	2.50E+06	RPMI,FBS, 1.4 ml	before	1µl in 3.2 ml	5 kV, ±, 25 Hz square	60870.00	62120.00	93%	91%	89%
15	10	10	2.50E+06	Colourless RPMI, FBS, 1.4 ml	before	1µl in 3.2 ml	8 kV, ±, 25 Hz square	81460.00	50530.00	95%	96%	98%
20	0.17	10	2.50E+06	Colourless RPMI, FBS, 1.4 ml	before	1µl in 3.2 ml	8 kV, ±, 25 Hz square	81490.00	89500.00	97%	97%	
20	10	10	2.50E+06	Colourless RPMI, FBS, 1.4 ml	before	1µl in 3.2 ml	3 kV, ±, 25 Hz square	93000.00	82000.00	95%	98%	
20	10	10	5.00E+06	Colourless RPMI, no FBS, 1.4 ml	before	1µl in 3.2 ml	8 kV, ±, 25 Hz square	248257.00	226870.00			
20	10	10	5.00E+06	Colourless RPMI, no FBS, 1.4 ml	before	1µl in 3.2 ml	8 kV DC	232965.00	196688.00	83%	90%	
20	10	10	5.00E+06	Premixed PBS, no FBS, 1.4 ml	before	1µl in 3.2 ml	8 kV, ±, 25 Hz square	159772.00	129426.00	93%	90%	89%
20	15	30	5.00E+06	Premixed PBS, no FBS, 1.4 ml	before	1µl in 3.2 ml	8 kV, ±, 25 Hz square	185801.00	144615.00	93%	84%	88%
15	0.07	15	2.50E+06	Colourless RPMI, FBS, 1.4 ml	before	1µl in 3.2 ml	-6kV DC	222194.00	183409.00	89%	92%	93%
15	5	15	2.50E+06	Colourless RPMI, FBS, 1.4 ml	before	1µl in 3.2 ml	-3 kV DC	188469.00	157947.00	89%	95%	96%
15	20	20	2.50E+06	Colourless RPMI, FBS, 1.4 ml	before	1µl in 3.2 ml	-6 kV DC	171601.00	105554.00	89%	93%	93%

Inter-electrode Distance (mm)	Corona Exposure Time (minutes)	Green Incubation Time (minutes)	Cell Concentration (cells/ml)	Medium	Addition of SYTOX Green	Concentration of SYTOX Green	Applied Voltage	Fluorescence (RFU)		Viability Before (%)	Viability After (%)	
								Control	Treatment	Treatment	Control	Treatment
20	10	15	2.50E+06	Colourless RPMI, FBS, 1.4 ml	before	0.5µl in 10.5 ml	6 kV, +, 25 Hz square	41294.40	25753.30	93%	95%	95%
40	10	15	2.50E+06	Colourless RPMI, FBS, 1.4 ml	before	0.5µl in 10.5 ml	8 kV, +, 25 Hz square	39712.60	40924.30	93%	91%	
20	15	15	2.50E+06	Colourless RPMI, FBS, 1.4 ml	after	0.5µl in 1.4 ml	-8 kV DC	109250.00	101835.00	91%	97%	98%
20	45	15	2.50E+06	Colourless RPMI, FBS, 1.4 ml	after	0.5µl in 1.4 ml	+8 kV DC	147019.00	112788.00	91%	95%	97%
20	10	10	2.50E+06	PBS(100 ul)	after	0.5ml(5ml PBS+1ul)	+7kV DC	6400.77	7879.33		71%	57%
20	10	10	2.50E+06	PBS(100 ul)	after	0.5ml(5ml PBS+1ul)	+7kV DC	7634.58	6035.35			84%
20	10	10	2.50E+06	PBS(100 ul)	after	0.5ml(5ml PBS+1ul)	+7kV DC	8762.52	7114.13			50%
20	10	10	2.50E+06	PBS+FBS(100ul)	after	0.5ml(5ml PBS+1ul)	+7kV DC	9839.52	8665.02			71%
20	10	10	2.50E+06	PBS+FBS(100ul)	after	0.5ml(5ml PBS+1ul)	+7kV DC	12886.8	13091.8			88%
20	10	10	2.50E+06	PBS+FBS(100ul)	after	0.5ml(5ml PBS+1ul)	+7kV DC	20206.2	14748.2			86%
20	10	10	2.50E+06	PBS+FBS(100ul)	after	0.5ml(5ml PBS+1ul)	+6kV DC	15396.3	12153.8			83%
20	10	10	2.50E+06	PBS+FBS(100ul)	after	0.5ml(5ml PBS+1ul)	+6kV DC	16494.4	15522.3			83%
20	10	10	2.50E+06	PBS+FBS(100ul)	after	0.5ml(5ml PBS+1ul)	+6kV DC	18467.5	15609.5			82%

(B) HeLa cells

Inter-electrode Distance (mm)	Corona Exposure Time (minutes)	SYTOX Green Incubation Time (minutes)	Medium	Addition of SYTOX Green	Concentration of SYTOX Green	Applied Voltage	Fluorescence (RFU)		Viability after treatment (%)		Comments
							Control	Treatment	Control	Treatment	
15	10	10	PBS(100ul)	after	0.5ml(5ml PBS+1ul)	-7 kV DC	8432.5	29788.3	99%	96%	No washing of cells. Fluorescence measurement in final mixture of PBS, trypsin, FBS, SYTOX. Exposure in 100 ul PBS.
15	10	10	PBS(100ul)	after	0.5ml(5ml PBS+1ul)	-7 kV DC	9687.7	23045.5	98%	98%	No washing of cells. Fluorescence measurement in final mixture of PBS, trypsin, FBS, SYTOX. Exposure in 100 ul PBS.
15	10	10	PBS(100ul)	after	0.5ml(5ml PBS+1ul)	-7 kV DC	7262.4	27152.3	99%	97%	No washing of cells. Fluorescence measurement in final mixture of PBS, trypsin, FBS, SYTOX. Exposure in 100 ul PBS.
15	10	10	PBS(100ul)	after	0.5ml(5ml PBS+1ul)	-7 kV, ±, 25 Hz square	8940.0	22611.0	98%	97%	No washing of cells. Fluorescence measurement in final mixture of PBS, trypsin, FBS, SYTOX. Exposure in 100 ul PBS.
20	10	10	PBS(100ul)	after	0.5ml(5ml PBS+1ul)	-7 kV, ±, 25 Hz square	5915.1	51005.6	98%	97%	No washing of cells. Fluorescence measurement in final mixture of PBS, trypsin, FBS, SYTOX. Exposure in 100 ul PBS.
20	10	10	PBS(100ul)	after	0.5ml(5ml PBS+1ul)	-7 kV, ±, 25 Hz square	9153.0	55116.1	92%	93%	No washing of cells. Fluorescence measurement in final mixture of PBS, trypsin, FBS, SYTOX. Exposure in 100 ul PBS.
							5415.2	16686.4			Fluorescence measurement on supernatant. Supernatant of treatment has higher fluorescence. Suggests free DNA in solution due to cell damage.
20	10	10	PBS(100ul)	after	0.5ml(5ml PBS+1ul)	-7 kV DC	7943.4	28599.6	88%	88%	
15	10	10	PBS(100ul)	after	0.5ml(5ml PBS+1ul)	6 kV, ±, 25 Hz square	11627.7	24538.3	99%	91%	
15	10	10	PBS(100ul)	before	100ul(5ml PBS+1ul)	6 kV, ±, 25 Hz square	2097.9	1713.3	98%	91%	Decrease in fluorescence
15	2	10	PBS(100ul)	after	0.5ml(5ml PBS+1ul)	6 kV, ±, 25 Hz square	10494.5	23257.7	97%	98%	
13	10	10	PBS(100ul)	after	0.5ml(5ml PBS+1ul)	-6 kV	6468.1	130187.0	99%	96%	
13	10	10	PBS(100ul)	after	0.5ml(5ml PBS+1ul)	-7 kV	14918.1	31402.3	97%	91%	
15	10	10	PBS(100ul)	after	0.5ml(5ml PBS+1ul)	-7 kV DC	23639.9	140917.0	97%	94%	

Inter-electrode Distance (mm)	Corona Exposure Time (minutes)	SYTOX Green Incubation Time (minutes)	Medium	Addition of SYTOX Green	Concentration of SYTOX Green	Applied Voltage	Fluorescence (RFU)		Viability after treatment (%)		Comments
							Control	Treatment	Control	Treatment	
15	10	10	PBS(100ul)	after	0.5ml(5ml PBS+1ul)	-6 kV DC	27757.8	113986.0	94%	90%	First of the results done in triplicate for diseertation and papers.
15	10	10	PBS(100ul)	after	0.5ml(5ml PBS+1ul)	-6 kV DC	14055.9	205923.0	94%	87%	
15	10	10	PBS(100ul)	after	0.5ml(5ml PBS+1ul)	-6 kV DC	14412.3	55303.9	93%	85%	
15	10	10	PBS(100ul)	after	0.5ml(5ml PBS+1ul)	-5 kV DC	11346.6	21643.3	98%	94%	Started using coloured RPMI for cell culture
15	10	10	PBS(100ul)	after	0.5ml(5ml PBS+1ul)	-5 kV DC	13715.6	141345.0	98%	93%	
15	10	10	PBS(100ul)	after	0.5ml(5ml PBS+1ul)	-5 kV DC	14431.1	21228.4	98%	97%	
15	10	10	PBS(100ul)	after	0.5ml(5ml PBS+1ul)	+6 kV DC	6477.2	10369.0	97%	88%	Recalculated medium volume and concentration for petri dishes. Increased trypsin for flask and petri dishes. Used coloured RPMI and FBS before fluorescence.
15	10	10	PBS(100ul)	after	0.5ml(5ml PBS+1ul)	+6 kV DC	6274.9	12535.8	95%	91%	
15	10	10	PBS(100ul)	after	0.5ml(5ml PBS+1ul)	+6 kV DC	7472.8	14248.9	97%	95%	
15	10	10	PBS(100ul)	after	0.5ml(5ml PBS+1ul)	+6 kV DC	4351.4	86846.4	98%	93%	
15	10	10	PBS(100ul)	after	0.5ml(5ml PBS+1ul)	+5 kV DC	9248.6	10242.5	97%	98%	Started using colourless RPMI before fluorescence measurement. This procedure is the final one to be used for the rest of the experiments on HeLa cells.
15	10	10	PBS(100ul)	after	0.5ml(5ml PBS+1ul)	+5kV DC	6754.7	12718.3	97%	96%	
15	10	10	PBS(100ul)	after	0.5ml(5ml PBS+1ul)	+5kV DC	6871.7	9758.3	95%	98%	
15	10	10	PBS(100ul)	after	0.5ml(5ml PBS+1ul)	+5kV DC	7403.4	16822.2	97%	97%	
15	10	10	PBS(100ul)	after	0.5ml(5ml PBS+1ul)	+6kV DC	5378.0	10403.1	98%	93%	
15	10	10	PBS(100ul)	after	0.5ml(5ml PBS+1ul)	+6kV DC	5899.7	17791.9	95%	85%	
15	10	10	PBS(100ul)	after	0.5ml(5ml PBS+1ul)	+6kV DC	9820.3	17911.9	96%	92%	
15	10	10	PBS(100ul)	after	0.5ml(5ml PBS+1ul)	+7kV DC	6206.4	16427.9	98%	86%	
15	10	10	PBS(100ul)	after	0.5ml(5ml PBS+1ul)	+7kV DC	5972.0	15332.6	97%	93%	

Inter-electrode Distance (mm)	Corona Exposure Time (minutes)	SYTOX Green Incubation Time (minutes)	Medium	Addition of SYTOX Green	Concentration of SYTOX Green	Applied Voltage	Fluorescence (RFU)		Viability after treatment (%)		Comments
							Control	Treatment	Control	Treatment	
15	10	10	PBS(100ul)	after	0.5ml(5ml PBS+1ul)	+7kV DC	8676.7	15441.3	97%	93%	
15	10	10	PBS(100ul)	after	0.5ml(5ml PBS+1ul)	-5kV DC	6682.0	113053.0	97%	93%	
15	10	10	PBS(100ul)	after	0.5ml(5ml PBS+1ul)	-5kV DC	6731.8	22676.7	98%	89%	
15	10	10	PBS(100ul)	after	0.5ml(5ml PBS+1ul)	-5kV DC	9043.0	20975.0	93%	93%	
15	10	10	PBS(100ul)	after	0.5ml(5ml PBS+1ul)	-5kV DC	9478.0	23619.1	97%	93%	
15	10	10	PBS(100ul)	after	0.5ml(5ml PBS+1ul)	-6kV DC	4246.4	16726.1	98%	95%	
15	10	10	PBS(100ul)	after	0.5ml(5ml PBS+1ul)	-6kV DC	4148.1	17350.0	81%	92%	
15	10	10	PBS(100ul)	after	0.5ml(5ml PBS+1ul)	-6kV DC	4408.3	15755.5	91%	93%	
15	10	10	PBS(100ul)	after	0.5ml(5ml PBS+1ul)	-7kV DC	7273.1	44952.1		92%	
15	10	10	PBS(100ul)	after	0.5ml(5ml PBS+1ul)	-7kV DC	7478.5	25007.7		82%	
15	10	10	PBS(100ul)	after	0.5ml(5ml PBS+1ul)	-7kV DC	7547.3	14987.8		93%	
15	10	10	PBS(100ul)	after	0.5ml(5ml PBS+1ul)	-7kV DC	7443.3	17234.8		90%	

APPENDIX II

All results with device 2

(A) Vero cells

Corona Exposure Time (minutes)	Green Incubation Time (minutes)	Medium	Addition of SYTOX Green	Concentration of SYTOX Green	Applied Voltage	Fluorescence (RFU)		Viability (%)	
						Control	Treatment	Control	Treatment
10	10	PBS	after exposure	0.5µl in 1 ml PBS	-6 kV DC	11150.80	9325.45	97%	95%
10	10	PBS	after exposure	0.5µl in 1 ml PBS	+6 kV, 50 Hz square	14139.20	14203.30		91%
10	10	PBS	after exposure	0.5µl in 10 ml PBS	+6 kV DC	1538.75	1423.02	94%	97%

(B) MT4 cells

Corona Exposure Time (minutes)	SYTOX Green Incubation Time (minutes)	Cell Concentration (cells/ml)	Medium	Addition of SYTOX Green	SYTOX Green Concentration	Applied Voltage	Fluorescence (FRU)		Viability Before (%)	Viability After (%)	
							Control	Treatment		Control	Treatment
10	15	2.50E+06	RPMI, 1.4 ml	after	0.5µl in 1.4 ml cells	+6 kV DC	129803.0	141228.0	97%	85%	80%
10	15	2.50E+06	RPMI, 1.4 ml	after	0.5µl in 1.4 ml cells	+8 kV, +, 25 Hz square	170071.0	141096.0	97%	80%	79%
30	45	2.50E+06	premixed PBS, 1.4 ml	after	0.5µl in 1.4 ml cells	-6 kV DC	195067.0	135569.0	96%	86%	80%
15	15	2.50E+06	premixed PBS	before	0.5µl in 1.4 ml cells	-5 kV DC	213549.0	178828.0	96%	84%	84%
15	10	2.50E+06	PBS, 1.4 ml	after	1µl in 2.8 ml cells	-7 kV DC	142800.0	140600.0	95%	92%	89%
10	10	2.50E+06	PBS, 1.4 ml	before	1µl in 2.8 ml cells	-7 kV DC	190004.0	151997.0	91%	75%	76%

(C) HeLa cells

Corona Exposure Time (minutes)	SYTOX Green Incubation Time (minutes)	Medium	Addition of SYTOX Green	Concentration of SYTOX Green	Applied Voltage	Fluorescence (RFU)		Viability after (%)		Comments
						Control	Treatment	Control	Treatment	
10	10	RPMI	after	0.5ul in petri dish	+6 kV DC	7600.0	3900.0	97%	94%	Medium discarded before trypsin but no washing.
10	30	PBS (250ul)	after	0.5ml(1ml PBS+0.5ul)	-6 kV DC	25850.0	85890.0	90%	91%	No washing of cells. Fluorescence measurement in final mixture of PBS, trypsin, FBS, SYTOX.
10	30	PBS (250ul)	after	0.5ml(1ml PBS+0.5ul)	-6 kV DC	62620.0	70610.0	88%	95%	No washing of cells. Fluorescence measurement in final mixture of PBS, trypsin, FBS, SYTOX.
10	30	PBS (250ul)	after	0.5ml(1ml PBS+0.5ul)	-6 kV DC			88%	93%	No washing of cells. Fluorescence measurement in final mixture of PBS, trypsin, FBS, SYTOX.
15	30	PBS (250ul)	after	0.5ml(1ml PBS+1ul)	-7 kV DC	105800.0	25280.0	98%	93%	No washing of cells. Fluorescence measurement in final mixture of PBS, trypsin, FBS, SYTOX.
10	30	PBS (250ul)	after	0.5ml(1ml PBS+0.5ul)	-6 kV DC	8640.4	24108.5	96%	97%	No washing of cells. Fluorescence measurement in final mixture of PBS, trypsin, FBS, SYTOX.
10	30	PBS (250ul)	after	0.5ml(1ml PBS+0.5ul)	-6 kV DC	26965.9	12246.0	99%	97%	No washing of cells. Fluorescence measurement in final mixture of PBS, trypsin, FBS, SYTOX.
10	20	PBS	before	0.5ml(2.5ml PBS+0.5ul)	-6 kV DC	15003.8	2086.4	98%	99%	Cell washed before trypsin while cells still attached.
10	10	PBS (250ul)	after	0.5ml(2.5ml PBS+0.5ul)	-6 kV DC	10735.0	23801.6	97%	97%	Cell washed before trypsin while cells still attached.
10	10	PBS(250ul)	after	0.5ml(2.5ml PBS+0.5ul)	-6 kV DC	4803.4	24002.4	98%	99%	Cells washed before trypsin while cells atill attached.
10	10	PBS(250ul)	after	0.5ml(5ml PBS+1ul)	-6 kV DC	21587.2	18342.9	95%	95%	cells washed before trypsin while cells still attached. Fluorescence in fresh PBS. Exposure in 250 ul PBS.
10	10	PBS(250ul)	after	0.5ml(5ml PBS+1ul)	-6 kV DC	25939.5	31034.1	100%	98%	cells washed before trypsin while cells still attached. Fluorescence in fresh PBS. Exposure in 250 ul PBS.
10	10	PBS(100ul)	after	0.5ml(5ml PBS+1ul)	-6 kV DC	9246.4	26924.2	100%	98%	Cells washed before trypsin while cells still attached. Fluorescence in fresh PBS. Exposure in 100 ul PBS.
10	10	PBS(100ul)	after	0.5ml(5ml PBS+1ul)	-7 kV DC	2115.0	10078.8	98%	97%	Cells washed before trypsin while cells still attached. Fluorescence in fresh PBS. Exposure in 100 ul PBS.
10	10	PBS(100ul)	after	0.5ml(5ml PBS+1ul)	-7 kV DC	3195.7	8258.5	97%	95%	Cells washed before trypsin while cells still attached. Fluorescence in fresh PBS. Exposure in 100 ul PBS.
10	10	PBS(100ul)	after	0.5ml(5ml PBS+1ul)	-7 kV DC	1828.5	8138.0	97%	98%	Cells washed before trypsin while cells still attached. Fluorescence in fresh PBS. Exposure in 100 ul PBS.

Corona Exposure Time (minutes)	SYTOX Green Incubation Time (minutes)	Medium	Addition of SYTOX Green	Concentration of SYTOX Green	Applied Voltage	Fluorescence (RFU)		Viability after (%)		Comments
						Control	Treatment	Control	Treatment	
10	30	PBS(100ul)	after	0.5ml(5ml PBS+1ul)	-7 kV DC	2191.8	8366.5	99%	98%	Cells washed before trypsin while cells still attached. Fluorescence in fresh PBS. Exposure in 100 ul PBS.
10	30	PBS(100ul)	after	0.5ml(5ml PBS+1ul)	-7 kV DC	2551.1	8889.7	98%	97%	Cells washed before trypsin while cells still attached. Fluorescence in fresh PBS. Exposure in 100 ul PBS.
10	10	PBS(100ul)	after	0.5ml(5ml PBS+1ul)	-7 kV DC	1600.7	2917.8	58%	60%	Wash cells by centrifuging at 1000 rpm for 7 minutes just before fluorescence measurement, ensures no cells discarded. Exposure in 100 ul PBS.
10	10	PBS(100ul)	after	0.5ml(5ml PBS+1ul)	-7 kV DC	7373.3	23044.1	98%	99%	No washing of cells. Fluorescence measurement in final mixture of PBS, trypsin, FBS, SYTOX. Exposure in 100 ul PBS.
10	10	PBS(100ul)	after	0.5ml(5ml PBS+1ul)	-7 kV DC	8893.4	33761.2	98%	97%	No washing of cells. Fluorescence measurement in final mixture of PBS, trypsin, FBS, SYTOX. Exposure in 100 ul PBS.
10	10	PBS(100ul)	after	0.5ml(5ml PBS+1ul)	-5 kV DC	4621.9	18634.3		98%	
10	10	PBS(100ul)	after	0.5ml(5ml PBS+1ul)	-5 kV DC	4968.7	18711.1		83%	
10	10	PBS(100ul)	after	0.5ml(5ml PBS+1ul)	-5 kV DC	4362.7	12900.4		84%	
10	10	PBS(100ul)	after	0.5ml(5ml PBS+1ul)	-5 kV DC	5165.5	13686.1		96%	
10	10	PBS(100ul)	after	0.5ml(5ml PBS+1ul)	-6kV DC	8945.0	27942.6		94%	
10	10	PBS(100ul)	after	0.5ml(5ml PBS+1ul)	-6kV DC	8147.4	19110.9		85%	
10	10	PBS(100ul)	after	0.5ml(5ml PBS+1ul)	-6kV DC	8454.3	24530.7		95%	
10	10	PBS(100ul)	after	0.5ml(5ml PBS+1ul)	-6kV DC	7423.7	22811.9		92%	
10	10	PBS(100ul)	after	0.5ml(5ml PBS+1ul)	-7kV DC	5532.1	15887.1		96%	
10	10	PBS(100ul)	after	0.5ml(5ml PBS+1ul)	-7kV DC	3904.1	13154.3		96%	
10	10	PBS(100ul)	after	0.5ml(5ml PBS+1ul)	-7kV DC	4373.2	17491.1		96%	
10	10	PBS(100ul)	after	0.5ml(5ml PBS+1ul)	+5kV DC	4740.2	6200.2		93%	
10	10	PBS(100ul)	after	0.5ml(5ml PBS+1ul)	+5kV DC	4290.6	7805.0		96%	
10	10	PBS(100ul)	after	0.5ml(5ml PBS+1ul)	+5kV DC	8636.7	7901.4		90%	
10	10	PBS(100ul)	after	0.5ml(5ml PBS+1ul)	+6kV DC	7963.7	23536.6		97%	

Corona Exposure Time (minutes)	SYTOX Green Incubation Time (minutes)	Medium	Addition of SYTOX Green	Concentration of SYTOX Green	Applied Voltage	Fluorescence (RFU)		Viability after (%)		Comments
						Control	Treatment	Control	Treatment	
10	10	PBS(100ul)	after	0.5ml(5ml PBS+1ul)	+6kV DC	9219.0	16109.2		96%	
10	10	PBS(100ul)	after	0.5ml(5ml PBS+1ul)	+6kV DC	11760.8	14097.4		97%	
10	10	PBS(100ul)	after	0.5ml(5ml PBS+1ul)	+6kV DC	8692.0	13985.3		99%	
10	10	PBS(100ul)	after	0.5ml(5ml PBS+1ul)	+7kV DC	5881.6	18012.4		97%	
10	10	PBS(100ul)	after	0.5ml(5ml PBS+1ul)	+7kV DC	6462.2	13726.6		96%	
10	10	PBS(100ul)	after	0.5ml(5ml PBS+1ul)	+7kV DC	4574.4	14830.4		97%	

APPENDIX III

All results with device 3

(A) MT4 cells

HV Electrode Distance above Suspension Surface	Corona Exposure Time (minutes)	Green Incubation Time (minutes)	Cell Concentration (cells/ml)	Medium	Addition of SYTOX Green	Concentration of SYTOX Green	Applied Voltage	Fluorescence (RFU)		Viability Before (%)	Viability After (%)	
								Control	Treatment		Control	Treatment
5 mm above surface	10	12	2.50E+06	PBS	before	1.5ul in 4.5 ml cells	-7 kV DC	138400.0	60240.0	91%	89%	76%
4 mm above surface	5	10	2.50E+06	PBS	after	0.7ul in 2 ml cells	-7 kV DC	309075.0	170055.0	96%	88%	83%
4 mm above surface	10	12	2.50E+06	PBS	before	1.5ul in 4.5 ml cells	+6 kV DC	57315.9	80442.8	96%	90%	84%
4 mm above surface	10	12	2.50E+06	PBS	before	1.5ul in 4.5 ml cells	+6 kV DC	120656.0	83854.4	95%	87%	81%
4 mm above surface	10	12	2.50E+06	PBS	before	1.5ul in 4.5 ml cells	+6 kV DC	133415.0	117045.0	95%	85%	83%

APPENDIX IV

All results with Vero cells

(A) Device 2

Corons Exposure Time (minutes)	SYTOX Green Incubation Time (minutes)	Medium	Addition of SYTOX Green	Concentration of SYTOX Green	Applied Voltage	Fluorescence (RFU)		Viability (%)	
						Control	Treatment	Control	Treatment
10	10	PBS	after exposure	0.5µl in 1 ml PBS	-6 kV DC	11150.80	9325.45	97%	95%
10	10	PBS	after exposure	0.5µl in 1 ml PBS	+6 kV, 50 Hz square	14139.20	14203.30		91%
10	10	PBS	after exposure	0.5µl in 10 ml PBS	+6 kV DC	1538.75	1423.02	94%	97%

APPENDIX V

All results with MT4 cells

(A) Device 1

Inter-electrode Distance (mm)	Corona Exposure Time (minutes)	SYTOX Green Incubation Time (minutes)	Cell Concentration (cells/ml)	Medium	Addition of SYTOX Green	Concentration of SYTOX Green	Applied Voltage	Fluorescence (RFU)		Viability Before (%)	Viability After (%)	
								Control	Treatment	Treatment	Control	Treatment
15	10	10	5.00E+06	RPMI,FBS, 1.4 ml	before	1µl in 3 ml	-3 kV DC	59697.2	98990.2			
20	10	10	2.50E+06	RPMI,FBS, 1.4 ml	before	0.6µl in 3 ml	8 kV, ±, 25 Hz square	102100.0	84720.0		94%	95%
20	1.5	10	2.50E+06	RPMI,FBS, 1.4 ml	before	1µl in 3.2 ml	8 kV, ±, 25 Hz square	92330.0	95610.0	99%	95%	96%
20	10	10	2.50E+06	PBS, 1.4 ml	before	1µl in 3.2 ml	8 kV, ±, 25 Hz square	296400.0	69490.0	93%	16%	11%
20	10	10	2.50E+06	RPMI,FBS, 1.4 ml	before	1µl in 3.2 ml	-5 kV DC	149900.0	146400.0	93%	84%	80%
20	10	10	2.50E+06	PBS, 1.4 ml	before	1µl in 3.2 ml	8 kV, ±, 25 Hz square	264100.0	63260.0	93%	37%	9%
15	10	10	2.50E+06	RPMI,FBS, 1.4 ml	before	1µl in 3.2 ml	5 kV, ±, 25 Hz square	60870.0	62120.0	93%	91%	89%
15	10	10	2.50E+06	Colourless RPMI, FBS, 1.4 ml	before	1µl in 3.2 ml	8 kV, ±, 25 Hz square	81460.0	50530.0	95%	96%	98%
20	0.17	10	2.50E+06	Colourless RPMI, FBS, 1.4 ml	before	1µl in 3.2 ml	8 kV, ±, 25 Hz square	81490.0	89500.0	97%	97%	
20	10	10	2.50E+06	Colourless RPMI, FBS, 1.4 ml	before	1µl in 3.2 ml	3 kV, ±, 25 Hz square	93000.0	82000.0	95%	98%	
20	10	10	5.00E+06	Colourless RPMI, no FBS, 1.4 ml	before	1µl in 3.2 ml	8 kV, ±, 25 Hz square	248257.0	226870.0			
20	10	10	5.00E+06	Colourless RPMI, no FBS, 1.4 ml	before	1µl in 3.2 ml	8 kV DC	232965.0	196688.0	83%	90%	
20	10	10	5.00E+06	Premixed PBS, no FBS, 1.4 ml	before	1µl in 3.2 ml	8 kV, ±, 25 Hz square	159772.0	129426.0	93%	90%	89%
20	15	30	5.00E+06	Premixed PBS, no FBS, 1.4 ml	before	1µl in 3.2 ml	8 kV, ±, 25 Hz square	185801.0	144615.0	93%	84%	88%
15	0.07	15	2.50E+06	Colourless RPMI, FBS, 1.4 ml	before	1µl in 3.2 ml	-6kV DC	222194.0	183409.0	89%	92%	93%

Inter-electrode Distance (mm)	Corona Exposure Time (minutes)	SYTOX Green Incubation Time (minutes)	Cell Concentration (cells/ml)	Medium	Addition of SYTOX Green	Concentration of SYTOX Green	Applied Voltage	Fluorescence (RFU)		Viability Before (%)	Viability After (%)	
								Control	Treatment	Treatment	Control	Treatment
15	5	15	2.50E+06	Colourless RPMI, FBS, 1.4 ml	before	1µl in 3.2 ml	-3 kV DC	188469.0	157947.0	89%	95%	96%
15	20	20	2.50E+06	Colourless RPMI, FBS, 1.4 ml	before	1µl in 3.2 ml	-6 kV DC	171601.0	105554.0	89%	93%	93%
20	10	15	2.50E+06	Colourless RPMI, FBS, 1.4 ml	before	0.5µl in 10.5 ml	6 kV, ±, 25 Hz square	21255.9	15788.1	93%	98%	96%
20	10	15	2.50E+06	Colourless RPMI, FBS, 1.4 ml	before	0.5µl in 10.5 ml	6 kV, +, 25 Hz square	41294.4	25753.3	93%	95%	95%
40	10	15	2.50E+06	Colourless RPMI, FBS, 1.4 ml	before	0.5µl in 10.5 ml	8 kV, +, 25 Hz square	39712.6	40924.3	93%	91%	
20	15	15	2.50E+06	Colourless RPMI, FBS, 1.4 ml	after	0.5µl in 1.4 ml	-8 kV DC	109250.0	101835.0	91%	97%	98%
20	45	15	2.50E+06	Colourless RPMI, FBS, 1.4 ml	after	0.5µl in 1.4 ml	+8 kV DC	147019.0	112788.0	91%	95%	97%
20	10	10	2.50E+06	PBS(100 ul)	after	0.5ml(5ml PBS+1ul)	+7kV DC	6400.8	7879.3		71%	57%
20	10	10	2.50E+06	PBS(100 ul)	after	0.5ml(5ml PBS+1ul)	+7kV DC	7634.6	6035.4			84%
20	10	10	2.50E+06	PBS(100 ul)	after	0.5ml(5ml PBS+1ul)	+7kV DC	8762.5	7114.1			50%
20	10	10	2.50E+06	PBS+FBS(100ul)	after	0.5ml(5ml PBS+1ul)	+7kV DC	9839.5	8665.0			71%
20	10	10	2.50E+06	PBS+FBS(100ul)	after	0.5ml(5ml PBS+1ul)	+7kV DC	12886.8	13091.8			88%
20	10	10	2.50E+06	PBS+FBS(100ul)	after	0.5ml(5ml PBS+1ul)	+7kV DC	20206.2	14748.2			86%
20	10	10	2.50E+06	PBS+FBS(100ul)	after	0.5ml(5ml PBS+1ul)	+6kV DC	15396.3	12153.8			83%
20	10	10	2.50E+06	PBS+FBS(100ul)	after	0.5ml(5ml PBS+1ul)	+6kV DC	16494.4	15522.3			83%
20	10	10	2.50E+06	PBS+FBS(100ul)	after	0.5ml(5ml PBS+1ul)	+6kV DC	18467.5	15609.5			82%

(B) Device 2

Corona Exposure Time (minutes)	SYTOX Green Incubation Time (minutes)	Cell Concentration (cells/ml)	Medium	Addition of SYTOX Green	SYTOX Green Concentration	Applied Voltage	Fluorescence (RFU)		Viability Before (%)	Viability After (%)	
							Control	Treatment		Control	Treatment
10	15	2.50E+06	RPMI, 1.4 ml	after	0.5µl in 1.4 ml cells	+6 kV DC	129803.0	141228.0	97%	85%	80%
10	15	2.50E+06	RPMI, 1.4 ml	after	0.5µl in 1.4 ml cells	+8 kV, +, 25 Hz square	170071.0	141096.0	97%	80%	79%
30	45	2.50E+06	premixed PBS, 1.4 ml	after	0.5µl in 1.4 ml cells	-6 kV DC	195067.0	135569.0	96%	86%	80%
15	15	2.50E+06	premixed PBS	before	0.5µl in 1.4 ml cells	-5 kV DC	213549.0	178828.0	96%	84%	84%
15	10	2.50E+06	PBS, 1.4 ml	after	1µl in 2.8 ml cells	-7 kV DC	142800.0	140600.0	95%	92%	89%
10	10	2.50E+06	PBS, 1.4 ml	before	1µl in 2.8 ml cells	-7 kV DC	190004.0	151997.0	91%	75%	76%

(C) Device 3

Distance of HV Electrode above Suspension Surface	Corona Exposure Time (minutes)	SYTOX Green Incubation Time (minutes)	Cell Concentration (cells/ml)	Medium	Addition of SYTOX Green	Concentration of SYTOX Green	Applied Voltage	Fluorescence (RFU)		Viability Before (%)	Viability After (%)	
								Control	Treatment		Control	Treatment
5 mm above surface	10	12	2.50E+06	PBS	before	1.5ul in 4.5 ml cells	-7 kV DC	138400.0	60240.0	91%	89%	76%
4 mm above surface	5	10	2.50E+06	PBS	after	0.7ul in 2 ml cells	-7 kV DC	309075.0	170055.0	96%	88%	83%
4 mm above surface	10	12	2.50E+06	PBS	before	1.5ul in 4.5 ml cells	+6 kV DC	57315.9	80442.8	96%	90%	84%
4 mm above surface	10	12	2.50E+06	PBS	before	1.5ul in 4.5 ml cells	+6 kV DC	120656.0	83854.4	95%	87%	81%
4 mm above surface	10	12	2.50E+06	PBS	before	1.5ul in 4.5 ml cells	+6 kV DC	133415.0	117045.0	95%	85%	83%

APPENDIX VI

Initial results with HeLa cells

(A) Device 1

Inter-electrode Distance (mm)	Corona Exposure Time (minutes)	SYTOX Green Incubation Time (minutes)	Medium	Addition of SYTOX Green	Concentration of SYTOX Green	Applied Voltage	Fluorescence (RFU)		Viability After (%)		Comments
							Control	Treatment	Control	Treatment	
15	10	10	PBS(100ul)	after	0.5ml(5ml PBS+1ul)	-7 kV DC	8432.5	29788.3	99%	96%	No washing of cells. Fluorescence measurement in final mixture of PBS, trypsin, FBS, SYTOX. Exposure in 100 ul PBS.
15	10	10	PBS(100ul)	after	0.5ml(5ml PBS+1ul)	-7 kV DC	9687.7	23045.5	98%	98%	No washing of cells. Fluorescence measurement in final mixture of PBS, trypsin, FBS, SYTOX. Exposure in 100 ul PBS.
15	10	10	PBS(100ul)	after	0.5ml(5ml PBS+1ul)	-7 kV DC	7262.4	27152.3	99%	97%	No washing of cells. Fluorescence measurement in final mixture of PBS, trypsin, FBS, SYTOX. Exposure in 100 ul PBS.
15	10	10	PBS(100ul)	after	0.5ml(5ml PBS+1ul)	-7 kV, ±, 25 Hz square	8940.0	22611.0	98%	97%	No washing of cells. Fluorescence measurement in final mixture of PBS, trypsin, FBS, SYTOX. Exposure in 100 ul PBS.
20	10	10	PBS(100ul)	after	0.5ml(5ml PBS+1ul)	-7 kV, ±, 25 Hz square	5915.1	51005.6	98%	97%	No washing of cells. Fluorescence measurement in final mixture of PBS, trypsin, FBS, SYTOX. Exposure in 100 ul PBS.
20	10	10	PBS(100ul)	after	0.5ml(5ml PBS+1ul)	-7 kV, ±, 25 Hz square	9153.0	55116.1	92%	93%	No washing of cells. Fluorescence measurement in final mixture of PBS, trypsin, FBS, SYTOX. Exposure in 100 ul PBS.
							5415.2	16686.4			Fluorescence measurement on supernatant. Supernatant of treatment has higher fluorescence. Suggests free DNA in solution due to cell damage.
20	10	10	PBS(100ul)	after	0.5ml(5ml PBS+1ul)	-7 kV DC	7943.4	28599.6	88%	88%	
15	10	10	PBS(100ul)	after	0.5ml(5ml PBS+1ul)	6 kV, ±, 25 Hz square	11627.7	24538.3	99%	91%	
15	10	10	PBS(100ul)	before	100ul(5ml PBS+1ul)	6 kV, ±, 25 Hz square	2097.9	1713.3	98%	91%	Decrease in fluorescence
15	2	10	PBS(100ul)	after	0.5ml(5ml PBS+1ul)	6 kV, ±, 25 Hz square	10494.5	23257.7	97%	98%	

Inter-electrode Distance (mm)	Corona Exposure Time (minutes)	SYTOX Green Incubation Time (minutes)	Medium	Addition of SYTOX Green	Concentration of SYTOX Green	Applied Voltage	Fluorescence (RFU)		Viability After (%)		Comments
							Control	Treatment	Control	Treatment	
13	10	10	PBS(100ul)	after	0.5ml(5ml PBS+1ul)	-6 kV	6468.1	130187.0	99%	96%	
13	10	10	PBS(100ul)	after	0.5ml(5ml PBS+1ul)	-7 kV	14918.1	31402.3	97%	91%	
15	10	10	PBS(100ul)	after	0.5ml(5ml PBS+1ul)	-7 kV DC	23639.9	140917.0	97%	94%	
15	101	10	PBS(100ul)	after	0.5ml(5ml PBS+1ul)	-6 kV DC	27757.8	113986.0	94%	90%	First of the results done in triplicate for diseertation and papers.
15	10	10	PBS(100ul)	after	0.5ml(5ml PBS+1ul)	-6 kV DC	14055.9	205923.0	94%	87%	
15	10	10	PBS(100ul)	after	0.5ml(5ml PBS+1ul)	-6 kV DC	14412.3	55303.9	93%	85%	
15	10	10	PBS(100ul)	after	0.5ml(5ml PBS+1ul)	-5 kV DC	11346.6	21643.3	98%	94%	Started using coloured RPMI for cell culture
15	10	10	PBS(100ul)	after	0.5ml(5ml PBS+1ul)	-5 kV DC	13715.6	141345.0	98%	93%	
15	10	10	PBS(100ul)	after	0.5ml(5ml PBS+1ul)	-5 kV DC	14431.1	21228.4	98%	97%	
15	10	10	PBS(100ul)	after	0.5ml(5ml PBS+1ul)	+6 kV DC	6477.2	10369.0	97%	88%	Recalculated medium volume and concentration for petri dishes. Increased trypsin for flask and petri dishes. Used coloured RPMI and FBS before fluorescence.
15	10	10	PBS(100ul)	after	0.5ml(5ml PBS+1ul)	+6 kV DC	6274.9	12535.8	95%	91%	
15	10	10	PBS(100ul)	after	0.5ml(5ml PBS+1ul)	+6 kV DC	7472.8	14248.9	97%	95%	
15	10	10	PBS(100ul)	after	0.5ml(5ml PBS+1ul)	+6 kV DC	4351.4	86846.4	98%	93%	
15	10	10	PBS(100ul)	after	0.5ml(5ml PBS+1ul)	+5 kV DC	9248.6	10242.5	97%	98%	Started using colourless RPMI before fluorescence measurement. This procedure is the final one to be used for the rest of the experiments on HeLa cells.
15	10	10	PBS(100ul)	after	0.5ml(5ml PBS+1ul)	+5kV DC	6754.7	12718.3	97%	96%	
15	10	10	PBS(100ul)	after	0.5ml(5ml PBS+1ul)	+5kV DC	6871.7	9758.3	95%	98%	
15	10	10	PBS(100ul)	after	0.5ml(5ml PBS+1ul)	+5kV DC	7403.4	16822.2	97%	97%	
15	10	10	PBS(100ul)	after	0.5ml(5ml PBS+1ul)	+6kV DC	5378.0	10403.1	98%	93%	

Inter-electrode Distance (mm)	Corona Exposure Time (minutes)	SYTOX Green Incubation Time (minutes)	Medium	Addition of SYTOX Green	Concentration of SYTOX Green	Applied Voltage	Fluorescence (RFU)		Viability After (%)		Comments
							Control	Treatment	Control	Treatment	
15	10	10	PBS(100ul)	after	0.5ml(5ml PBS+1ul)	+6kV DC	5899.7	17791.9	95%	85%	
15	10	10	PBS(100ul)	after	0.5ml(5ml PBS+1ul)	+6kV DC	9820.3	17911.9	96%	92%	
15	10	10	PBS(100ul)	after	0.5ml(5ml PBS+1ul)	+7kV DC	6206.4	16427.9	98%	86%	
15	10	10	PBS(100ul)	after	0.5ml(5ml PBS+1ul)	+7kV DC	5972.0	15332.6	97%	93%	
15	10	10	PBS(100ul)	after	0.5ml(5ml PBS+1ul)	+7kV DC	8676.7	15441.3	97%	93%	
15	10	10	PBS(100ul)	after	0.5ml(5ml PBS+1ul)	-5kV DC	6682.0	113053.0	97%	93%	
15	10	10	PBS(100ul)	after	0.5ml(5ml PBS+1ul)	-5kV DC	6731.8	22676.7	98%	89%	
15	10	10	PBS(100ul)	after	0.5ml(5ml PBS+1ul)	-5kV DC	9043.0	20975.0	93%	93%	
15	10	10	PBS(100ul)	after	0.5ml(5ml PBS+1ul)	-5kV DC	9478.0	23619.1	97%	93%	
15	10	10	PBS(100ul)	after	0.5ml(5ml PBS+1ul)	-6kV DC	4246.4	16726.1	98%	95%	
15	10	10	PBS(100ul)	after	0.5ml(5ml PBS+1ul)	-6kV DC	4148.1	17350.0	81%	92%	
15	10	10	PBS(100ul)	after	0.5ml(5ml PBS+1ul)	-6kV DC	4408.3	15755.5	91%	93%	
15	10	10	PBS(100ul)	after	0.5ml(5ml PBS+1ul)	-7kV DC	7273.1	44952.1		92%	
15	10	10	PBS(100ul)	after	0.5ml(5ml PBS+1ul)	-7kV DC	7478.5	25007.7		82%	
15	10	10	PBS(100ul)	after	0.5ml(5ml PBS+1ul)	-7kV DC	7547.3	14987.8		93%	
15	10	10	PBS(100ul)	after	0.5ml(5ml PBS+1ul)	-7kV DC	7443.3	17234.8		90%	

(B) Device 2

Corona Exposure Time (minutes)	SYTOX Green Incubation Time (minutes)	Medium	Addition of SYTOX Green	Concentration of SYTOX Green	Applied Voltage	Fluorescence (RFU)		Viability after (%)		Comments
						Control	Treatment	Control	Treatment	
10	10	RPMI	after	0.5ul in petri dish	+6 kV DC	7600.0	3900.0	97%	94%	Medium discarded before trypsin but no washing.
10	30	PBS (250ul)	after	0.5ml(1ml PBS+0.5ul)	-6 kV DC	25850.0	85890.0	90%	91%	No washing of cells. Fluorescence measurement in final mixture of PBS, trypsin, FBS, SYTOX.
10	30	PBS (250ul)	after	0.5ml(1ml PBS+0.5ul)	-6 kV DC	62620.0	70610.0	88%	95%	No washing of cells. Fluorescence measurement in final mixture of PBS, trypsin, FBS, SYTOX.
10	30	PBS (250ul)	after	0.5ml(1ml PBS+0.5ul)	-6 kV DC			88%	93%	No washing of cells. Fluorescence measurement in final mixture of PBS, trypsin, FBS, SYTOX.
15	30	PBS (250ul)	after	0.5ml(1ml PBS+1ul)	-7 kV DC	105800.0	25280.0	98%	93%	No washing of cells. Fluorescence measurement in final mixture of PBS, trypsin, FBS, SYTOX.
10	30	PBS (250ul)	after	0.5ml(1ml PBS+0.5ul)	-6 kV DC	8640.4	24108.5	96%	97%	No washing of cells. Fluorescence measurement in final mixture of PBS, trypsin, FBS, SYTOX.
10	30	PBS (250ul)	after	0.5ml(1ml PBS+0.5ul)	-6 kV DC	26965.9	12246.0	99%	97%	No washing of cells. Fluorescence measurement in final mixture of PBS, trypsin, FBS, SYTOX.
10	20	PBS	before	0.5ml(2.5ml PBS+0.5ul)	-6 kV DC	15003.8	2086.4	98%	99%	Cell washed before trypsin while cells still attached.
10	10	PBS (250ul)	after	0.5ml(2.5ml PBS+0.5ul)	-6 kV DC	10735.0	23801.6	97%	97%	Cell washed before trypsin while cells still attached.
10	10	PBS(250ul)	after	0.5ml(2.5ml PBS+0.5ul)	-6 kV DC	4803.4	24002.4	98%	99%	Cells washed before trypsin while cells atill attached.
10	10	PBS(250ul)	after	0.5ml(5ml PBS+1ul)	-6 kV DC	21587.2	18342.9	95%	95%	cells washed before trypsin while cells still attached. Fluorescence in fresh PBS. Exposure in 250 ul PBS.
10	10	PBS(250ul)	after	0.5ml(5ml PBS+1ul)	-6 kV DC	25939.5	31034.1	100%	98%	cells washed before trypsin while cells still attached. Fluorescence in fresh PBS. Exposure in 250 ul PBS.
10	10	PBS(100ul)	after	0.5ml(5ml PBS+1ul)	-6 kV DC	9246.4	26924.2	100%	98%	Cells washed before trypsin while cells still attached. Fluorescence in fresh PBS. Exposure in 100 ul PBS.
10	10	PBS(100ul)	after	0.5ml(5ml PBS+1ul)	-7 kV DC	2115.0	10078.8	98%	97%	Cells washed before trypsin while cells still attached. Fluorescence in fresh PBS. Exposure in 100 ul PBS.
10	10	PBS(100ul)	after	0.5ml(5ml PBS+1ul)	-7 kV DC	3195.7	8258.5	97%	95%	Cells washed before trypsin while cells still attached. Fluorescence in fresh PBS. Exposure in 100 ul PBS.
10	10	PBS(100ul)	after	0.5ml(5ml PBS+1ul)	-7 kV DC	1828.5	8138.0	97%	98%	Cells washed before trypsin while cells still attached. Fluorescence in fresh PBS. Exposure in 100 ul PBS.
10	30	PBS(100ul)	after	0.5ml(5ml PBS+1ul)	-7 kV DC	2191.8	8366.5	99%	98%	Cells washed before trypsin while cells still attached. Fluorescence in fresh PBS. Exposure in 100 ul PBS.

Corona Exposure Time (minutes)	SYTOX Green Incubation Time (minutes)	Medium	Addition of SYTOX Green	Concentration of SYTOX Green	Applied Voltage	Fluorescence (RFU)		Viability after (%)		Comments
						Control	Treatment	Control	Treatment	
10	30	PBS(100ul)	after	0.5ml(5ml PBS+1ul)	-7 kV DC	2551.1	8889.7	98%	97%	Cells washed before trypsin while cells still attached. Fluorescence in fresh PBS. Exposure in 100 ul PBS.
10	30	PBS(100ul)	after	0.5ml(5ml PBS+1ul)	-7 kV DC	2243.8	11231.4	98%	99%	Cells washed before trypsin while cells still attached. Fluorescence in fresh PBS. Exposure in 100 ul PBS.
10	10	PBS(100ul)	after	0.5ml(5ml PBS+1ul)	-7 kV DC	1600.7	2917.8	58%	60%	Wash cells by centrifuging at 1000 rpm for 7 minutes just before fluorescence measurement, ensures no cells discarded. Exposure in 100 ul PBS.
10	10	PBS(100ul)	after	0.5ml(5ml PBS+1ul)	-7 kV DC	7373.3	23044.1	98%	99%	No washing of cells. Fluorescence measurement in final mixture of PBS, trypsin, FBS, SYTOX. Exposure in 100 ul PBS.
10	10	PBS(100ul)	after	0.5ml(5ml PBS+1ul)	-7 kV DC	8893.4	33761.2	98%	97%	No washing of cells. Fluorescence measurement in final mixture of PBS, trypsin, FBS, SYTOX. Exposure in 100 ul PBS.
10	10	PBS(100ul)	after	0.5ml(5ml PBS+1ul)	-5 kV DC	4621.9	18634.3		98%	
10	10	PBS(100ul)	after	0.5ml(5ml PBS+1ul)	-5 kV DC	4968.7	18711.1		83%	
10	10	PBS(100ul)	after	0.5ml(5ml PBS+1ul)	-5 kV DC	4362.7	12900.4		84%	
10	10	PBS(100ul)	after	0.5ml(5ml PBS+1ul)	-5 kV DC	5165.5	13686.1		96%	
10	10	PBS(100ul)	after	0.5ml(5ml PBS+1ul)	-6kV DC	8945.0	27942.6		94%	
10	10	PBS(100ul)	after	0.5ml(5ml PBS+1ul)	-6kV DC	8147.4	19110.9		85%	
10	10	PBS(100ul)	after	0.5ml(5ml PBS+1ul)	-6kV DC	8454.3	24530.7		95%	
10	10	PBS(100ul)	after	0.5ml(5ml PBS+1ul)	-6kV DC	7423.7	22811.9		92%	
10	10	PBS(100ul)	after	0.5ml(5ml PBS+1ul)	-7kV DC	5532.1	15887.1		96%	
10	10	PBS(100ul)	after	0.5ml(5ml PBS+1ul)	-7kV DC	3904.1	13154.3		96%	
10	10	PBS(100ul)	after	0.5ml(5ml PBS+1ul)	-7kV DC	4373.2	17491.1		96%	
10	10	PBS(100ul)	after	0.5ml(5ml PBS+1ul)	+5kV DC	4740.2	6200.2		93%	

Corona Exposure Time (minutes)	SYTOX Green Incubation Time (minutes)	Medium	Addition of SYTOX Green	Concentration of SYTOX Green	Applied Voltage	Fluorescence (RFU)		Viability after (%)		Comments
						Control	Treatment	Control	Treatment	
10	10	PBS(100ul)	after	0.5ml(5ml PBS+1ul)	+5kV DC	4290.6	7805.0		96%	
10	10	PBS(100ul)	after	0.5ml(5ml PBS+1ul)	+5kV DC	8636.7	7901.4		90%	
10	10	PBS(100ul)	after	0.5ml(5ml PBS+1ul)	+6kV DC	7963.7	23536.6		97%	
10	10	PBS(100ul)	after	0.5ml(5ml PBS+1ul)	+6kV DC	9219.0	16109.2		96%	
10	10	PBS(100ul)	after	0.5ml(5ml PBS+1ul)	+6kV DC	11760.8	14097.4		97%	
10	10	PBS(100ul)	after	0.5ml(5ml PBS+1ul)	+6kV DC	8692.0	13985.3		99%	
10	10	PBS(100ul)	after	0.5ml(5ml PBS+1ul)	+7kV DC	5881.6	18012.4		97%	
10	10	PBS(100ul)	after	0.5ml(5ml PBS+1ul)	+7kV DC	6462.2	13726.6		96%	
10	10	PBS(100ul)	after	0.5ml(5ml PBS+1ul)	+7kV DC	4574.4	14830.4		97%	

APPENDIX VII

Attempt at achieving homogeneity by cell lysis using Triton X-100 and CyQuant on HeLa cells

Inter-electrode Distance (mm)	Corona Exposure Time (minutes)	SYTOX Green Incubation Time (minutes)	Medium	SYTOX Green Concentration	Applied Voltage	Fluorescence of Cells (FRU)		Fluorescence of Supernatant (RFU)		Viability After (%)		Comments
						Control	Treatment	Control	Treatment	Control	Treatment	
15	10	10	PBS(100 ul)	0.5ml(5ml PBS+1ul)	+6kV DC	before x-100		1092.9	1523.7	87%	87%	use x-100 on ice for 15 minutes
						6636.1	11296.4	1083.3	1574.0			
						5947.9	62561.7	1088.8	1587.6			
						8325.0	13157.7					
						after x-100						
						2022.1	2288.9					
						2241.5	5211.9					
						1348.6	38066.4					
15	10	10	PBS(100ul)	0.5ml(5ml PBS+1ul)	+6kV DC	5412.7	88790.3	1199.7	2289.3		95%	Use CyQuant cell lysis buffer
						5825.4	16467.3	1207.4	2267.1			
						6241.1	15022.3	1214.1	2306.7			
						Next day after freezing						
						1417.2	11636.4					
						1768.4	54551.0					
						1886.9	10240.6					
15	10	10	PBS(200ul)	0.5ml(5ml PBS+1ul)	+6kV DC	7568.2	18477.9				96%	
						7925.4	20556.5					
						8056.2	46831.7					

Inter-electrode Distance (mm)	Corona Exposure Time (minutes)	SYTOX Green Incubation Time (minutes)	Medium	SYTOX Green Concentration	Applied Voltage	(FRU)		Supernatant (RFU)		Viability After (%)		Comments
						Control	Treatment	Control	Treatment	Control	Treatment	
15	10	10	PBS(100ul)	0.5ml(5ml PBS+1ul)	+6kV DC	10490.7	11923.3	1134.5	1374.2			
						8618.4	16989.1	1109.0	1345.3			
						7809.0	11575.7	1104.1	1362.4			
						after x-100						use x-100 on ice for 30 minutes
						2979.5	54373.8					
						2280.3	104391.0					
						2608.5	2680.0					
15	10	10	PBS(100 ul)	0.5ml(5ml PBS+1ul)	+6kV DC	5642.7	18407.9	1146.3	2133.5			Use CyQuant cell lysis buffer and ultrasound
						6269.0	15743.1	1139.7	2114.1			
						5694.6	88512.0	1158.4	2095.1			
						Next day after freezing						
						1366.9	3016.2					
						1412.5	2857.1					
						1386.3	2733.4					

Inter-electrode Distance (mm)	Corona Exposure Time (minutes)	SYTOX Green Incubation Time (minutes)	Medium	SYTOX Green Concentration	Applied Voltage	(FRU)		Supernatant (RFU)		Viability After (%)		Comments
						Control	Treatment	Control	Treatment	Control	Treatment	
15	10	10	PBS(100 ul)	0.5ml(5ml PBS+1ul)	+6kV DC	17635.1	15540.5	2343.0	2173.0			Use ultrasound
						15530.3	16082.8	2446.7	2201.6			
						16150.8	15115.8	2465.3	2192.0			
						Next day after freezing						
						3966.5	6896.6					
						4143.1	38875.6					
						4991.6	19032.9					
20	10	10	PBS(100 ul)	0.5ml(5ml PBS+1ul)	+6kV DC	6033.2	10404.1				98%	
						5734.5	5446.5					
						7539.7	5130.4					
15	2	10	PBS(100 ul)	0.5ml(5ml PBS+1ul)	+6kV DC	6597.2	8574.8				98%	
						6021.1	7800.7					
						6659.2	8451.5					
15	5	10	PBS(100 ul)	0.5ml(5ml PBS+1ul)	+6kV DC	5606.6	12379.4	1155.2	1694.2		84%	No freezing with x-100
						5658.2	10273.4	1159.7	1651.6			
						5104.5	12093.3	1173.3	1656.3			
						after x-100						
						3008.1	22342.6					
						2573.8	17743.6					
						2854.1	18688.8					

Inter-electrode Distance (mm)	Corona Exposure Time (minutes)	SYTOX Green Incubation Time (minutes)	Medium	SYTOX Green Concentration	Applied Voltage	(FRU)		Supernatant (RFU)		Viability After (%)		Comments
						Control	Treatment	Control	Treatment	Control	Treatment	
15	3.5	10	PBS(100 ul)	0.5ml(5ml PBS+1ul)	+6kV DC	11122.3	10151.6				98%	
						10759.1	9570.4					
						10552.1	13616.7					
15	10	10	PBS(200 ul)	0.5ml(5ml PBS+1ul)	+6lV DC	after x-100		1343.4	1381.7	96%	95%	Use x-100 with no freezing
						4074.2	17333.9	1429.6	1417.2			
						5996.2	2954.2	1507.0	1396.8			
						7630.6	6367.8					
15	10	10	PBS(200 ul)	0.5ml(5ml PBS+1ul)	+6kV DC	2045.4	1901.1	2045.4	1901.1		97%	washed after SYTOX
						1528.2	1737.3	1528.2	1737.3			
						1469.1	1972.7	1469.1	1972.7			
15	3.5	10	PBS(100 ul)	0.5ml(5ml PBS+1ul)	+6kV DC	3330.7	11118.3	1412.3	1642.0			wash before fluorescence measurement and resuspend in 1 ml PBS
						3829.4	11427.1	1424.6	1711.7			
						4306.4	11278.5	1446.6	1571.7			
15	5	10	PBS(100 ul)	0.5ml(5ml PBS+1ul)	+6kV DC	5029.9	14888.7	1479.9	2025.4	97%	98%	
						4045.2	10104.2	1518.8	2044.4			
						4909.3	17924.4	1513.9	2060.6			

APPENDIX VIII

Optimization of exposure time

Inter-electrode Distance (mm)	Corona Exposure Time (minutes)	SYTOX Green Incubation Time (minutes)	Medium	Concentration of SYTOX Green	Applied Voltage	Fluorescence of cells (RFU)		Fluorescence of Supernatant (RFU)		Viability After (%)		Cell Concentration (cells/ml)	
						Control	Treatment	Control	Treatment	Control	Treatment	Control	Treatment
15	1	10	PBS(100 µl)	0.5ml(5ml PBS+1µl)	+6kV DC	1573.8	5087.0	1715.7	1995.3	97%	98%	1.10E+06	7.40E+05
						1560.3	6242.9	1796.5	2042.9				
						1647.2	8545.3	1852.6	1957.7				
15	2	10	PBS(100 µl)	0.5ml(5ml PBS+1µl)	+6kV DC	1896.9	3392.8	1861.3	1820.3	96%	98%	1.10E+06	8.40E+05
						1770.8	8467.6	1831.6	1830.3				
						1707.1	4922.3	1861.7	1807.4				
15	4	10	PBS(100 µl)	0.5ml(5ml PBS+1µl)	+6kV DC	2010.1	10199.5	1657.4	2350.7	96%	94%	1.20E+06	9.40E+05
						1617.4	5607.3	1722.1	2281.9				
						1577.7	4990.5	1701.0	2375.8				
15	5	10	PBS(100 µl)	0.5ml(5ml PBS+1µl)	+6kV DC	1229.1	9372.2	1141.6	1718.3	95%	95%	1.20E+06	9.30E+05
						1281.8	7877.7	1129.0	1696.9				
						1245.3	8048.6	1130.0	1688.7				
15	6	10	PBS(100 µl)	0.5ml(5ml PBS+1µl)	+6kV DC	1238.7	5772.3	1054.9	1872.6	99%	95%	1.30E+06	1.00E+06
						1082.3	11530.8	1059.9	1845.2				
						1064.6	5357.4	1039.0	1923.7				

Inter-electrode Distance (mm)	Corona Exposure Time (minutes)	SYTOX Green Incubation Time (minutes)	Medium	Concentration of SYTOX Green	Applied Voltage	(RFU)		Supernatant (RFU)		Viability After (%)		(cells/ml)	
						Control	Treatment	Control	Treatment	Control	Treatment	Control	Treatment
15	8	10	PBS(100 µl)	0.5ml(5ml PBS+1µl)	+6kV DC	1225.8	9980.1	1118.3	2321.3	96%	94%	1.30E+06	1.10E+06
						1278.3	11977.6	1121.9	2297.2				
						1473.7	8216.5	1145.6	2307.1				
15	10	10	PBS(100 µl)	0.5ml(5ml PBS+1µl)	+6kV DC	1368.9	8444.3	1113.4	2531.2	95%	92%	1.20E+06	1.30E+06
						1418.5	16501.1	1121.7	2636.9				
						1393.9	6403.8	1147.4	2596.2				
15	3	10	PBS(100 µl)	0.5ml(5ml PBS+1µl)	+6kV DC	2516.8	4493.0	1218.5	1736.1	98%	93%	1.40E+06	1.00E+06
						1562.3	3106.6	1210.9	1771.6				
						1818.5	3682.4	1197.0	1663.5				
15	7	10	PBS(100 µl)	0.5ml(5ml PBS+1µl)	+6kV DC	1223.3	8547.4	1107.6	1990.9	97%	93%	1.40E+06	1.10E+06
						1271.1	6927.7	1095.7	2016.9				
						1216.4	9961.2	1096.5	2038.3				
15	9	10	PBS(100 µl)	0.5ml(5ml PBS+1µl)	+6kV DC	1163.2	9795.0	1130.5	2290.2	96%	92%	1.60E+06	1.20E+06
						1191.0	13011.5	1148.0	2320.2				
						1171.3	13260.4	1158.6	2308.4				

APPENDIX IX

Optimization of volume of liquid

(A) Device 1

Inter-electrode Distance (mm)	Corona Exposure Time (minutes)	SYTOX Green Incubation Time (minutes)	Medium	SYTOX Green Concentration	Applied Voltage	Fluorescence of Cells (RFU)		Fluorescence of Supernatant (RFU)		Viability After (%)		Cell Concentration (cells/ml)	
						Control	Treatment	Control	Treatment	Control	Treatment	Control	Treatment
15	1	10	PBS(100 ul)	0.5ml(5ml PBS+1ul)	+6kV DC	1573.8	5087.0	1715.7	1995.3	97%	98%	1.10E+06	7.40E+05
						1560.3	6242.9	1796.5	2042.9				
						1647.2	8545.3	1852.6	1957.7				
15	1	10	PBS(200 ul)	0.5ml(5ml PBS+1ul)	+6kV DC	1338.2	2067.6	1135.5	1408.9	90%	98%	1.60E+06	1.40E+06
						1485.9	2006.6	1150.8	1439.3				
						1387.9	2217.8	1146.1	1417.8				
15	1	10	PBS(300 ul)	0.5ml(5ml PBS+1ul)	+6kV DC	2019.8	1685.9	1958.9	2092.2	95%	95%	1.10E+06	1.10E+06
						2035.8	1685.3	2136.2	2188.4				
						1965.2	1668.2	2112.5	2128.0				
15	1	10	PBS(400 ul)	0.5ml(5ml PBS+1ul)	+6kV DC	1788.5	1713.1	2086.7	1822.2	98%	97%	1.20E+06	1.20E+06
						1836.0	2278.9	1919.4	1827.8				
						1834.0	1763.4	1915.4	1761.4				

APPENDIX X

Optimization of incubation time with SYTOX Green

Inter-electrode Distance (mm)	Corona Exposure Time (minutes)	SYTOX Green Incubation Time (minutes)	Medium	Concentration of SYTOX Green	Applied Voltage	Fluorescence of Cells (RFU)		Fluorescence of Supernatant (%)		Viability After (%)		Cell Concentration (cells/ml)	
						Control	Treatment	Control	Treatment	Control	Treatment	Control	Treatment
15	1	5	PBS(100 µl)	0.5ml(5ml PBS+1µl)	+6kV DC	1804.8	4338.0	1930.1	3767.5	94%	95%	1.20E+06	1.10E+06
						1792.1	3935.9	1932.8	3753.9				
						1882.4	4035.9	1875.6	3596.1				
15	1	8	PBS(100µl)	0.5ml(5ml PBS+1µl)	+6kV DC	4145.6	3978.8	1197.9	1593.2	97%	97%	6.00E+05	6.70E+03
						5531.0	5237.3	1226.5	1580.8				
						2372.9	4155.7	1187.3	1507.6				
15	1	6	PBS(100µl)	0.5ml(5ml PBS+1µl)	+6kV DC	1498.8	1899.4	1384.1	3003.8	96%	98%	1.00E+06	9.50E+05
						1511.0	2281.7	1375.4	2990.0				
						1484.4	1692.5	1344.1	2943.3				
15	1	4	PBS(100µl)	0.5ml(5ml PBS+1µl)	+6kV DC	1187.4	4133.7	1594.7	2694.6	98%	95%	1.10E+06	9.80E+05
						1725.6	3656.7	1623.1	2650.5				
						1120.5	3175.9	1596.3	2621.2				
15	1	12	PBS(100µl)	0.5ml(5ml PBS+1µl)	+6kV DC	2325.6	3402.9	3348.8	1807.8	94%	93%	1.00E+06	1.10E+06
						2168.1	4215.6	1703.3	1839.6				
						2374.3	3689.2	1738.5	1853.2				
15	1	2	PBS(100µl)	0.5ml(5ml PBS+1µl)	+6kV DC	1378.7	5442.4	2197.2	2605.2	96%	97%	1.00E+06	1.10E+06
						1356.2	5355.4	2229.7	2501.5				
						1362.3	6587.6	2200.5	2494.7				

Inter-electrode Distance (mm)	Corona Exposure Time (minutes)	SYTOX Green Incubation Time (minutes)	Medium	Concentration of SYTOX Green	Applied Voltage	(RFU)		Supernatant (%)		Viability After (%)		(cells/ml)	
						Control	Treatment	Control	Treatment	Control	Treatment	Control	Treatment
15	1	10	PBS(100µl)	0.5ml(5ml PBS+1µl)	+6kV DC	1341.0	1518.1	1604.8	2193.8	95%	96%	1.10E+06	1.20E+06
						1327.1	1421.8	1659.4	2261.4				
						1328.6	1473.3	1582.1	2168.6				
15	7	10	PBS(100µl)	0.5ml(5ml PBS+1µl)	+6kV DC	1298.3	6169.0	1385.1	3351.4	99%	97%	1.20E+06	1.30E+06
						1278.2	5381.2	1445.7	3316.4				
						1314.5	5449.9	1459.6	3324.5				
15	7	8	PBS(100µl)	0.5ml(5ml PBS+1µl)	+6kV DC	1567.2	7038.3	1770.1	2615.3	96%	96%	1.20E+06	1.40E+06
						1538.4	6808.4	1884.5	2694.0				
						1502.9	6481.0	1889.5	2612.2				
15	7	6	PBS(100µl)	0.5ml(5ml PBS+1µl)	+6kV DC	1569.7	5471.9	2133.3	2477.2	97%	97%	1.60E+06	1.40E+06
						1361.9	5708.3	2168.5	2520.0				
						1406.0	6884.9	2187.4	2423.0				
15	7	4	PBS(100µl)	0.5ml(5ml PBS+1µl)	+6kV DC	1495.4	11104.6	2382.9	2643.3	99%	96%	1.20E+06	1.20E+06
						1552.9	10647.3	2405.9	2659.0				
						1639.2	9522.5	2382.9	2600.1				
15	7	2	PBS(100µl)	0.5ml(5ml PBS+1µl)	+6kV DC	1649.5	6802.8	1938.2	3188.3	98%	95%	1.30E+06	1.30E+06
						1569.9	6720.1	1911.6	3194.9				
						1580.9	7171.5	1920.0	3136.1				

APPENDIX XI

Optimization of inter-electrode distance

Inter-electrode Distance (mm)	Corona Exposure Time (minutes)	SYTOX Green Incubation Time (minutes)	Medium	Concentration of SYTOX Green	Applied Voltage	Fluorescence of Cells (RFU)		Fluorescence of Supernatant (RFU)		Viability After (%)		Cell Concentration (cells/ml)	
						Control	Treatment	Control	Treatment	Control	Treatment	Control	Treatment
17	7	2	PBS(100ul)	0.5ml(5ml PBS+1ul)	+6kV DC	1346.1	3158.1	1798.4	2900.7	98%	99%	1.40E+06	1.70E+06
						1362.8	3109.5	1826.3	2805.6				
						1393.3	3169.1	1971.4	2719.1				
19	7	2	PBS(100ul)	0.5ml(5ml PBS+1ul)	+6kV DC	1858.7	1804.9	1951.7	2521.6	98%	98%	1.40E+06	1.60E+06
						1700.5	1709.4	2067.8	2557.5				
						1741.6	3078.2	2132.1	2542.7				
13	7	2	PBS(100ul)	0.5ml(5ml PBS+1ul)	+6kV DC	1651.8	3129.3	2240.8	3598.5	98%	96%	1.20E+06	1.30E+06
						1666.6	2969.6	2290.1	3572.3				
						1715.6	3605.8	2193.3	3582.5				
15	7	2	PBS(100ul)	0.5ml(5ml PBS+1ul)	+6kV DC	1649.5	6802.8	1938.2	3188.3	98%	95%	1.30E+06	1.30E+06
						1569.9	6720.1	1911.6	3194.9				
						1580.9	7171.5	1920.0	3136.1				

APPENDIX XII

Initial results of investigation of applied voltage

Fluorescence measurements are made in 200 µl volume, and not per cell

Inter-electrode Distance (mm)	Exposure Time (minutes)	SYTOX Green Incubation Time (minutes)	Medium	Concentration of SYTOX Green	Applied Voltage	Fluorescence of Cells (RFU)		Fluorescence of Supernatant (RFU)		Viability After (%)		Cell concentration	
						Control	Treatment	Control	Treatment	Control	Treatment	Control	Treatment
15	7	2	PBS(100ul)	0.5ml(5ml PBS+1ul)	+1kV DC	2134.9	3033.1	2809.0	2851.2	98%	97%	1.30E+06	1.30E+06
						2225.3	3047.4	2293.9	2820.0				
						2786.2	3173.3	2432.3	2713.4				
15	7	2	PBS(100ul)	0.5ml(5ml PBS+1ul)	+2kV DC	1659.3	1676.1	2202.0	2930.8	98%	97%	1.30E+06	1.30E+06
						1679.6	1646.5	2338.9	2967.6				
						1607.5	1724.1	2394.3	2978.4				
15	7	2	PBS(100ul)	0.5ml(5ml PBS+1ul)	+3kV DC	1780.9	1467.3	2321.6	2105.8	98%	97%	1.50E+06	1.60E+06
						2050.6	1456.6	2439.8	2019.9				
						1861.0	1453.9	2403.6	2077.1				
15	7	2	PBS(100ul)	0.5ml(5ml PBS+1ul)	+4kV DC	1468.3	6093.4	2694.0	4318.7	97%	98%	1.10E+06	1.50E+06
						1494.8	5702.5	2663.8	4320.2				
						1506.0	7916.5	2725.1	4327.5				
15	7	2	PBS(100ul)	0.5ml(5ml PBS+1ul)	+5kV DC	1310.8	2389.6	2234.7	4418.2	97%	99%	1.20E+06	1.10E+06
						1305.7	2390.9	2233.6	4398.5				
						1277.8	2201.3	2249.1	4201.4				
15	7	2	PBS(100ul)	0.5ml(5ml PBS+1ul)	+6kV DC	9791.5	9186.0	5840.7	6028.6	97%	94%	1.10E+06	1.40E+06
						9972.7	10384.4	6156.2	5881.5				
						10244.8	13398.2	5879.9	6010.9				

Inter-electrode Distance (mm)	Exposure Time (minutes)	SYTOX Green Incubation Time (minutes)	Medium	Concentration of SYTOX Green	Applied Voltage	(RFU)		Supernatant (RFU)		Viability After (%)		Cell concentration	
						Control	Treatment	Control	Treatment	Control	Treatment	Control	Treatment
15	7	2	PBS(100ul)	0.5ml(5ml PBS+1ul)	+7kV DC	1321.1	4505.5	2566.0	5143.9	98%	96%	1.40E+06	1.70E+06
						1319.5	5015.7	2539.3	5135.6				
						1334.3	5951.3	2581.7	5085.2				
15	7	2	PBS(100ul)	0.5ml(5ml PBS+1ul)	+8kV DC	2561.9	21794.1	2912.5	6658.4	96%	93%	1.20E+06	1.10E+06
						3266.1	18781.4	2894.6	6516.4				
						2736.2	28482.4	2935.6	6638.1				
15	7	2	PBS(100ul)	0.5ml(5ml PBS+1ul)	+5kV DC	3315.6	10692.8	2878.6	4490.8	97%	98%	1.20E+06	1.20E+06
						3456.3	8799.9	2893.6	4509.1				
						3244.5	10786.4	2810.7	4403.3				
15	7	2	PBS(100ul)	0.5ml(5ml PBS+1ul)	+5kV DC	1800.8	7396.7	2304.9	4660.0	98%	94%	1.80E+06	1.50E+06
						1822.1	8694.6	2413.8	4854.0				
						1850.8	6961.2	2350.6	4872.8				
15	7	2	PBS(100ul)	0.5ml(5ml PBS+1ul)	+6kV DC	1364.8	12151.6	1851.3	4478.2	97%	97%	1.30E+06	8.90E+05
						1300.6	15372.6	1910.8	4567.0				
						1312.9	13183.2	1893.7	4521.3				

Inter-electrode Distance (mm)	Exposure Time (minutes)	SYTOX Green Incubation Time (minutes)	Medium	Concentration of SYTOX Green	Applied Voltage	(RFU)		Supernatant (RFU)		Viability After (%)		Cell concentration	
						Control	Treatment	Control	Treatment	Control	Treatment	Control	Treatment
15	7	2	PBS(100ul)	0.5ml(5ml PBS+1ul)	+6kV DC	1352.6	11346.1	2043.0	4978.7	98%	94%	1.20E+06	8.70E+05
						1391.9	11374.3	2057.7	4997.9				
						1487.9	10514.2	2077.3	4981.5				
15	7	2	PBS(100ul)	0.5ml(5ml PBS+1ul)	+7kV DC	1257.1	8414.4	1650.7	5521.1	96%	96%	1.30E+06	1.10E+06
						1252.1	9596.4	1636.5	5070.6				
						1239.7	9443.3	1648.6	750.2				
15	7	2	PBS(100ul)	0.5ml(5ml PBS+1ul)	+7kV DC	1548.6	5732.4	1883.6	3919.7	92%	84%	1.30E+06	8.80E+05
						1730.9	5844.7	1919.8	3930.3				
						1591.3	140183.0	1901.8	3924.6				
15	7	2	PBS(100ul)	0.5ml(5ml PBS+1ul)	+8kV DC	2113.7	7367.0	2537.5	9535.7	95%	90%	1.40E+06	1.40E+06
						2113.7	6451.4	2689.5	9969.5				
						2627.7	6774.7	2835.0	9611.4				
15	7	2	PBS(100ul)	0.5ml(5ml PBS+1ul)	+8kV DC	1843.9	10311.2	2680.1	7647.8	91%	91%	1.10E+06	1.40E+06
						1896.2	7325.9	3032.9	7971.8				
						1881.4	6769.1	3071.4	8022.0				
15	7	2	PBS(100ul)	0.5ml(5ml PBS+1ul)	+4kV DC	1593.8	6255.5	2315.9	7654.8	86%	90%	1.50E+06	1.40E+06
						1657.6	6735.2	2261.2	7717.5				
						1596.7	6662.3	2388.8	7731.9				

Inter-electrode Distance (mm)	Exposure Time (minutes)	SYTOX Green Incubation Time (minutes)	Medium	Concentration of SYTOX Green	Applied Voltage	(RFU)		Supernatant (RFU)		Viability After (%)		Cell concentration	
						Control	Treatment	Control	Treatment	Control	Treatment	Control	Treatment
15	7	2	PBS(100ul)	0.5ml(5ml PBS+1ul)	+4kV DC	1645.0	17563.8	2827.0	6448.5	80%	85%	1.30E+06	1.00E+06
						1655.7	15866.0	2913.7	6738.5				
						1694.0	20927.4	2908.4	6614.2				
15	7	2	PBS(100ul)	0.5ml(5ml PBS+1ul)	-6kV DC	1335.1	13028.9	1683.1	4408.0	96%	96%	1.30E+06	1.40E+06
						1312.6	8090.5	1682.9	4466.1				
						1323.6	8080.0	1712.7	4448.1				
15	7	2	PBS(100ul)	0.5ml(5ml PBS+1ul)	-7kV DC	1426.6	24503.2	2066.1	4656.9	97%	92%	1.50E+06	9.80E+05
						1335.1	16270.7	2078.1	4459.2				
						1457.7	16487.7	2077.7	4450.9				
15	7	2	PBS(100ul)	0.5ml(5ml PBS+1ul)	-8kV DC	1615.2	12342.4	1984.0	5973.6	95%	82%	1.30E+06	1.10E+06
						1605.5	10927.3	1996.5	6002.1				
						1661.3	11502.3	2028.1	6064.0				
15	7	2	PBS(100ul)	0.5ml(5ml PBS+1ul)	-8kV DC	1450.4	4468.4	1957.0	6317.1	97%	69%	1.30E+06	1.20E+06
						1445.6	4441.7	2020.9	6324.9				
						1500.2	4589.5	2022.1	6246.7				

APPENDIX XIII

Final results of investigation of applied voltage

Fluorescence measurements are made per 250 000 cells.

Inter-electrode Distance (mm)	Exposure Time (minutes)	SYTOX Green Incubation Time (minutes)	Medium	Concentration of SYTOX Green	Applied Voltage	Fluorescence of Cells (RFU)		Fluorescence of Supernatant (RFU)		Viability After (%)		Cell Concentration (cells/ml)	
						Control	Treatment	Control	Treatment	Control	Treatment	Control	Treatment
15	7	2	PBS(100ul)	0.5ml(5ml PBS+1ul)	+4kV DC	967.4	3470.4	1200.7	2654.2	98%	98%	2.40E+06	1.90E+06
						977.1	2971.8	1204.0	2582.2				
						980.7	3422.9	1204.5	2519.6				
15	7	2	PBS(100ul)	0.5ml(5ml PBS+1ul)	+5kV DC	1094.9	1452.6	1633.2	2340.2	98%	95%	2.10E+06	2.10E+06
						1203.7	1420.7	1637.9	2295.7				
						1007.2	1411.6	1691.4	2289.4				
15	7	2	PBS(100ul)	0.5ml(5ml PBS+1ul)	+6kV DC	981.7	1932.1	1193.3	3129.3	97%	95%	2.70E+06	2.60E+06
						977.1	2389.4	1208.5	3120.0				
						1008.1	1693.1	1232.8	3139.6				
15	7	2	PBS(100ul)	0.5ml(5ml PBS+1ul)	+7kV DC	1178.3	2902.8	1839.9	5125.7	98%	90%	2.50E+06	2.10E+06
						1162.7	2768.7	1844.4	4899.0				
						1146.7	2776.3	1851.8	4965.1				
15	7	2	PBS(100ul)	0.5ml(5ml PBS+1ul)	+8kV DC	1041.0	7590.0	1468.6	5681.8	93%	93%	2.70E+06	1.40E+06
						1029.6	8534.8	1456.4	5833.8				
						1092.5	6903.5	1552.6	5963.9				

Inter-electrode Distance (mm)	Exposure Time (minutes)	SYTOX Green Incubation Time (minutes)	Medium	Concentration of SYTOX Green	Applied Voltage	Cells (RFU)		Supernatant (RFU)		Viability After (%)		(cells/ml)	
						Control	Treatment	Control	Treatment	Control	Treatment	Control	Treatment
15	7	2	PBS(100ul)	0.5ml(5ml PBS+1ul)	+4kV DC	1098.7	3095.2	1740.7	4501.1	97%	94%	2.40E+06	2.10E+06
						1118.8	3002.0	1767.0	4465.3				
						1094.7	3789.4	1840.6	4452.5				
15	7	2	PBS(100ul)	0.5ml(5ml PBS+1ul)	+5kV DC	993.5	2107.3	1495.5	5198.3	96%	91%	2.60E+06	2.00E+06
						999.2	2174.6	1524.3	5382.7				
						996.8	2196.1	1529.3	5128.2				
15	7	2	PBS(100ul)	0.5ml(5ml PBS+1ul)	+6kV DC	1480.9	2376.0	2108.8	3632.8	97%	93%	2.40E+06	2.80E+06
						1386.0	2345.2	2143.3	3865.8				
						1432.9	2390.5	2257.6	3801.7				
15	7	2	PBS(100ul)	0.5ml(5ml PBS+1ul)	+7kV DC	1036.9	5191.3	1802.8	4000.9	96%	78%	2.50E+06	2.10E+06
						1021.9	5553.0	1849.4	4084.1				
						1033.1	5930.1	1815.9	4027.4				
15	7	2	PBS(100ul)	0.5ml(5ml PBS+1ul)	+4kV DC	1315.4	1293.6	2349.5	2926.5	98%	98%	3.00E+06	2.70E+06
						1299.7	1490.1	2256.2	2975.6				
						1294.9	1310.1	2306.9	3041.9				
15	7	2	PBS(100ul)	0.5ml(5ml PBS+1ul)	+5kV DC	1035.5	1436.0	1981.9	3457.5	98%	98%	2.70E+06	2.40E+06
						1019.9	1443.8	1890.4	3423.2				
						1036.8	1359.8	1988.0	3548.5				
15	7	2	PBS(100ul)	0.5ml(5ml PBS+1ul)	+6kV DC	990.9	9381.4	1951.2	4214.6	97%	96%	3.00E+06	2.20E+06
						1013.1	7690.0	1996.2	4101.2				
						992.2	4924.0	2035.1	4016.7				

Inter-electrode Distance (mm)	Exposure Time (minutes)	SYTOX Green Incubation Time (minutes)	Medium	Concentration of SYTOX Green	Applied Voltage	Cells (RFU)		Supernatant (RFU)		Viability After (%)		(cells/ml)	
						Control	Treatment	Control	Treatment	Control	Treatment	Control	Treatment
15	7	2	PBS(100ul)	0.5ml(5ml PBS+1ul)	+7kV DC	977.5	4715.8	1762.5	4265.7	98%	95%	3.00E+06	2.70E+06
						966.9	4523.0	1795.2	4262.5				
						969.6	5271.9	1859.2	4248.6				
15	7	2	PBS(100ul)	0.5ml(5ml PBS+1ul)	+8kV DC	1286.8	6421.6	2105.6	5179.8	97%	88%	2.20E+06	2.10E+06
						1474.6	6553.7	2137.6	5317.0				
						1406.2	6833.7	2199.5	5072.5				
15	7	2	PBS(100ul)	0.5ml(5ml PBS+1ul)	+8kV DC	993.6	4315.8	1814.9	3965.7	97%	90%	2.60E+06	2.50E+06
						995.4	5299.8	1771.4	4054.0				
						1001.3	6276.4	1847.3	4073.6				
15	7	2	PBS(100ul)	0.5ml(5ml PBS+1ul)	-7kV DC	953.7	3459.1	1568.2	4075.2	97%	94%	3.10E+06	2.40E+06
						978.2	1970.9	1637.7	4070.4				
						956.1	2013.6	1585.0	4143.6				

Inter-electrode Distance (mm)	Exposure Time (minutes)	SYTOX Green Incubation Time (minutes)	Medium	Concentration of SYTOX Green	Applied Voltage	Cells (RFU)		Supernatant (RFU)		Viability After (%)		(cells/ml)	
						Control	Treatment	Control	Treatment	Control	Treatment	Control	Treatment
15	7	2	PBS(100ul)	0.5ml(5ml PBS+1ul)	-8kV DC	978.7	3864.1	1377.6	6373.0	98%	89%	2.00E+06	1.80E+06
						968.8	3731.6	1368.1	6330.6				
						977.0	3501.9	1394.4	6489.4				
15	7	2	PBS(100ul)	0.5ml(5ml PBS+1ul)	-7kV DC	1055.8	12681.2	1896.1	5438.6	97%	86%	2.10E+06	1.60E+06
						1031.8	7113.6	1845.2	5512.2				
						1037.5	11497.9	1822.8	5526.5				
15	7	2	PBS(100ul)	0.5ml(5ml PBS+1ul)	-6kV DC	1056.1	5190.0	1622.2	5542.4	97%	88%	2.00E+06	2.30E+06
						1048.0	5896.3	1687.4	5460.1				
						1030.8	4518.2	1706.0	5020.6				
15	7	2	PBS(100ul)	0.5ml(5ml PBS+1ul)	-6kV DC	954.8	1639.7	1687.0	2933.6	99%	91%	3.00E+06	3.00E+06
						974.6	1280.8	1749.5	3089.9				
						932.0	1332.2	1701.6	3015.3				
15	7	2	PBS(100ul)	0.5ml(5ml PBS+1ul)	-5kV DC	1037.0	4975.3	1644.6	4687.2	96%	90%	2.40E+06	2.40E+06
						1065.6	4770.2	1662.6	4775.4				
						1078.1	4203.5	1659.2	4718.9				

Inter-electrode Distance (mm)	Exposure Time (minutes)	SYTOX Green Incubation Time (minutes)	Medium	Concentration of SYTOX Green	Applied Voltage	Cells (RFU)		Supernatant (RFU)		Viability After (%)		(cells/ml)	
						Control	Treatment	Control	Treatment	Control	Treatment	Control	Treatment
15	7	2	PBS(100ul)	0.5ml(5ml PBS+1ul)	-6kV DC	1169.6	2929.0	1662.3	6311.2	97%	86%	2.50E+06	2.30E+06
						1046.9	2818.2	1731.3	6229.9				
						1021.2	3286.6	1756.0	6284.8				
15	7	2	PBS(100ul)	0.5ml(5ml PBS+1ul)	-5kV DC	1274.7	4012.6	1892.7	3749.3	96%	92%	1.60E+06	2.60E+06
						1200.9	4165.3	1852.6	3757.2				
						1182.8	2712.4	1899.3	3743.6				
15	7	2	PBS(100ul)	0.5ml(5ml PBS+1ul)	-5kV DC	950.7	3609.0	1666.5	4963.6	97%	92%	3.10E+06	2.10E+06
						920.3	3456.3	1693.9	5288.4				
						944.3	3898.8	1720.0	5155.0				
15	7	2	PBS(100ul)	0.5ml(5ml PBS+1ul)	-7kV DC	1012.9	3066.5	1696.2	5000.4	98%	95%	2.60E+06	2.10E+06
						1007.8	3298.0	1787.6	5160.5				
						995.2	3060.9	1813.5	4947.4				

APPENDIX XIV

Matlab program for plotting a single page of current pulses

```
clear;
clc;
%Import voltage waveform across current transformer
%Import in binary form because of the excel limitation in Matlab
load 'one.mat';
y=A;

%Convert voltages to current for data from the current transformer
y1 = (y*1e-3)/2.5;
t=0:200e-12:(5000003*200e-12);
Plot current versus time graph
subplot(1,1,1);
plot(t,y1);
grid on;
xlabel('Time (s)')
ylabel('Current (A)')
title('Corona Current versus Time: +6 kV DC at 5 GS/s','FontSize',14)
```

APPENDIX XV

Matlab program for measuring rise-time and width of pulses

```
clear;
clc;

%Import voltage waveform across current transformer
%Import in binary form becaues of the excel limitation in Matlab
load 'one.mat';
y=A;

%Convert voltages to current for data from the current transformer
y1 = (y*1e-3)/2.5;
t=0:200e-12:(5000003*200e-12);

% Corona Signal of Interest
y1n=y1(241167:241502);
t1=t(241167:241502);

%Graph of Corona Current versus time for identified pulse
subplot(1,1,1)
plot(t1,y1n);
grid on;
xlabel('Time (s)')%ylabel('Corona Current (A)')
ylabel('Current (A)')
title('Corona Current for Identified Pulse versus Time','FontSize',14)
```

APPENDIX XVI

Matlab program for calculating average amplitude and spacing of pulses

```
clear;
clc;

format long;

%Import voltage waveform across current transformer
%Import in binary form because of the excel limitation in Matlab
load 'three.mat';
y=A;

%Convert voltages to current (A) for data from the current transformer
y1 = y/2.5;

%Plot current versus sampling point
subplot(3,1,1);
plot(y1);
grid on;
xlabel('Sampling Point')
ylabel('Current (A)')
title('Corona Current versus Sampling Point','FontSize',14)

%Plot Peaks (To compare with full signal above to check all peaks are found)
subplot(3,1,2)
[pks,locs]=findpeaks(y1,'MinPeakProminence',0.006,'MinPeakHeight',0.0025,'MinPeakDista
nce',1000);
stem(locs,pks);
grid on;
xlabel('Sampling Point')
ylabel('Current (A)')
title('Corona Pulse Peaks versus Sampling Point','FontSize',14)
```

```
%Put locs(x value of peaks) and pks (magnitude of peaks) into arrays
A=locs;
B=pks;

%Plot only the peaks versus datapoint to compare to graph above to check that arrays are
correct
subplot(3,1,3);
stem(A,B);
grid on;
xlabel('Sampling Point')
ylabel('Current (A)')
title('Corona Current of Pulse Peaks versus Sampling Point','FontSize',14)

%Calculate average amplitude of peaks
AverageAmplitude=mean(B)

%Calculate average spacing of pulses
a=numel(A);
X=0;
for n=2:a
   X=X + abs((A(n)-A(n-1)));
end;
AveragePulseSpacing=(X/(a-1))*200e-12 %in seconds
```

APPENDIX XVII

Matlab program for calculating the characteristic frequencies of a pulse

```
clear;
clc;

format long;

%Import voltage waveform across current transformer
%Import in binary form because of the excel limitation in Matlab
load 'three.mat';
y=A;

%Convert voltages to current for data from the current transformer
y1 = y/2.5;

%Define sampling time intervals
t=0:200e-12:(5000003*200e-12);

%Plot graph of Current versus Sampling Point
subplot(3,1,1);
plot(y1);
grid on;
xlabel('Sampling Point')
ylabel('Current (A)')
title('Corona Current versus Sampling Time','FontSize',14)


% FFT analysis
% Inverse of sampling rate gives sampling frequency
fs=1/(200e-12);

% Single corona pulse of interest to be analyzed
y1n=y1(4295550:4295857);
```

```
t1=t(4295550:4295857);

%Graph of Corona Current versus time for identified pulse
subplot(3,1,2)
plot(t1,y1n);
grid on;
xlabel('Time (s)')%ylabel('Corona Current (A)')
ylabel('Current (A)')
title('Corona Current for Identified Pulse versus Time','FontSize',14)

% FFT ANALYSIS
L1=length(y1n);
NFFT1 = 2^nextpow2(L1);
Yh1 = fft(y1n,NFFT1)/L1;

% Frequency range of interest
f1 = (fs/2*linspace(0,1,NFFT1/2+1))/1e6;
subplot(3,1,3);
%stem(f1,2*abs(Yh1(1:NFFT1/2+1)));
%Assign coordinates of FFT analysis to matrices
A=f1;
B=2*abs(Yh1(1:NFFT1/2+1));

%Plot the identified frequencies
stem(A,B);

%Output the coordinates of the first two frequencies to screen for
%noting for later analysis
X(1,1)=A(2);
X(1,2)=B(2);
X(2,1)=A(3);
X(2,2)=B(3);
X(3,1)=A(4);
X(3,2)=B(4);
```

```
%Display the matrix X
X

%Format chart
xlim([0 50]);
ylim([0 0.005]);
xlabel('Frequency (MHz)')
ylabel('Current (A)')
title('Dominant Frequencies of Corona Pulse','FontSize',14)
grid on;
```

APPENDIX XVIII

Results of pulse width and pulse rise-time calculations

Applied Voltage (kV)	Current Pulse Width (ns)	Current Pulse Rise Time (ns)	Standard Error of Pulse Width (ns)	Standard Error of Rise Time (ns)
4	61.3	23.6	1.4	1.5
5	64.9	25.1	3.5	3.3
6	59.9	21.0	1.3	1.6
7	58.9	21.4	0.8	0.8
8	59.5	21.5	0.6	0.6

APPENDIX XIX

Peak amplitude and pulse spacing

Applied Voltage (kV)	Amplitude of Current Pulse (mA)	Standard Error of Amplitude (mA)	Spacing of Current Pulses (nS)	Standard Error of pulse spacing (nS)
4	6.5	2.4	121.9	74.0
5	6.4	2.2	156.8	73.2
6	9.6	3.4	58.0	21.6
7	6.2	2.0	22.7	1.3
8	6.9	2.0	14.4	3.8